Design and Development of a New Hand and Wrist Rehabilitation Robot-Assisted System; Equipped With Game-Based Therapy, ROM and Tip-Pinch Force Self-Assessment Approaches

Thesis for the Degree of Doctor of Philosophy (PhD)

by: Husam Abdulkareem Almusawi

Supervisor: Dr. Husi Géza

UNIVERSITY OF DEBRECEN

Doctoral Council of Natural Sciences and Information Technology

Doctoral School of Informatics

Debrecen, 2021

Hereby I declare that I prepared this thesis within the Doctoral Council of Natural Sciences and Information Technology, Doctoral School of Informatics, University of Debrecen in order to obtain a PhD Degree in Informatics at Debrecen University.

The results published in the thesis are not reported in any other PhD theses.

Debrecen, 2021/08/10 ……

signature of the candidate

Hereby I confirm that Husam Abdulkareem Neamah Almusawi, candidate conducted his studies with my supervision within the Informatics Doctoral Program of the Doctoral School of University of Debrecen between 2017 and 2021 The independent studies and research work of the candidate significantly contributed to the results published in the thesis.

I also declare that the results published in the thesis are not reported in any other theses.

I support the acceptance of the thesis.

Debrecen, 2021/08/10 ……

signature of the supervisor

Design and Development of a New Hand and Wrist Rehabilitation Robot-Assisted System; Equipped With Game-Based Therapy, ROM and Tip-Pinch Force Self-Assessment Approaches

Dissertation submitted in partial fulfillment of the
requirements for the doctoral (PhD) degree in Informatics

Written by Husam AbdulKareem Neamah Almusawi ..... certified in Mechatroniccs Engineering

Prepared in the framework of the Informatics doctoral school
of the University of Debrecen
(Industrial and Scientific Applications of Informatics)

Dissertation advisor: Dr. Husi Géza

The official opponents of the dissertation:

Dr. ....

Dr. ....

The evaluation committee:

chairperson: Dr. ....

members: Dr. ....

Dr. ....

Dr. ....

Dr. ....

The date of the dissertation defense: …… 2021

Acknowledgments

I want to express my deep gratitude to Almighty Allah for providing me with the chance and wisdom to complete this research and the competence and strength.

I would like to express my heartfelt appreciation to Dr Habil Husi Géza, my supervisor and dean of the engineering faculty, for his unwavering support, excellent guidance, patience, care, and unflinching efforts in providing me with adequate technical expertise during my PhD studies and research.

My gratitude will never be enough for my loving parents (AbdulKareem Neamah and Bahyia Naser), who have allowed me to pursue my aspirations and raised me to be the best version of myself; without them, this dream would never come true.

Special thanks to my wonderful and lovely wife, Zahraa Alarer, who has always stood by my side and she is always willing to help us.

Thanks to my friend, Mr Mohammed Aad, who was always there for me when I needed his unwavering support, sympathy, and encouragement. Also, I'd like to express my gratitude to my wonderful colleagues, especially Dr Krisztina Toth and Ms Nora Toth.

I would like to express my gratitude to the reviewers. I appreciate the time and effort put in by the reviewers in offering important criticism on this dissertation. Their insightful remarks and stunning observations aided in the development of this work from numerous angles.

I would also want to thank Prof. Dr János Sztrik DSc, Head of the Doctoral School, for his assistance. Likewise, a big thank you to Dr Kocsis Gergely. I would also like to express my gratitude to all of the Committee members for their efforts. I'd want to express my gratitude to Prof. Dr András Hajdu DSc, the Chairman. Eventually, I would like to say a special thanks for the work to all those who contributed to my dissertation.

Table of Contents

ACKNOWLEDGMENTS ..... **I**

LIST OF FIGURES: ..... **VI**

LIST OF TABLES: ..... **IX**

CHAPTER 1: INTRODUCTION **1**

1.1. Overview 1

1.2. Research Motivation 4

1.3. AIMS AND OBJECTIVES 5

1.4. Contribution 7

1.5. Methodology 10

CHAPTER 2: BACKGROUND AND LITERATURE REVIEW OF THE HAND REHABILITATION DEVICES AND THEIR ASSOCIATED TECHNOLOGIES **13**

2.1. Dysfunction of hand after stroke 13

2.2. Considerations On Recovery and Rehabilitation 14

2.2.1. Recovery Attributes: Range Of Motion 15

2.2.2. Recovery Attributes: Spasticity 16

2.3. Hand Conventional Therapy: Techniques Review 17

2.4. Robot-Assisted Therapies for Stroke Rehabilitation 18

2.5. State of the Art of The Rehabilitation Robotics 19

2.5.1. Type of the Mechanical Structure 20

2.5.2. Assistive mode types 28

2.5.3. Actuator Types 30

CHAPTER 3: CASE STUDY AND SYSTEM DESIGN REQUIREMENTS **32**

3.1. Introduction 32

3.2. Essential Clinical Requirements and Considerations 33

3.2.1. Design Technical Specifications 35

3.3. Biomechanical Constraints Based on the Case Study: (Parameterization) 36

3.3.1. Problem Study 36

CHAPTER 4: HUMAN FINGER KINEMATIC MODEL AND FINGER'S TRAJECTORY DETERMINING 42

4.1. Background 42

4.2. Kinematics of a Single Finger 43

4.2.1. Homogeneous transformation 45

4.2.2. Hand Kinematic: Forward kinematics 47

4.3. Thumb finger Kinematics modelling 49

4.4. Simulation Results and Evaluation 52

4.4.1. 2D Index finger workspace modelling 54

4.1. Finger's Trajectory Planner Mechanism 55

4.2. Initial Design and Development 56

CHAPTER 5: MECHANICAL SYSTEM AND MECHANISM DESIGN 61

5.1. Design overview 61

5.2. Actuation Unit 62

5.3. Four Fingers Design Description 63

.5.3.1 Transmission and Driving mechanism 63

5.3.2. Rack and Pinion Mechanism 64

5.3.3. Exoskoleten fingertip holder design 68

5.3.4. The mechanism for (extension and flexion) of the fingers 70

5.3.5. Mechanical Range Determining ..... **Error! Bookmark not defined.**

5.4. Thumb Rehabilitation Mechanism Design 72

5.4.1. Thumb rehabilitation mechanism Design process 74

5.5. Forearm Support and Cover Design 78

5.6. Assembly 79

5.7. Wrist and Forearm Mechanism Design 80

5.7.1. Wrist F/E and R/U Mechanism 81

5.7.2. Wrist F/E Mechanism 83

5.7.3. Wrist-Robot Assembly Integration 83

5.7.4. Wrist Ulnar/Radial Deviation Mechanism Design 85
5.8. Stress analysis and kinematic modelling and simulation 86
5.8.1. structural Stress Analysis.....**Error! Bookmark not defined.**
5.8.2. Forward Kinematic model of the proposed system..... 87

CHAPTER 6: HARDWARE AND SOFTWARE DEVELOPMENT.....94

6.1. Electrical System Design..... 94
6.2. Servo motor speed and position control..... 98
6.3. Design And Development an Integrative Grabbing Force Sensing Unit 100
6.3.1. Design Of the Integrative Force Sensing and Working Principle 101
.6.3.2 Electromechanical Implementation 103
6.3.3. Force-sensitive resistors..... 105
6.3.4. Analog to digital converters..... 108
6.3.5. Inter-Integrated Circuit Communication Protocol..... 109
6.4. The Power Supply Unit Design and Hardware Implementation..... 110
6.5. Software: Back-End and Front-End Development..... 112
6.5.1. State Management System..... 114
6.5.2. UI – Servo and UI – ADC Controller Communication..... 115
6.5.3. Data collection development and storage..... 116
6.6. Interactive based Game Rehabilitation..... 121

CHAPTER 7: EXPERIMENTAL RESULTS AND DISCUSSION.....124

7.1 Experimental Procedure..... 124
7.2 Passive Therapy: Experimental Test..... 126
7.2.1 Experimental human-robot integration and software setup 126
7.2.2 Motion Capture System Setup..... 130
7.2.3 Passive Fingers F/E Experimental Results and Discussion 132
7.3 Active Therapy with Assistance..... 134
7.3.1 The Force Measurement and Evaluation..... 138
7.4 Wrist Rehabilitation Experimental Results..... 139
7.4.1 Wrist F/E and U/R result's Discussion..... 144

7.4.2 Wrist uniaxial and boundary motions 144
7.4.3 Interactive game-based rehabilitation experimental results 146
7.5 Time-based Performance Assessment: UI Results 148
7.6 Subjective Study and Results 151
7.6.1 Questionnaire For Cpm Device Functionality And Safety Feedback 151
7.6.2 Evaluated Result With Healthy Participants 152
CHAPTER 8: CONCLUSION AND FUTURE WORK 153
8.1. Conclusion and Future Work 153
8.2. Theses 154
8.3. Publications 156
REFERENCES.....161

List of Figures:

Figure 1: summarized diagram of the working process 12
Figure 2: Anatomy of Hand and Wrist[21] 14
Figure 3: Spasticity 16
Figure 4: End-Effector devices in literature 24
Figure 5: a group of rehabilitation devices based on grounded-exoskeleton-based 28
Figure 6: Human Hand Motion (DOF) 33
Figure 7: Measuring the Extension of the wrist of stroke patient by the Goniometer provided by the Rehabilitation Department 37
Figure 8: Measuring the patient's upper limb 37
Figure 9: Measured Range of Motion (ROM) values of impaired and unimpaired hand of Subject 1 41
Figure 10: Measured Range of Motion (ROM) values of impaired and unimpaired hand of Subject 2 41
Figure 11: representation the coordinate frame of the three-link index 43
Figure 12: DH Frame Assignment 44
Figure 13: representation the coordinate frame of the two-link thumb 50
Figure 14: Simulation results for index finger; 53
Figure 15: Simulation results for thumb. 54
Figure 16: theoretical trajectories and workspace of the finger's F/E 55
Figure 17**:** The grounded exoskeleton of the finger's rehabilitation 57
Figure 18:. Block diagram of the actuation system workflow 59
Figure 19: A real-time experimental setup of the index finger's workspace trajectories measurement: 60
Figure 20: 3D structure of the employed Driving mechanism 65
Figure 21: the proposed linear guide mechanism: 66
Figure 22: Ultimate 3D design of four-driving mechanism assembly: 68
Figure 23: 3D model of the distal fingertip's holder assembly: 69
Figure 24: 3D assembly of four fingertips holder and support that connected with the guiding shaft. 70

Figure 25: 3D structure assembly model of the proposed system concept's integrations 71
Figure 26: Thumb range of motion;..... 74
Figure 27: 3D CAD structure model of the proposed thumb rehabilitation mechanism with its implementation. 76
Figure 28: 3D CAD assembly top view, demonstrate the active ROM of the proposed system's links..... 77
Figure 29: 3D CAD assembly front view demonstrate the proposed thumb rehabilitation mechanism for both right and left hands..... 78
Figure 30: the proposed system with its cover and forearm support design..... 78
Figure 31: 3D structure implementation of the cover and forearm support design woven belts 79
Figure 32: 3D CAD model of the arm-robot models;..... 80
Figure 33: 3D structure of the proposed wrist and forearm rehabilitation system 81
Figure 34: 3D CAD assembly model of the wrist F/E and R/U mechanism: 82
Figure 35: 3D CAD assembly of the proposed system F/E ROM:..... 83
Figure 36: 3D model assambly of human-robot integration for the wrist 84
Figure 37: 3D model assembly of human-robot integration for the wrist 85
Figure 38: 3D CAD assembly of the proposed system F/E ROM:..... 85
Figure 39: final 3D structure design assembly 86
Figure 40: Coordinate frame of the proposed finger rehabilitation system. 87
Figure 41: Detailed view of the robotic arm..... 88
Figure 42: Robot's end-effector workspace plot 90
Figure 43: X and Z position for the end-effector..... 92
Figure 44: Driving transmission mechanism of the proposed system end-effector: 93
Figure 45: 3D assembly of the proposed electric and electronic schematic circuit..... 98
Figure 46: Servo motor position control..... 99
Figure 47: Servo motor speed and position control block diagram..... 99
Figure 48: Motors connected to the 3D printed parts 100
Figure 49: Force-sensing resistor:..... 102
Figure 50: Electromechanical Implementation..... 104

Figure 51: The proposed integrative force for the thumb. 105
Figure 52: Voltage divider circuit 106
Figure 53: Second order active low pass filter 107
Figure 54: Bode plot of second-order active low pass filter. 107
Figure 55:Connections 108
Figure 56: Delta-sigma ADC architecture 109
Figure 58: I2C Message 110
Figure 59: A low power consumption. illustrates the hardware composition and relationship. 111
Figure 60: Front-end of a specially developed (Patient information tab on GUI) 113
Figure 61: Flow chart of Flux architecture [159] 115
Figure 62: HTTP vs Socket.io 116
Figure 63: Clamping function 119
Figure 64: Updating GUI based on the sensor reading. 120
Figure 65: Servo position and speed control 120
Figure 66: Controlling servo motors and updating GUI based on the sensor reading. 121
Figure 67: the proposed 2D game development which was used for the hand rehabilitation interactive game 122
Figure 68:The proposed System implementation 125
Figure 69: human-robot integration setup 126
Figure 70: Hand parameters tab on UI 128
Figure 71: Therapy settings tab on UI 128
Figure 72: Real-time, passive finger F/E therapy training. 129
Figure 73: A real-time experimental setup of fingers-robot integration and the index finger's workspace trajectories measurement: 131
Figure 74: Continuous passive motion rehabilitation experiment of s typical finger flexion and extension displacement. 133
Figure 75: The developed control dashboard: hand parameters selection 135
Figure 76: illustrates the real-time performance of active therapy with assistance. 137
Figure 77: the developed force integration UI of fingertip-pinch force evaluator 139

Figure 78: The real-time experiments of wrist F/E workspace trajectories and ROM. 140
Figure 79: The real-time experiments of wrist R/U workspace trajectories and ROM. 142
Figure 80: Continuous passive motion rehabilitation experiment of s typical. 144
Figure 81: wrist active uniaxial motions 145
Figure 82: wrist elliptical motion: 146
Figure 83: the developed game-based interactive rehabilitation 147
Figure 84: Session's information tab on the developed dashboard 148
Figure 85: Time-based monitoring of the performance assessment. 150
Figure 86: Bar graph showing the Functionality and Safety measure of CPM device given by 06 healthy participants 152

List of Tables:

Table 1: Range of motion (ROM) measurement[26] 16
Table 2: Recent elated work. 19
Table 3: Measured values of the fingers of Impaired hand and Wrist 38
Table 4: Measured values of the fingers of unimpaired hand and Wrist 39
Table 5: DH Parameters (Index finger) 46
Table 6: DH parameters for the Thumb finger 50
Table 7: DH Parameters 88

Chapter 1: INTRODUCTION

1.1. Overview

The hand is one of the foremost vital limbs of humans; it is a multi-fingered extremity at the end of the arm. It consists of five fingers and a wrist. It is one means by which humans have changed the world by creating gigantic buildings and machines. Human hands are an influential part of the human body since they are extraordinarily mobile and can execute a delicate and extensive range of duties, covering activity of daily living (ADL) (e.g., gripping different objects, holding things, transporting, moving, writing, eating, touching, and even changing the world). Unfortunately, many conditions, including stroke, spinal cord injury, tendon shatters, and fall-related injuries, can lead to the impairment of hand motor and sensorimotor functions of the upper extremity (UE). Approximately 80% stroke or Cerebral vascular accidents survivors develop hemiparesis in the upper arm, the dominant symptom of which is an inability to grasp an object [1]. Moreover, Stroke is also the second-leading cause of mortality worldwide [2]. It is estimated that over 15 million people each year have a stroke over the world. There are five million deaths and another five million who are permanently incapacitated due to their motor disability [3]. The majority of them will necessitate care and neurorehabilitation [4]. This process called rehabilitation Which helps re-learning of movement [5]. Neuroplasticity, also termed neuroplasticity, is a concept that claims that neurons can form new connections through the repetition of learning and experience [6]. The goal of rehabilitation is to restructure and reinvigorate the neuronal connections in these motor patterns that were destroyed due to disease or an accident, with a detrimental impact on patients' upper limbs. These help individuals who survived to deal with their disabilities. Physio-therapists aid patients in regaining lost abilities during conventional rehabilitation, these approaches

draw upon methods and approaches similar to physical therapy, which works to restore motion and exercise, as well as occupational therapy, which works to teach patients how to do their daily routines, including eating, drinking, and personal care. Current medical evidence and Rehabilitation care recommendations are suggesting that patients receive care for brain injury as soon as possible [7].

However, it is important to identify possible obstacles, as well as possible advantages, because recovery of upper extremity functions may be limited as well as further hampered by the lack of available resources. (e.g., enough trained physiotherapist, facilities) which further complicated problem. While physiotherapy appointments with professionals do allow only a limited number of exercises, unfortunately, this is often due to scheduling constraints and patient preference. Usually, the therapist starts with the primary focus to rehabilitate the lower extremity to help victims regain their balance and mobility, which usually leads to neglect of the UE, putting the stroke victims at a greater risk of hand and arm disability. Due to the rising number of patients, there are not enough resources to treat them with traditional methods, making those methods costly and hard to handle. These facts lead to the majority of stroke patients not receiving sufficient treatment, and according to statistics, only approximately 12% of stroke patients show a considerable improvement in their capability to use their upper limbs [8].

Therefore, there is a critical need to develop technologies that can relieve the burden on health professionals, provide the necessary active and passive exercises, motivate the patients, contribute to strengthening the active range of motion AROM, and grasp force.

Over the last years, the researchers came up with various ergonomically strategies by combining the power of robotic technology with sophisticated medical therapies to work hand in hand.

The robot-assisted rehabilitation devices are a mechatronic device in which a specially designed external mechanism is coupled to the individual body and deliver a necessary force to perform the required gestures of the human limb. These assistive motions can be formed with different modes, including active, passive, Continuous Passive Motion (CPM), and interactive modes. Moreover, these devices then transfer the generated motion link to the affected limb, depending on the mechanical structure and the diver transmission mechanism.

A significant advancement in conventional recovery approaches has contributed to assistive robotics. Assistive rehabilitation robotic has progressed and increased the human quality of life significantly. Increasing emphasis was given to technical advances in robotics during refurbishment training [9], [10]. Additionally, it should be noted that these therapeutic robotics are not meant to replace therapists; their purpose is to assist the time-consuming, and challenging tasks therapists must conduct. [11], [12].

Additionally, numerous considerations should be taken into mind when designing robot-assisted rehabilitation that integrates directly with the human body, such as strike technical and clinical requirements. Additionally, the human hands represent a higher challenge to the invention of robotics that integrates with it because of their complex anatomy shape, since the designers must follow this complexity.

1.2. Research Motivation

Human beings have had a variety of health difficulties from the dawn of time. Some of these health problems can occur in particular environments, such as heredity, villages, or countries. Some are global illnesses and accidents, such as cerebrovascular accidents and brain traumas, which result in limitations in the upper limb, including the most mobile and functional component, the hand. Since there are too many patients and little resources, physiotherapists are unable to train each patient adequately. Nothing can be more motivational for the author to design a machine to help other human sufferings from disabilities regain their independent hand and sensorimotor functionalities. Since intense therapeutic training of movements involves repetitive tasks, the physiotherapist usually performs these repetitive passive motions manually. However, the efficiency of manual motion is a very long, tiring, and tedious process that may be influenced by the capabilities of the physiotherapist to recover their hand functions.

Moreover, the recovery efficiency will depend on the physiotherapist mood. Therefore, to resolve these challenges, a robot or machine could be developed that combines neurorehabilitation methods and standards for motor learning and repetitive assistance for people with various conditions that affect the nervous system, such as stroke, brain injury, and physical injury, and neurological damage. Since the advent of human assistive technology, research on machine-human interactions has become a key concern. As a result, experts in robotics have developed an increased interest in the subject. Finally, restoration and physiotherapy are successful techniques for people with severe injuries, neurological impairments, and various disorders to restore the capability to regulate their body movements. Upper-limb power aid and/or rehabilitation robots have been created in order to solve all of these

concerns. Couples with ideas to advance current rehab approaches for restoring arm function.

1.3. AIMS AND OBJECTIVES

The primary goal of this dissertation is to demonstrate a novel design and development of self-assessment fingers, and wrist rehabilitation mechatronic system to aid with the recovery progress of survivors who suffer hemiparesis of the upper arm caused by brain injury, spinal cord injury, tendon shatters, or fall-related injuries. The aimed system step forward to improve the related existing devices. The objective of the proposed system is to help the users regain both right and/or left-hand functionality and sensory-motor and reduce spasticity, muscle tone on the hand, and observe and evaluate their recovery steps. The intended system is designed to be a single device that capable of performing the basic movements of the hand movement, including one fingers flexion/ Extension (F/E) including the thumb (F/E); plus, two wrist movements wrist flexion/ Extension (F/E), and Wrist Radial/ulnar (R/U) deviation; and one forearm pronation/supination (P/S). Additional benefits of this project include helping to minimize the overall cost of rehabilitation and providing a better solution for the market, besides the proposed system aimed to develop a game-based therapy that motivates the patients during their active therapy. A self-assessment feature was considered during software development to evaluate the rehabilitation progress at the end of each therapy session. Including all these characteristics will give more people easier access towards a creative and cost-effective approach to exercise rehabilitation.

the following objectives are in place to ensure the achievement of these goals:

- Construct a sensor-based rehabilitation approach for usage with either hand fingers and/or wrist using a robot-based rehabilitation strategy.
- It follows the natural movement of attached joints.
- Single finger and thumb gestures can be assisted in various ways, including passive, interactive, active, and CPM.
- The device is capable of doing multiple functions by providing the fingers all together or independently.
- It is rapid and straightforward to set up end-users (patients). And it is usable for users with Spasticity
- Developing a grabbing force and ROM assessment programs and Objective evaluations and reporting
- Develop a user-friendly dashboard GUI development to set, control, report the therapy parameters and progress.
- The development of a game-based therapy with different changeable gaming levels motivates and improves the patient's muscle strength and motor learning.
- Safety considerations: The device should not force or access the possible active ROM in the mechanical design, especially for spastic patients. In the electrical and electronics design, several electrical protections must be considered, including emergency stop buttons. The software level enables the therapy to be immediately to be pause or stop.
- The fingertips and wrist attachment should be removable to be sterilized easily and easy to wear for the patients without hurting them, and it can be fit for different hand sizes, and a programmed part subject

to be easily reused by the end-user for both the patients and the therapist.

- Adjustable forearm supports can be changed quickly depending on the user's hand size.

- The selection of the material (e.g., type of actuators, sensors, design, electrical component, filaments, etc.) is defined according to the model's productivity, cost-effectiveness, and ergonomics.
- Consider the safety of the patient and the therapist who attended to use the machine by implementing an emergency control in the mechanical, electrical, electronic, and software designs, enabling the first and end-users to pause or stop the machine instantly.

1.4. Contribution

Although, a set of assistive-robots rehabilitation systems has been developed. Nevertheless, there are numerous limitations in the existed hand rehabilitation approaches; most of them are very expensive for local rehabilitation centres, heavy-weighted, complex structured, noisy, too challenging to operate, and too many mechanical parts linked to the patients' arms can be unconformable to both therapists and patients. In addition, specific devices are a static platform and intended for some specific applications and specific hand and joints and neglecting the thumb and the wrist from their designs. Furthermore, many existing devices control over an external PC without embedded control implementation. Besides, most of the existing solutions are not outfitted with an automated diagnostic system, self-assessment and feedback system interactive game, and a gripping force measurement instrument. All work together to facilitate accurate patient feedback and continuous motivation throughout a long repetitive rehabilitation process.

Taken together, these facts show that worldwide stroke overall survival is rising, and the death rate is climbing, which indicates a necessity towards greater and improved therapeutic facilities in the future. Therefore, considering all these limitations along with technical and clinical requirements, the proposed system also intended to step forward of improving the existing solution, this thesis describes a novel system that is capable of rehabilitating four fingers and thumb plus the wrist joints in one device, along with the process of mechanical, electronic design, and software design and development. Theoretically, the human fingers were modelled as kinematic objects and direct measurements regarding their AROM, and grabbing force was made from stroke survivors to better understand the problem. The proposed system takes advantage of the combination ground-exoskeleton and end-effector mechanism to provide the desired motions to the desired joints. The concept and the design of the proposed system were developed at Debrecen University with respect to the technical and strict clinical requirements. The system is designed for research investigations and prototyping with the help of rehabilitation practitioners. Furthermore, essential to notice, the result of this project will be a product, not medication or a surgical procedure.

Along with cost reductions: The following are the primary contributions of this dissertation:

- Develop and build a new mechanical structure and motion transmission mechanism to provide a repetitive active, passive, and continuous passive training for four fingers F/E, capable of assisting all fingers together independently for both right and left hand.
- Develop and build a new thumb rehabilitation mechanism capable of providing active and passive training to the right and left thumb F/E.

- Develop and construct a new mechanical structure and mechanism for wrist joints rehabilitation, capable of performing wrist F/E, R/U deviation and circular movements with different assistive modes, including active, passive, and interactive training.

- The development and implementation hardware embedded system can safely, control, actuate, and sense, and drive the desired singles and sufficient power to the entire proposed system.

- Owning kinematics and workspace representation of the human Index Finger F/E, and thumb F/E anatomy and the proposed mechanism using forward kinematic analysis to profoundly investigate the fingers, trajectories, ROM, and workspace MATLAB software.

- Construct and integrate the mechanical and electrical systems for the fingers and wrist, and implement a forearm cuff support that can be adjusted and fasten depend on the targeted therapy and the user's hand size.

- Develop a biofeedback sensory, which provides valuable data including the ROM, grabbing force, and muscle activities through EMG signals.

- Develop and implement an embedded software and user's friendly dashboard through graphical users' interface (GUI), which enable the therapist to set and save the patient information, including the name, age, case date, insurance number, the therapist's name, type of brain injury, the affected side, the joint to be rehabilitated, and eventually the case description.

- Develop local database storage to store the user's info and perform ROM, grabbing forces, gaming scores, and the therapist notes.

- Develop a diagnostic system that provides self-assessment feedback regarding the patient recovery progress. To evaluate the patient ROM and grasping force progress by analysing and reporting each therapy session's parameters.

- Develop and implement interactive game-based therapy to enhance the therapy progress and motivate the patients.

1.5. **Methodology**

As Figure 1 summarized the development steps, the following phases will be used to execute the methodology to accomplish the proposed development:

1- Previous research on rehabilitation devices and/or any relevant topic has been studied to gain a comprehensive knowledge of the robot-assisted rehabilitation research field and the entire design system (e.g., the employed actuators, control modes, mechanical designs, power transmissions, biofeedback sensors, and so on). This review has also given a comprehensive awareness of several research areas in robot-assisted rehabilitation.

2- The initial stage in any research effort is to define the problem that needs to be addressed. This is done by evaluating existing knowledge and identifying the deficiencies of existing robot-based rehabilitation strategies.

3- Verifying the possible approaches, assessing their effectiveness, and ensuring they are included in the rehab therapeutic system's optimizations.

4- Design and manufacturing a novel motion driver system that enables the fingers and the wrist to execute the necessary motions.
5- Develop a kinematic analysis model for human index and thumb fingers and the proposed fingers rehabilitation mechanism.
6- Develop and integrate embedded hardware and controller for entire proposed system capable of driving sufficient signals and power.
7- Developing a user's friendly dashboard GUI to set, control, and report the therapy parameters and progress
8- Developing a game-based therapy for the active training
9- Developing self-management adjustable data analytics to report each therapy session.
10- Proposed mechanical designs are put to the test and evaluated: During the development of an equivalent kinematics model and workspace representation for the proposed end-effector, as well as a Stress analysis to further investigate and test the system behaviour in such conditions as the maximum stress that can be applied to the mechanical parts, as well as simulation of the system's end-effectors' trajectories, velocities, and workspaces
11- Performing various experiments to evaluate and validate the proposed system integration
12- Sustained design adjustment as a result of evaluation results, with the aim of improving system functionality and experimental validation.
13- The PhD completion, publications, and submission for PhD thesis defence

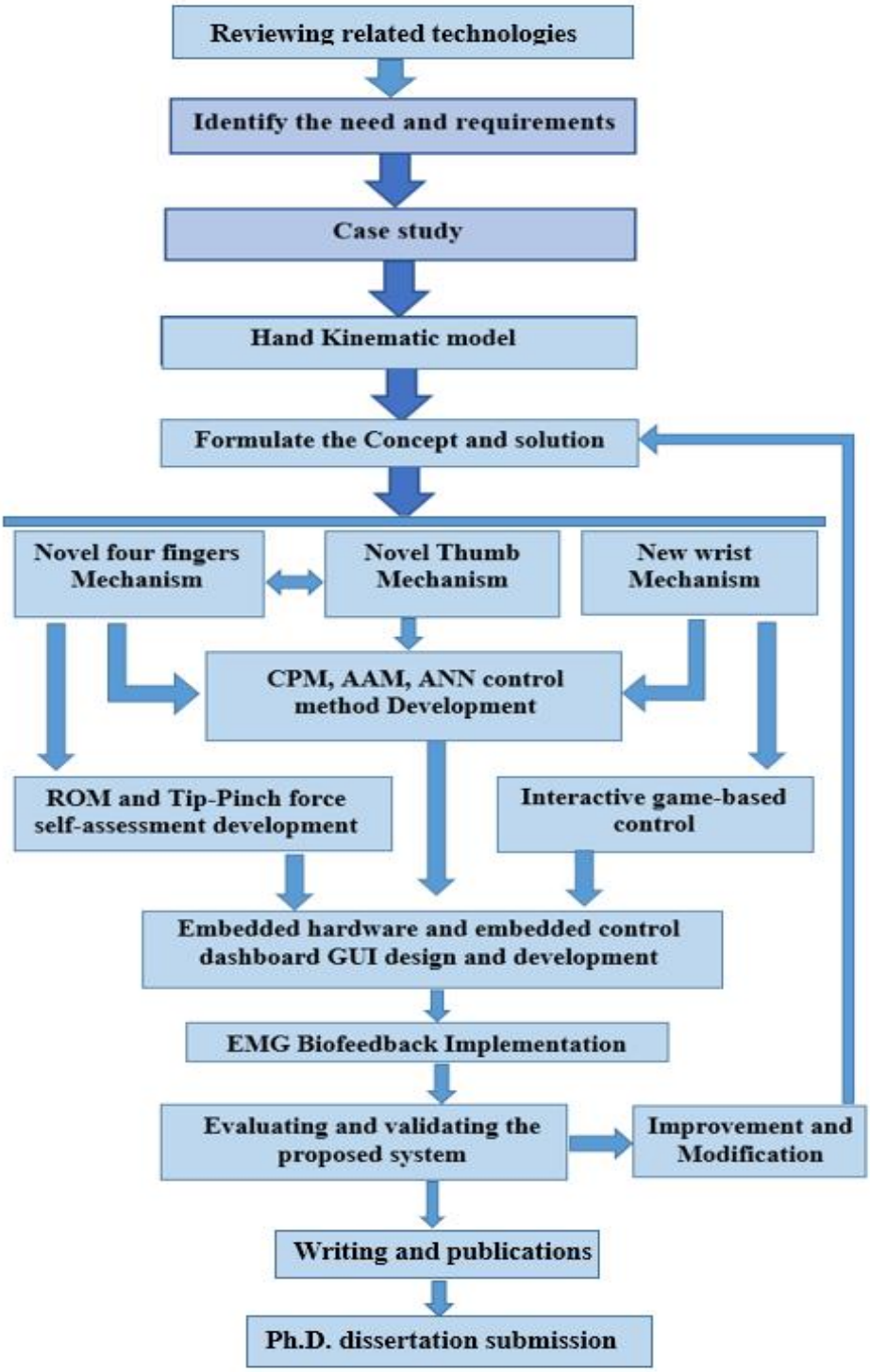

Figure 1: summarized diagram of the working process

Chapter 2: Background and Literature review of the Hand Rehabilitation devices and their associated Technologies.

2.1. Dysfunction of hand after stroke

Daily living activities are often affected by a stroke, and symptoms include spasticity, hemiparesis, and lack of coordination. The study concludes that nearly two-thirds of stroke patients have motor difficulties with their upper limbs. After getting ischemic or haemorrhagic lesions to the motor cortex, premotor cortex, motor tracts or related ways in the cerebellum or cerebrum can lead to serious injuries in the human brain that adversely affect the body's functionality in general [13]. Daily living activities are often affected by a stroke, and symptoms include spasticity, hemiparesis, and lack of coordination [14]. The study concludes that nearly two-thirds of stroke patients have motor difficulties with their upper limbs [15]. Stroke affects hand motor function, resulting in disordered movement, mirroring disordered neural connections. Disability can range from total impairment to being a relatively minor disability. Typically, a lack of muscle strength resulting from the stroke, particularly in the fingers and wrist, is the hand motor deficiency contributing factor [16] [17]. Loss of control is due to fatigue, spasticity, and various muscle activity trends. In contrast, loss of feedback is due to weakness, e.g., a failure to extend the fingers induced by motoneuron, the lack of reciprocal inhibition and hyperexcitement is due to weakness and unnecessary coactivation of finger extender and flexor muscles. [18].Finger disability occurs because of the failure to separate particular muscles and because force generation is irrelevant in a task [19]. However, the separation between the finger regulation and the grip strength can be seen with the ipsilesional side, demonstrating dexterity abnormalities. The disparity between the grip

capacity and the coordination of individual fingers is obviously demonstrated by the fact that, while grip strength is maintained, the ipsilesial Hand can exhibit dexterity anomalies. Figure 2 illustrates the composition of human hands and wrists to better explain the bones anatomy[20] . To clearly understand the bones anatomy, Figure 2 demonstrates human hand and wrist composition.

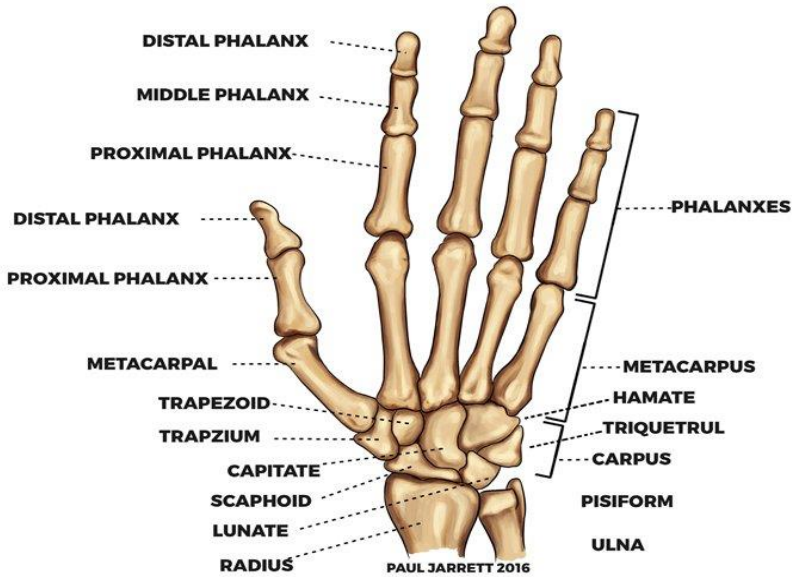

Figure 2: Anatomy of Hand and Wrist[21]

2.2. Considerations On Recovery and Rehabilitation

Recovering the stroke hand is an ongoing research initiative. Engineers performed experiments to integrate robotics with the field of rehabilitation. To train a victim of a stroke, his physical, social and physiological steps are maximized; coordinated medical, vocational and special schooling is utilized for stroke therapy. From the clinical studies, it is clear that the early onset of treatment is complimented by an immense recovery process. Delayed care can lead to secondary complications such as deconditioning and contractures [22].

Motor rehabilitation and hemiparesis are the best researched of all stroke impairments since almost 88 per cent of severe stroke cases are hemiparesis. The stroke begins with the UE (upper extremity) being higher than the LE (lower extremity). This causes motor activation to be greater at the upper end than at the lower end. The crucial period to restore the hand to action is the magnitude of the top extremity defect which is known as real motor recovery qualities in the EU. However, 58 studies have reported that the predominant magnitude of motor deficiency is the most significant predictor factor for upper-leg rehabilitation [23]. Nevertheless, the recovery phase aims at enhancing mobility range which is known as the range of motion, muscle power, physical and cognitive ability.

2.2.1. Recovery Attributes: Range Of Motion

The range of movement can be described as calculating the degree to which the joints' usual range motions can be carried. It is a very helpful index to assess the recovery of patients who can lift their joints. There are two forms of ROM in rehabilitation care exercises, i.e., Active and Passive. With active motion range (AROM), patients may do exercises without support in the joint movement, although passive motion range (PROM) is one in which the therapist assists a patient to shift the joint across the motion range. The calculation (ROM) is measured by the therapist using a goniometer and inclinometer to calculate the motion range of each joint in degrees [24], [25]. However, with age, sex, and genetic context, the usual scope of movement differs. The reference values are demonstrated in Table 1.

Table 1: Range of motion (ROM) measurement[26]

Joint		ROM	
Wrist		Flexion	0° - 75°
		Extension	0° – 70°
		Radia	0° - 20°
		Ulnar	0° - 35°
Thumb	Basal joint	Palmar Adduction	0°
		Palmar Abduction	0° - 45°
		Radial Adduction	0°
		Radial Abduction	0° - 60°
	Interphalangeal	Hyperextension	0° - 15°
		Flexion	0° - 80°
	Metacarpophalangeal	Hyperextension	0° - 10°
		Flexion	0° - 55°
Fingers DIP joints		Extension	0°
		Flexion	0° - 80°
Fingers PIP joints		Extension	0°
		Flexion	0° - 10°
Fingers MCP joints		Hyperextension	0° - 45°
		Flexion	0° - 90°

2.2.2. Recovery Attributes: Spasticity

Spasticity is characterized as a motor dysfunction attributable to muscle hyperactivity; stroke defects in the brain allow the muscles to contract unconsciously [27]. The tendons and soft tissue around a muscle cannot achieve their maximum motion due to tightness. This makes it even tougher to extend the muscle. The elbow, knee, hand and fingertips of the spastic upper limb suffer seriously. Figure 3 indicates the above-mentioned positions explicitly.

Figure 3: Spasticity

(a): Bent wrist (b): Pronated forearm (c): Clenched fist, (d): Thumb in palm[28]

2.3. Hand Conventional Therapy: Techniques Review

This section reviews and summarize the traditional techniques used to recover hand functions after stroke. Generally, in this Technique, the interdisciplinary team works hand in hand and requires recovery professionals and medical providers primarily responsible for rehabilitation services. These treatments include regular assessment, task-based care and evaluation. The therapy mechanism utilizes external inputs such as stretching to enhance muscle function and activation, which is fully neurological dependent [29]. Two major fundamental recovery approaches are physical Therapy (PT) addition to occupational therapy (OT) [30]. Brunnstrom is one of the neurological activities that stress the synergic activity habits that form during rehabilitation. Another method called Rood focuses on the tasks of growth, the description of muscle work and sensory feedback. The most common technique is Bobath to emphasize the control response from weakened postural structures [31]. The PNF (propositive neuromuscular facilitation) is typically used in clinical studies towards boosting the active and passive ROM to maximize mobility efficiency and improvement help [32]. This approach has efficient outcomes and is useful for patients with strokes. However, the conductive therapy for learning theory is used to manage psychological disorders, and the motor relearning theory is used for practical activities and regular relearning [33].

Another medication known as botulinum toxin is used in hospitals to suppress sound, even if the active action of hand and arm does not alter. The subject must make an attempt to make such an operation affected by the procedure itself [34]. The treatment of acupuncture is often known as a rehabilitation technique for stoked patients, where needles are manipulated and placed more clearly into particular areas of a body, nerve endings are used to alleviate discomfort.

The technique of Functional Electric Stimulation (FES) is often used for stroke treatment, and this procedure offers a shock for the nerves of the muscle of the patient to raise and render it functional. Particularly to grip and release, it is an effective technique for hand-rehabilitation. FES helps paralyzed or partly paralyzed muscles to re-move through the stroke [35]. In several case studies, the recovery phase has been strengthened by FES [36], whereas some contend that the stroke patient does not look successfully took effect [37]. However, several options for stroke recovery are available since there is a "task-specific training" style that includes holistic exercise as well as physically-based challenges where one must use multiple motor skills at different degrees of freedom (DOFS) [38]. in addition, different traditional training approaches employ constraint-induced movement therapy (CIMT) to help patients with recovering limbs [39], Transcutaneous Electrical Nerve Stimulation (TNS)[40], Transcranial Magnetic Stimulation (TMS)[41], Bimanual therapy[42], Mirror therapy [43], Observation to imitate [44], and Mental Motor Imagery [45]. All these approaches are noninvasively advancing which are widely used in Conventional therapy for sensory re-education and motor rehabilitation following a stroke.

2.4. Robot-Assisted Therapies for Stroke Rehabilitation

Robotic therapy (RT) is becoming increasingly crucial for post-stroke care to optimize rehabilitation and rehabilitate a stroke victim's function [46]. Compared with traditional procedures, consistent preparation, good results, and precision assessment have various advantages [47]. Robotic therapeutic training facilitates people management's economic utilisation and the quality control of recovery therapies. The procedure could be accomplished quicker and more effectively if clinicians and physiotherapists only had to run the robot instead of performing therapy by themselves. This increases therapy session efficiency and patient monitoring while reducing overall treatment

time [48]. According to the aim of this project, this thesis focuses on and discuss the therapeutic devices for the motor recovery of Hand and Wrist. The new literary reviews carried out by universities and academic institutes from the literature and studies concentrate on designing and creating robot-based recovery devices for the upper limb. The latest developments in upper-limb construction are addressed in Table 2. in which in the following table, the systems are sorted based on their training method they provide, transmission mechanism they adopt, type of actuator they powered by, and the movement and joints they acuate.

Table 2: Recent related work.

System	Training Mode	Transmission Schematic	Type of Actuator	Mechanical Structure Type	Supported Movements
[49]	Passive	parallel mechanism	2* Servo motors	Exoskeleton	Elbow (F/E) and shoulder (F/E)
[50]	Passive and active	SPRM) with the parallel mechanism	DC motor	Exoskeleton	1 finger
[51]	Passive and active	parallel mechanism	2* pneumatic actuator	End-effector	Wrist (F/E, R/U)
[52]	CPM	rope + toothed belt	DC motors Harmonic motors	End-effector and exoskeleton	shoulder (F/E, I/E, A/A), elbow (F/E, I/E); wrist (F/E).
[53]	Active and Passive	Cable-driven and differential rotation	PMS	exoskeleton	1 finger (F/E)

2.5. State of the Art of The Rehabilitation Robotics

According to the latest state-of-the-art literature, [57]–[60], assistive robotics is rehabilitation instrument that may be split into several categories according

to their particular concept, mainly divided into classes: The first one is the portable devices that support daily living activities ADLs. This group of systems has consisted of wearable devices; They may even be linked to tables; They are designed to guide manipulators of patients at home to conduct ADL (e.g., holding things, grasping, and using a phone). But portability is not essential at the early stage of stroke, provided that patients are unable to execute regular ADLs. However, challenges in these frameworks must be taken into consideration; More actuators are required as the set of joints to be trained increases. These facts, of course, would contribute to increasing energy supply, weight, complexity and expense. The second group is based on the therapeutic systems that are more relevant than ADL supportive technologies in assistive-robotic devices. These are mostly for therapeutic hospitals and too pricey even for certain small clinical services because of their complexity, size, weight and scale.

However, both the ADL devices and the therapeutic devices can be further classified and grouped by other bases and terminologies, including the type of mechanical structure, actuation unit type, driving unit, transmission mechanism, control strategy, assistive type, a system of transfer of electricity, a technique for deliberate sensing, DOFs.

2.5.1. Type of the Mechanical Structure

the mechanical properties are the most challenging part of designing a device that can integrate and provide the desired motion to the upper limb since it is the part that attaches, actuates, and transfer the motion to the target joints and travels across the mechanical system through the damaged limbs. The most popular architectures for assist robots are the exoskeleton-based framework and end-effector systems. The distinction between the two methods is that the exoskeleton-based frame represents the configuration of the skeleton of the

target limb. Exoskeleton-based structure facilitating the movement of individual joints of varying degrees of freedom DOFs. The end-effector-based devices are a more precise and reasonable solution, where the intended limb connects with the terminal unit with fewer mechanical integrations.

A. End Effector

The End Effector is a system beyond the patient extremity that provides the necessary assistance or resist the gestures by the end of the user's extremity. In a broader context, the end effector mechanism is the assistive robotics component that interacts with the human limb. The feature of end effect robots is easily customized to each patient because the user and machine and the joint angles do not have to be set the same. The production of end-effect robots has been proven in rehabilitating disabled individuals, and it has also reached the marketplace, such as Amadeo, Tyromotion [54], another typical end-effector development; My Scrivener, Obslap Reseach, LLC; Palsbo [55], this system provides 3 DOFs. Another example of end-effector-based robot presented by authors in [52], shown in Figure 4 (f), they developed a heavy stationary end-effector robot performing in total six DOFs: dividing as (1), three DOF of the shoulder joint with different: (F/E), internal/external rotation (I/E), abduction/adduction (A/A); (2), one DOF of the elbow joint: (F/E); one DOFs: (I/E); one DOF of the wrist joint: (F/E). The proposed end-effector system with a tension mechanism based on cable-driven modular parallel joint driven by a toothed belt, the transmission mechanism used a rear-mount to transmit motion for the end joints, derived by DC Servo motors and harmonic motors. The authors used an external computer-controlled machine to perform continuous passive rehabilitation. An End-effector-based device termed MIT MANUS [56], which was developed by the Massachusetts Institute of Technology (MIT), cooperated with the Burke Rehabilitation Clinic in the

USA. There are four units: three of them are actively used for vertical, planar, and wrist movements, and one is passive: which is used for grasping [57]. This system features 2 DOFs, which are programmed to practice and replicate motions of the arm. The patient's hand is fastened to the end of the robot that will help the hand extend and practice the grip by adjusting its diameter [56]. It should, however, be restricted by a limited ROM and cannot train the opening hand from a closed hand. Another Device labelled INMOTION [58], [59], consists of three innovative tools for robotic care established by Interactive Motion Technologies: In Motion ARM, In Motion WRIST, and Motion HAND. These systems use Interactive gaming to show the patient impairment and it is used throughout patients' recovery to monitor improvements in functioning motor and intellectual capabilities [60]. In the Motion Hand module, An adaptive device is continuously utilized for an extension with the In Motion Arm system primarily used to release and catch the patient intensities, except this In Motion Wrist module is an exoskeleton robot adaptable to gestures of the wrist [61]. Two of the In Motion technologies are shown in Figure 4 (a, b). A system named MIME [69] (Mirror Image Movement Enabler) was developed by cooperation between Veteran Administrative Medical Center and Stanford University. on the basis of robotic activity for upper limb instruction. This device consists of 6 DOFs with unilateral and bilateral modes along with four therapy stages (active-assisted, passive, constrained, bimanual) [62]. Usage of 6 DOF place digitizer to direct an oppressed limb according to master-slave law with the bilateral therapy of a three DOF shoulder – elbow movement with a non-paretic arm. In active mode, patients must start activity and have to operate with a computer, while the robot performs resistance at active constraints to the patient's purpose [63]. Both modes of the device are illustrated in Figure 4 (e). Another end-effector based system so-called BI-MANU TRACK[64], it

was founded by Stefan Hesse as a community of researchers in Germany. This system is a computerized motorized arm trainer able to have two separate movement strategies for bilateral training: wrist flexion and extension and forearm pronation and supination. The Bi-Manu-Track provides repeated training in three realistic modes, as seen in Figure 4 (d). The active-passive mode follows the defective upper limb, while the less deficient upper limb pushes the handle. Both arms are operated by machines during the passive mode, while both arms actively exceed initial isometric resistance in active-active mode. The motions of this system may be parallel (antiphase) or reflective (in-phase). Several clinical trials have been done to determine the effectiveness of stroke patients in which the improvement in recovery has been observed [65], [66]. A system is known as NEREBOT [67], this system, utilizing a cable-driven mechanism to help stabilize and direct the victim's forearms during treatment to guide the physiotherapy treatments. This instrument enables three-dimensional rotation, pronation, and elbow flexion on a patient. This system can be seen in Figure 4 (j). The robot is built of manually adjustable wheels and overhead structures. It consists of three wires that power the shaft that the forearm rests on. In the learning process, the therapist shifts the arm through those particular system points while the control system generates interpolated paths for the motors during the process of therapy to render the movement comfortable and smooth [68]. An Additional device called ARM-GUIDE [69] was established at the Chicago Institute for Recovery by W. Zev Rymer. Assisted Rehabilitation and Measurement (ARM)-Guide directs the scope and tests the range of the arm motion, targets irregular situations and spastic reflections. The unit is a linear limit, which is fitted with a six-axis load cell and an optical encoder. In addition, a computer-operated torque motor is used in the system to use pressures or regulated motions in the arm around the linear limit. The unit may

be positioned vertically in various directions. A wood cone wrapps the wrist and a splint is applied to the forearm. The calculation is accomplished by the optical encoder and force measurement by the six-load cell between linear restriction and splint. [70], [71]. One more device termed ARMIN [72], ARMin is a grounded semi-exoskeleton device composed of a 6-DOF unit whereby 4 are responsive, and others are inactive and used for complete arm recovery. The orthotic shell may be moved from left to right limbs to rehabilitate all extremities. The personalization function is used according to the duration and range of the patient's arm. Without support, a patient will shift his arm to the target, and Armin can direct you if the action cannot be identified. It is also used for many case studies of the augmented reality framework [73].

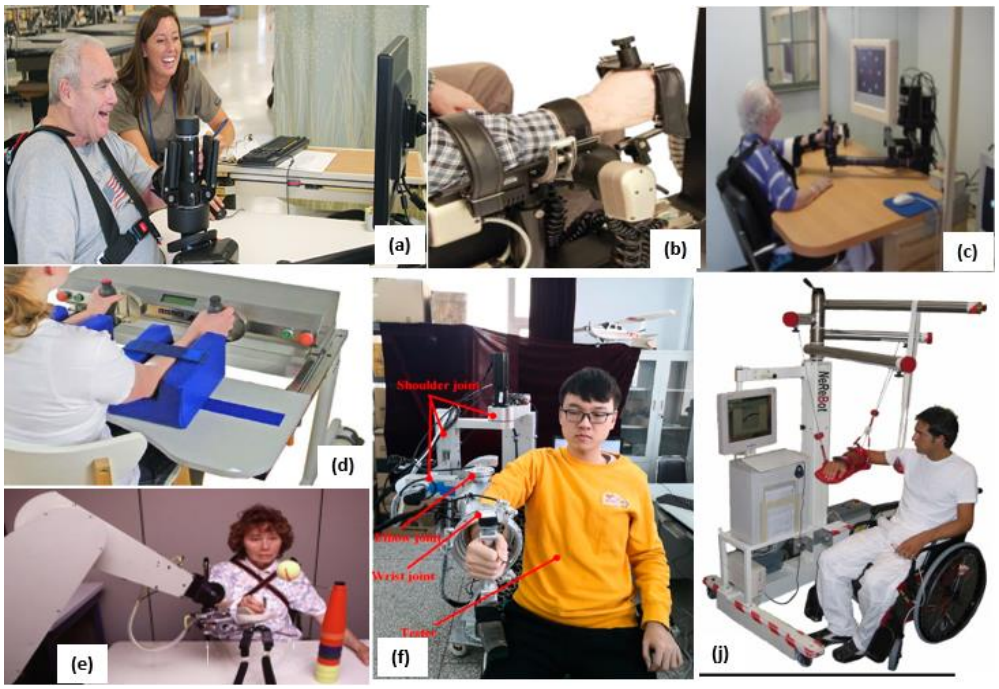

Figure 4: End-Effector devices in literature

(a): In Motion Arm (b): In Motion Wrist (c): MIT-MANUS (d): Bi-Manu-Track (e): Unilateral MIME

Exoskeleton Devices

Generally, exoskeleton-based robots are more complex and end-effector-based because the exoskeleton-based robots are designed to actuate each individual joint and parallelly integrate with the bone skeleton of the target joint. But since the human hand is a complicated system, exoskeleton-based robots must comply with this complexity. The exoskeleton-based structure can be split into grounded and ungrounded. exoskeleton-based devices have an exterior mechanism that permits them to be Freestanding is known as grounded exoskeleton devices. They can be changed in length, fitness and comfort. The approach of adaptation in the grounded exoskeleton facilitates completion of the task since ungrounded exoskeleton and end-effector equipment lack this element. The therapy is extremely effective since it targets the whole arm like hand and various joints. In this sense, researchers analyse the greater range of motion (ROM) and fine motor function more intensively [74]. a distinctive exoskeleton-based device called Kawasaki [75], supports 18 DOF and uses 22 Servo motors. RUPERT IV [76], with 5 DOFs, is another exoskeleton-based device. Lambercy [77] also uses two DC brushed engines and provides a 2 DOF unit named the Haptic Knob. Another typical example of a grounded-exoskeleton device that is commercially available, known as the hand of hope [78], shown in Figure 5 (b), which is driven by five linear actuators. Another example presented in [50], the authors developed a portable mechatronic exoskeleton device focused on active and passive single-finger recovery regulation approaches. This system is powered by an Android smartphone application by a Field Programmable Gate Array (FPGA). They have a parallel process operated by a pinion and rack device (SPRM). The approach developed is a compact mechatronic device using a DC motor. Using a hand exoskeleton module that is attached to the patient's arm, the authors employed a rear module that links the hand exoskeleton configuration of the

Bowden cord. As shown in Figure 5 (c). In [51], the authors developed a parallel wrist rehabilitation robot (PWRR), Appropriate mainly for hypertonic, stroke or wrist wounds. The proposed approach is focused on an end-effector structure that continuously trains the rehabilitation of the wrist joints, consisting of two rotational DOFs for wrist F/E and R/U movements. Two pneumatic actuators power the proposed PWRR to transfer the movement to the wrist R/U and F/E joints, respectively. As shown in Figure 5 (d). Moreover, other examples of grounded-exoskeleton-based devices are discussed as follows. Another exoskeleton-based system termed HWARD [79], which is a Hand-wrist assisting device. HOWARD perform 3 DOFs which can switch and extend thumb and fingers, as seen in Figure 5 (e), to a broad range of motion. The palm side may be adjoined to the dorsal side for a tactile sensation of objects in real-time, of varying sizes and shapes of hand. The treatment may be pushed out, thereby working with reduced friction in a passive state. The patient can wave his hand easily and can measure arm motions in kinematics. This device can produce a force of up to 122.8 N and can be regulated to 4-15 N. It has an emergency shutdown and hyperextension avoidance feature [80]. A device called PUREFORM, which is a haptic exoskeleton built to provide power feedback to the index finger and thumb as seen in the figure Figure 5 (f), this system performs 6 DOFs, the relation between the forearm and an external grounding unit facilitates weight reduction and offers power for haptic input while at the same time gathering the data for the arm location. It is especially used for exploring, orienting, and forming artefacts [81]. While a system labelled HIRO III [82], it is a five-finger haptic instrument positioned before the hand on the table, and with passive magnetic joints, the fingers are connected as opposed to being behind the hand. Without ever losing the connection to the machine through helping magnetic joints, the fingers may be arranged in various ways. Each finger has 3 DOF and three actuated motors

for a total of 1five DOF. For all fingers, flexion-extension, and abduction-abduction, it allows 3-dimensional force for up to 3.6 N. The machine contains six DOF arm interfaces and motors, allowing for up to 56 N of force along with an additional working area for the trunk, shoulder training abduction-abduction, flexion-extension and internal-external rotation as shown in Figure 5 (j) [80]. Another exoskeleton-based system known as MAHI EXO II [83], it is considered as a second-generation exoskeleton. It has 5 DOF, three of them are for the wrist, one for forearm and other for the elbow. The workspace is aiming the complete range of motion of the healthy individual due to the 3 revolute-prismatic-spherical (RPS) and revolute joints platform for the wrist. It can be worn by the left or right arm. There are two fittings for the various sizes of hands and handicaps, it also has flexible braces to accommodate the size of the bicep. This device has three approaches of therapy: triggered, active-constrained, and passive which augments the individualization of therapy [84]. Whereas RICE WRIST [85], is grounded haptic exoskeleton is the amalgamation of the wrist structure of Mahi Exo II and MIME end-effector device. It is primarily crafted by targeting the forearm, wrist, and angle of coliptic joints for enhanced hand use. The user can reproduce the natural movement by the support of the RPS platform, forearm joints, and inverse kinematics. The Rice Wrist can control the force feedback integrated with the virtual reality system, which enhances the rehabilitation process [82]. An example for both the devices is given in Figure 5 (h). Another commercially available product called MEASTRA HAND AND WRIST [86], Several commercial robotics deliver constant passive motions (CPM) of the hand to avoid the formation of joints stiffness. Hand CPM technology comprises devices that can be attached with braces to the hand and to the wrist and attached to the fingertips with differing portability. Most machines can shift the fingers passively, lift them to open their hands and switch the action

around. However, these devices are not ideally designed for spasticity patients and cannot train active finger motions, and most Hand CPM devices do not include training for the thumb Figure 5 (k).

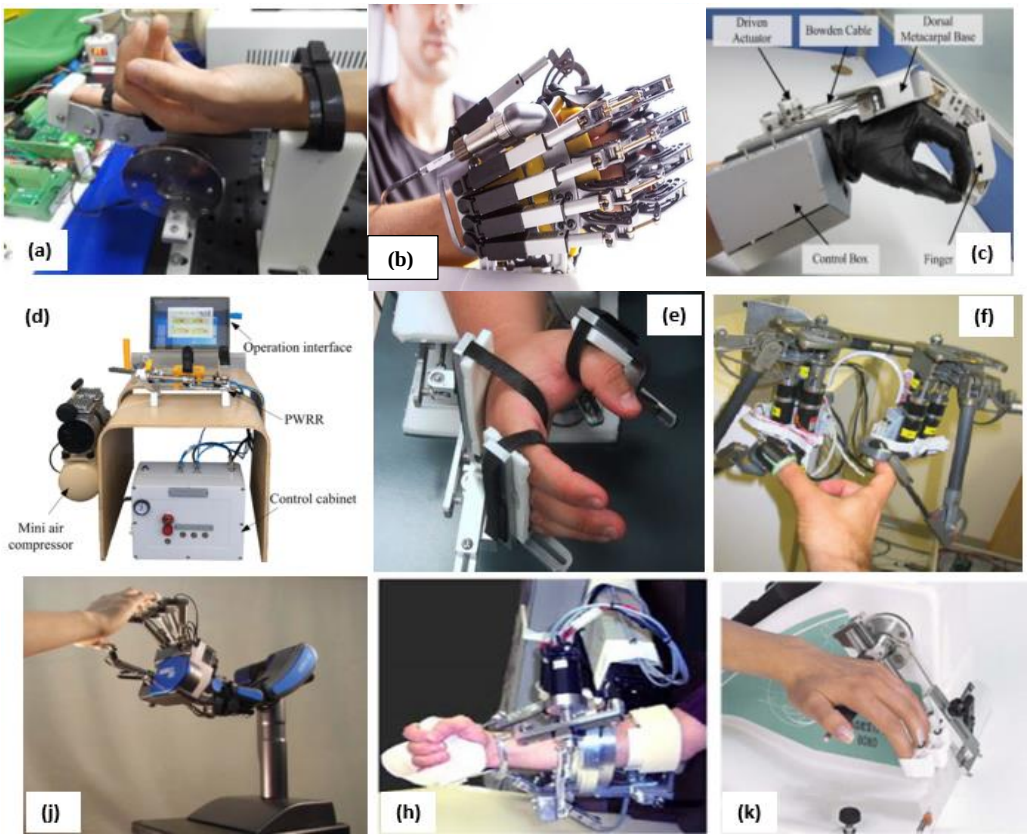

Figure 5: a group of rehabilitation devices based on grounded-exoskeleton-based

2.5.2. Assistive mode types

The therapeutic devices may be categorized into a different group based on the assistive mode that they can provide to the patient's limb. The assistive mode types can be listed below.

- **Passive assistive motion** Rehabilitation programs are more commonly reported. In contrast, passive support systems can control the activity of the patient's limb. Certain devices are only appropriate for persons

with strokes that can raise their limbs; Consequently, these devices also need not be powered by an actuator [87], [88]. Passive devices thus usually consume fewer energy than active devices and are lighter in weight [89].

- **AAM devices** equipped with the actuation unit, one of the most used actuators in robotic systems for neurorehabilitation, is electric motors [90]. AAM device is used to move patient limbs continuously; They are best used where basic ADL gestures cannot be carried out. However, certain active devices treat the end-user initiative as passive; The end-user stays inactive in operation as the system pushes the integrated joint dynamically. These systems help guide and guarantee that the patient's limb follows the planned workspace trajectory by providing continuous passive motion (CPM) [89].
- **Interactive Assistive mode:** The patient is shown a scenario or game, and the patient provides feedback on its output using voice, picture, touch, and other sensory equipment. This setting will increase the complexity of the game as the patient gets better. This reveals that the rehab program has been designed specifically to work around the patient's current constraints. Passive or active software can be used in conjunction with this mode if system sensors and actuators support it.
- **CPM** machines are among the most widely quoted therapy approaches assisted by the therapeutic exoskeletons produced. Early recovery of muscle contractures is helpful through the passive mode. In comparison to the current exoskeletons in literature, the CPM machine was beneficial in the initial level. Improving the range of motions, movement and grab the ability of the neurorehabilitation robotics for wrist or finger dependent on CPMs was indicated to be significant in number. In addition, they are the industry's most common technology

to boost motor sensory incapacity for upper limbs. In the market commercial, CPM-based development can be found [54], [65], [72], [86], [91], [92]. The most highly developed existing commercial products are Amadeo, Tyromotion [54], which is focused on the concept of a end-effector that trains five fingers for each hand using an electrical generator. Another popular CPM machine developed by MEASTRA [86], this system targets the fingers and wrist. Another commercially available Hand Mentor TM, Kinematic Muscles [92], Is a wearable orthosis that uses the wrist and four digits with a pneumatic actuator. Inventions are also available for healing, publication and experiments in academic laboratories, targeting upper limbs and more precisely for finger and wrist capture, which is not available on the market. AMES, Cordo [93], is a stationary system that supports one DOF; both [55], [93] use electric actuator and train both fingers and wrist. Another Stationary system called HWARD, Takahashi [79] supports 3 DOF and uses three Pneumatic actuators. While Hasegawa [94] is a grasp assistance device that uses 11 DC motors and supports 11 DOF. A recently published robot-looks called EULRR [95], uses two commercial manipulators, each manipulator's hand 7 DOF.

2.5.3. Actuator Types

An actuator is a device or portion of a machine that transmits energy to regulate and control the movement of a system. Generally, the assist robot for hand and wrist rehabilitation is designed to aid the user by guiding the fingers to do active tasks. It is possible to create a particular type of movement with a variety of actuators. There are mainly six types of actuators in hand recovery models: electrical, hydraulic, pneumatic, pneumatic artificial muscle, series elastic, and functional electrical stimulation. Electric DC Motors Electric motor is an actuator that uses voltage and current to generate mechanical

torque and regulator velocity. They are the most frequent form of actuator used to actuate the assist-robot since they are easy and quick to regulate, and widely available in the market. However, there are several different types of electric actuators, and these actuators are capable of providing both linear and rotational movements.. Using brushed motors, rotational motion can be accomplished [50] [94] [96]–[101], or brushless motors. To provide linear movement, linear DC motors are used [78] [102]–[106] DC motors that can have their axes rotated or motors with linear trackers [107]–[109][42], [46]. rotary or linear Servo motors often used in rehabilitation robotics [110], [111, p.], [112], [113]. They performed high torque, energy-efficient, they self-contain of position close-loop, and accurate position control. A further variety of actuator is the pneumatic actuator, which utilizes pneumatic cylinders and pneumatic cylinders to regulate the flow of hydraulic or air via compressors. [114], [115] and some uses an air balloons [116] , air bladder [117], soft actuation [118] [55] or pneumatic artificial muscles, often used in rehabilitation robotics [119, p. 1], [120]–[122]. Basically, their output is like a pneumatic push, Basically, they are a special pneumatic actuator type, an internal bladder with flexible non-extensible threaded mesh shell [89]. At minimal cost, they are capable of high power and speed adjustments. Remotely controlled exoskeletons might manage the capacity of the compressor because of the compressor's capacity.

Chapter 3: Case study and system design Requirements

3.1. Introduction

To ensure that the proposed system meets its technological and clinical requirements, as the mechanical design concern, this thesis presents a new design and development of a cost-efficient Fingers and Wrist Rehabilitation Mechatronic System Concerning the mechanical structure. The proposed system combines a grounded exoskeleton and end-effector structures to repeatable, active, passive, interactive, and continuous passive motion for either hand left or right. The stroke patients' hand recovery is based on moving their impaired hand with the help of proper training and exercises, as already discussed in chapter 2. However, this section will clarify more specifically about the movement of the hand, which is presented with the collaboration of neurologists. The proposed system performs four basic movements of the hand, which illustrated in Figure 6; the targeted joints movement are including one fingers flexion/ Extension (F/E); two wrist movements, flexion/ Extension (F/E), and Wrist Radial/ulnar (R/U), deviation; forearm pronation/supination (P/S). These motions are critical for conducting activities of daily living (ADL) as instructed by therapists. The supination/pronation and dorsiflexion are considered for grasping an object [123], whereas fine finger movements are used for smaller objects. The fingers are flexed caused to extensor muscular weakness, and patients are incapable of releasing or manipulating their hands. Therefore, it is mandatory that the rehabilitation device should train initially to the finger extension and afterwards, finger flexion training will strengthen the weak muscles [124]. to obtain that goal, several designs were made, tested and evaluated. However, in the designing phase, the first step towards developing hand and wrist orthosis for the purpose of rehabilitation is to analyse targeted joints specific anatomical and mechanical constraints such as structural shape, power, and since our study and primary

objective to develop hand and wrist rehabilitation system for the upper limb disabilities. Therefore, it is crucial to understand the technical and clinical requirements. In the progressive stage of rehabilitation, the training and measurements of the independence of the finger movements are significant and to clearly understand the devices' mechanism according to the patient's desired therapy.

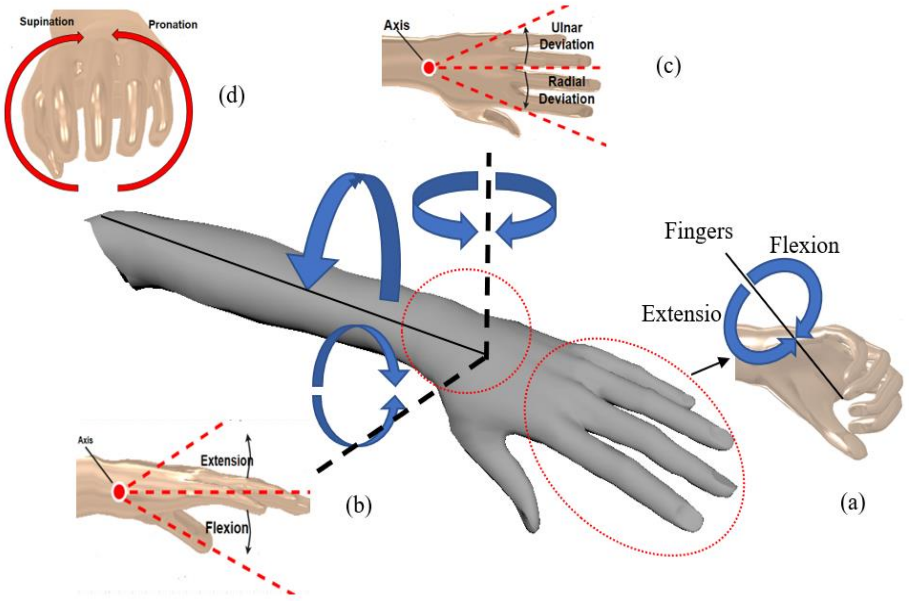

Figure 6: Human Hand Motion (DOF)

3.2. Essential Clinical Requirements and Considerations

From the designers' and therapists' perspective, some clinical and technical criteria should be considered when designing a mechatronics system that interacts with humans. It is essential to integrate the motor-learning standards and practice in any neurorehabilitation assistive design. Health considerations still need to be considered in the design process of the assistive-robots rehabilitation system. Since, in some cases, the fingers are flexed because of the muscular weakness of the extender. At any rate, both the therapist and the patients should psychologically accept the rehabilitation robot [87]. Surly, in

a robotic-assisted therapy exercise, safety is critical in the recovery process. Since the therapist usually determines and schedules the rehabilitation process and sessions. The therapist is the vital factor in the recovery process; in fact, the rehabilitation robotics advancement should help the therapist (first-user) to support the patients (end-user) in the treatment period; thus, the therapist should control the force between the robot's end-effector and the extremity affected. During the development of the rehabilitation device, systematic analysis is considered to identify design considerations and critical issues. Concerning the different kinds of hand difficulties, the various rehabilitation guidelines suggested by the number of researchers are considered. Different possible outcomes of these rehabilitation guidelines could arise if they are applied to rehabilitative equipment, which is considered as:

- Complexity of Hand movements: Understating the required level of therapy for the patient may include basic movements of the fingers necessary for ADL, grasping of an object, pinching precision, etc.
- Rehabilitation Environment: Focusing on the real surroundings that consists of the therapist or assistance sometimes required when using the devices or Virtual reality (VR), which includes simulator and software configuration for enhancing motor learning and even helps boost the motivation level of the patient.
- complexity of exercises: Simple training and strenuous activities help define the sort of exercise for developing finger mobility, while strenuous and rigorous workouts can restore control of hand movements.

Mostly the overall structure of the robotic system strictly depends on these categories. .

3.2.1. Design Technical Specifications

According to the literature survey and available rehabilitation modules, some common characteristics and other specific concerns about the mechanical design, electronic system and control strategy. Probably the best possible device is not available, mainly because the rules for system design and operation have not been determined, as the system is quite complicated and every change needs to be considered.". The designer of rehabilitation devices has to go through several choices, like Degree of Freedom (DOFs), transmission mechanism, control and architecture etc. However, the design objectives depend upon the designer's experience and issues recognised on the project goals to be achieved and the target market.

Additionally, based on the affected limbs' functionality and mobility, the therapist must regulate the ROMs, motion Speed, and the device's repetition times towards the patient's limbs. The designer must consider the anatomy of the targeted limbs, the number of DOFs created by these limbs, ROMs' limitations, and the forces needed to move them.

Moreover, particular concerns about the external mechanical structure, such as the exoskeleton fingertip's attachments of the rehabilitation robot that directly integrate with different patients' limbs, should be non-toxic material and serializable material. However, it would be worthwhile if they are removable and replaceable in winding up. The set-up should quickly and effortlessly fix the patient's arms without hurting them, and it can be fit for different hand sizes. Also, the device must move in a manner similar to that of the human fingers in their natural range of motion (ROM). Other than that, human hand shapes and adaptability should be considered a critical and mandatory requirement so that many patients must use the device. The device must be capable enough to be slightly modified, which can be done by implementing compliant connections or passive joints.

3.3. Biomechanical Constraints Based on the Case Study: (Parameterization)

To identify the hand kinematics and associated trajectories for investigating the appropriate required data to make the target device, it was difficult to find the reference values from the literature analysis due to the inconsistency of data. For this purpose and to satisfy the design concerns as it is the first step towards the objective, the case study is being conducted on the stroke patients currently getting treatment from the Clinic of the University of Debrecen. By the guidelines of the rehabilitation department and their assistance, we made measurements of hand kinematics for making the reference values of our device.

3.3.1. Problem Study

The study is seeking to investigate and determine the level of the impact that the strokes can cause to the hand and wrist movements and force and be able to select the right specifications to the planned device, such as the torque value that will be induced by the proposed system towards the patient's fingers. The feasibility study is based on the scales given for Range of Motion (ROM) for measuring the patients impaired and unimpaired hand range of motion and Modified Ashworth Scale (MAS) for obtaining the wrist and finger spasticity. These values are used as a reference for our CPM device to be designed and programmed according to the desired therapies for the patients to retaliate their motor skills. The measurements are taken in the Clinic of the University of Debrecen as illustrated in Figure 7 and Figure 8.

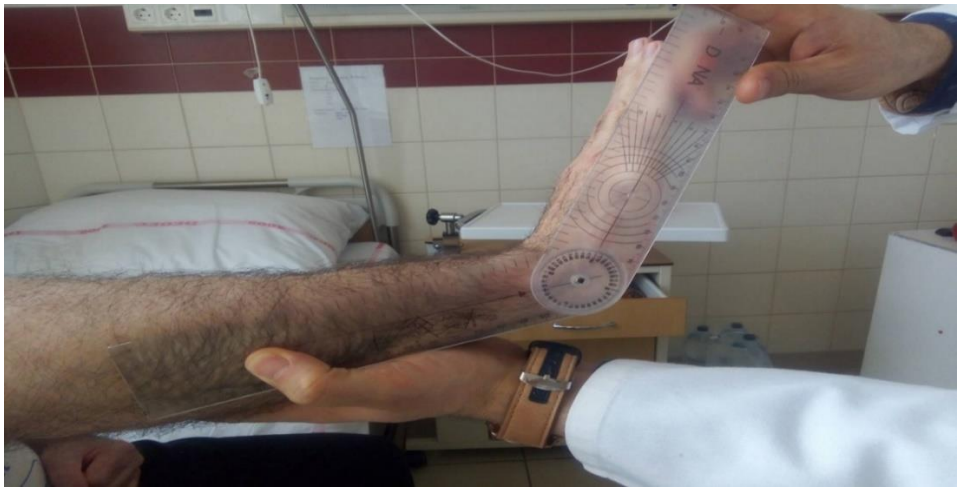

Figure 7: Measuring the Extension of the wrist of stroke patient by the Goniometer provided by the Rehabilitation Department

Figure 8: Measuring the patient's upper limb

(a): Obtaining the individual finger force of the stroke patient's impaired hand (b): The actual position of the patient to get the therapy by the CPM

Table 3 illustrates the study done on stroke patients' impaired hands in the rehabilitation department of the University of Debrecen Clinic, where ten stroke patients' have been observed and their data associated with each finger (Index, Middle, Ring, Little), thumb and wrist have been measured by the

weighing scale. The data for MCP-PIP, PIP-DIP and DIP-Tip is highlighted for each finger along with the calculated average. In contrast, wrist angle dorsiflexion (UP), palmer flexion (DOWN), radial deviation (LEFT) and ulnar deviation (RIGHT) is measured in degrees. The spasticity of the wrist and fingers is graded by the Modified Ashworth Scale (MAS) [125]; this six-fold scale ranges from 0 (No Spasticity) to 4 (fixed muscle contracture).

Table 3: Measured grabbing force (the unit of the values is Kg) and ROM values of the fingers of Impaired hand and Wrist

	Sub 1	**Sub 2**	**Sub 3**	**Sub 4**	**Sub 5**	**Sub 6**	**Sub 7**	**Sub 8**	**Sub 9**	**Sub 10**
					Index Finger					
MCP-PIP	0.41	0.47	0.10	0.12	0.10	0.13	0.03	0.01	0.13	0.05
PIP-DIP	0.21	0.22	0.11	0.12	0.11	0.16	0.10	0.07	0.17	0.09
DIP-Tip	0.41	0.20	0.12	0.13	0.12	0.10	0.09	0.07	0.14	0.08
Average	0.34	0.29	0.11	0.12	0.11	0.13	0.07	0.05	0.14	0.07
					Middle Finger					
MCP-PIP	0.60	0.25	0.11	0.14	0.05	0.08	0.10	0.01	0.11	0.10
PIP-DIP	0.31	0.25	0.11	0.13	0.05	0.12	0.10	0.08	0.14	0.08
DIP-Tip	0.60	0.12	0.13	0.13	0.02	0.11	0.09	0.05	0.19	0.10
Average	0.50	0.20	0.11	0.13	0.04	0.10	0.09	0.04	0.14	0.09
					Ring Finger					
MCP-PIP	0.50	0.32	0.13	0.12	0.11	0.18	0.06	0.02	0.09	0.10
PIP-DIP	0.41	0.26	0.10	0.03	0.10	0.17	0.10	0.03	0.10	0.12
DIP-Tip	0.49	0.22	0.11	0.09	0.10	0.16	0.08	0.05	0.09	0.13
Average	0.46	0.26	0.11	0.08	0.10	0.17	0.08	0.03	0.09	0.11
					Little Finger					
MCP-PIP	0.30	0.12	0.10	0.11	0.14	0.11	0.10	0.03	0.16	0.09
PIP-DIP	0.30	0.14	0.10	0.02	0.10	0.17	0.09	0.06	0.14	0.10
DIP-Tip	0.42	0.10	0.10	0.07	0.11	0.17	0.08	0.06	0.10	0.10
Average	0.34	0.12	0.1	0.06	0.11	0.15	0.09	0.05	0.13	0.09
					Thumb					
MCP-PIP	0.31	0.23	0.09	0.11	0.12	0.22	0.05	0.03		0.11
PIP-DIP	0.21	0.15	0.09	0.11	0.15	0.21	0.04	0.04		0.12
DIP-Tip	0.30	0.20	0.06	0.11	0.12	0.17	0.10	0.06		0.01
Average	0.27	0.19	0.08	0.11	0.13	0.20	0.06	0.04		0.08

					Wrist					
	MAS score of Wrist (0-4)	1	0	1		0	2	1	0	3	
	MAS score of Finger (0-4)	0	0	1		0	1+	0	0	2	
Wrist Angle (Degrees)	Up (Dorsiflexion)	12°	70°	50°	0°	60°	25°	12°	0°		3°
	Down (Palmer Flexion)	63°	100°	53°	80°	40°	77°	43°	80°	40°	70°
	Right (Ulnar Deviation)	3°	30°	25°	10°	40°	20°	30°	0°		31°
	Left (Radial Deviation)	6°	30°	30°	10°	30°	30°	20°	0°		12°

Table 4: Measured grabbing force (the unit of the values is Kg) and ROM values of the fingers of unimpaired hand and Wrist

	Sub 1	**Sub 2**	**Sub 3**	**Sub 4**	**Sub 5**	**Sub 6**	**Sub 7**	**Sub 8**	**Sub 9**	**Sub 10**
				Index Finger						
MCP-PIP	1.10	0.40	0.32	0.13	0.25	0.33	0.18	0.09	0.20	0.24
PIP-DIP	1.07	0.67	0.29	0.23	0.26	0.33	0.20	0.12	0.22	0.21
DIP-Tip	1.28	0.69	0.29	0.17	0.25	0.30	0.24	0.15	0.22	0.22
Average	1.15	0.58	0.30	0.17	0.25	0.32	0.20	0.12	0.21	0.22
				Middle Finger						
MCP-PIP	1.28	0.53	0.21	0.10	0.20	3.87	0.37	0.11	0.25	0.21
PIP-DIP	1.18	0.62	0.25	0.24	0.16	0.31	0.20	0.16	0.26	0.26
DIP-Tip	1.38	0.67	0.29	0.12	0.18	0.30	0.23	0.18	0.26	0.19
Average	1.28	0.60	0.25	0.15	0.18	1.49	0.26	0.15	0.25	0.22
				Ring Finger						
MCP-PIP	1.18	0.60	0.20	0.10	0.20	0.35	0.19	0.16	0.27	0.33
PIP-DIP	1.08	0.62	0.27	0.24	0.18	0.32	0.23	0.17	0.25	0.29
DIP-Tip	1.31	0.50	0.30	0.10	0.10	0.30	0.23	0.13	0.25	0.25
Average	1.19	0.57	0.25	0.14	0.16	0.32	0.21	0.15	0.25	0.29
				Little Finger						
MCP-PIP	0.99	0.50	0.30	0.13	0.10	0.37	0.19	0.14	0.20	0.20

PIP-DIP	0.99	0.47	0.30	0.20	0.16	0.30	0.22	0.19	0.25	0.20
DIP-Tip	1.29	0.61	0.30	0.11	0.21	0.31	0.21	0.18	0.23	0.22
Average	1.09	0.52	0.3	0.14	0.15	0.32	0.20	0.17	0.22	0.20
				Thumb						
MCP-PIP	0.69	0.43	0.32	0.17	0.21	0.34	0.20	0.15	0.32	0.20
PIP-DIP	0.68	0.50	0.23	0.26	0.20	0.40	0.22	0.20	0.30	0.22
DIP-Tip	0.60	0.50	0.28	0.20	0.25	0.30	0.27	0.20	0.30	0.20
Average	0.65	0.47	0.27	0.21	0.22	0.34	0.23	0.18	0.30	0.20
				Wrist						
MAS score of Wrist (0-4)	0	0	0	0	0	0	0	0	0	0
MAS score of Finger (0-4)	0	0	0	0	0	0	0	0	0	0
Wrist Angle (Degrees) Up (Dorsiflexion)	55°	110°	63°	80°	50°	30°	15°	16°	62°	72°
Down (Palmer Flexion)	110°	70°	70°	80°	70°	80°	20°	83°	70°	90°
Right (Ulnar Deviation)	33°	50°	53°	30°	55°	30°	40°	20°	34°	40°
Left (Radial Deviation)	33°	52°	42°	30°	54°	24°	19°	13°	20°	40°

For better analysis of our design objective, the unimpaired hand of the same patients has been observed and measured, as shown in Table 4. An overview has been given in the form of bar graph for better understanding the individual measurement of stroke patients, specifically for their impaired and unimpaired hand, as shown in Figure 9 and Figure 9.

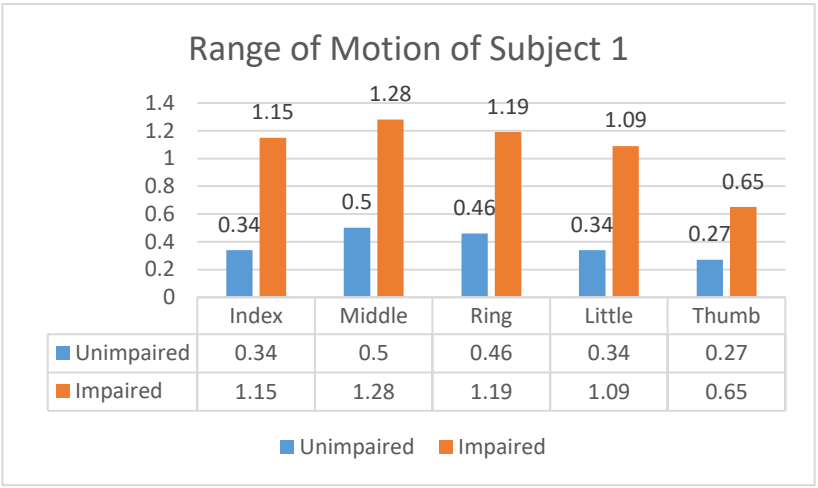

Figure 9: Measured grabbing force values (the unit of the values is Kg) of the impaired and unimpaired hand of Subject 1

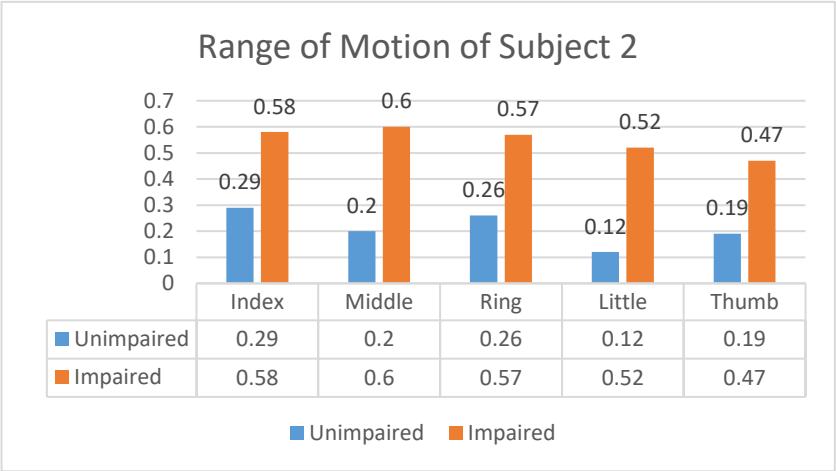

Figure 10: Measured grabbing force values (the unit of the values is Kg) of the impaired and unimpaired hand of Subject 2

Chapter 4: Human finger kinematic Model and Finger's Trajectory determining

4.1. Background

To design a rehabilitation device, it is needed to deeply understand all the characteristics of the human hand to develop a mechanism interacting it; hence, the human hand kinematics analyses of the hand movement configurations is needed so that a robotic system could be able to mimic its natural movement. These models are relevant in numerous disciplines, and because of that, the use of these models is quite active in scientific study. The diversity of existing hand kinematic models[126]–[128]. However, the human hand has many DoF compacted within a much smaller region, making it a tough challenge to simulate. In short, it's conceivable to employ mechanical theories to examine the hand [129]. The hand consists of two components: muscles. The muscle and joints function as an actuator, which transfers force and motion to other muscles, tendons, bones, and joints [131] and. We can consider the human hand as a rigid body system that consists of three links. Kinematic models, in general, explain the motion of objects and systems in terms of position, direction, and acceleration without taking into account the factors that induce the movement.

In this section a 3D-dimensional kinematic model of hand finger model includes a single finger F/E. and the thumb F/E, and Ab/Ad. However, only the Index finger will be modelled for simplicity's sake since the index and pinkie, middle, and ring fingers follow the exact mechanism of flexing and extending. Additionally, the thumb will be modelled too, since the thumb has its own mechanism. These models will be simulated using MATLAB software and its plugin called Peter Corke pagcke.

4.2. Kinematics of a Single Finger

This section provides the Kinematic model of the index finger representation. The model equation is calculated utilizing Denavit-Hartenberg (DH). Figure 11, depicts the kinematic model of the hand as well as the coordinate frames. The structure shown in the kinematic model will be replicated in the proposed finger design as shown in Figure 12, with three links corresponding to the human finger phalanxes phalanges (distal, middle, and proximal phalanxes, respectively), and two active revolute joints (2DOF for each) and one Universal (2DOF). Which associate the finger Flexion/Extension (F/E) movement. Another factor to consider is that the metacarpophalangeal joint (middle knuckle) was also examined as it is fixed in contact with the wrist. Moreover, the parametric dates, such as the size of the proximal phalanx, medial phalanx, and the distal phalanx skeletons, were also employed to drive the D-H parameters. The designer's hand was used to estimate the modelled index finger.

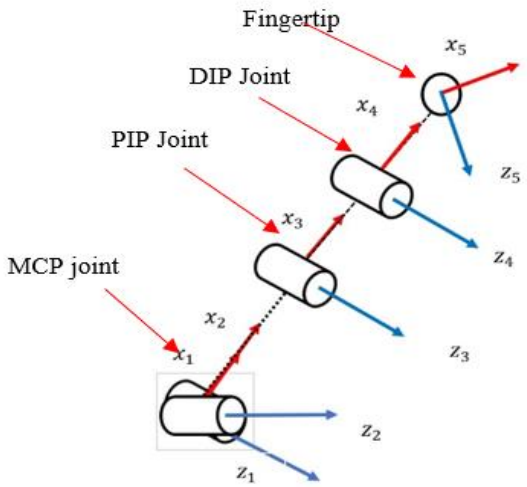

Figure 11: representation of the coordinate frame of the three-link index

To solve the kinematics, a theory of robotics was employed in conjunction with the theory of movement to describe four degrees of freedom in the index

finger [130]. Since each joint connects two links, an N-joint finger manipulator will have an N+1 link. Whereas the link was numbered from 0 to n starting from the base, the joint was numbered from 1 to n. Thus, the joint I links link i-1 to link I, and joint i-1 moves link i. Link 0, the first link, cannot move while the joint is activated since it is attached to the ground.

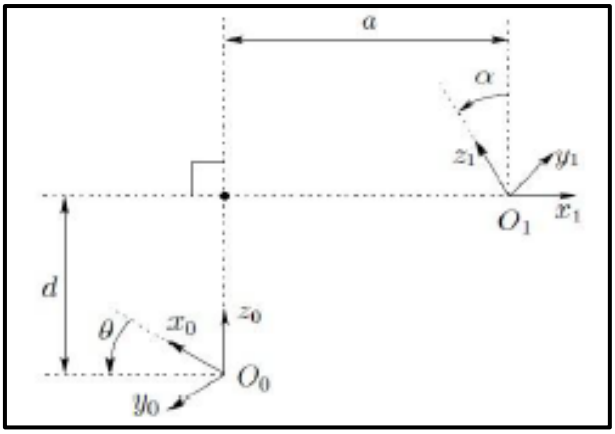

Figure 12: DH Frame Assignment

Ti can get depend on four primary transformations:

$$T_i = Rot(z,\theta_i)\ Trans(z,d_i)Trans(x,a_i)Rot(x,\alpha_i) \qquad Eq\ 1$$

So from Eq 1, we can transfer from i frame to i+1 frame

$Rot(x,\alpha_i)$: Rotation around x axes a_i angle.

$Trans(x,a_i)$: Transformation x axes a_i angle.

$Rot(z,\theta_i)$: Rotation around z axes θ_i angle.

$Trans(z,d_i)$: Transformation z axes d_i angle.

T_i The final matrix will be the result of multiple of those matrixes.

$$T_i = \begin{bmatrix} c_{\theta i} & -s_{\theta i} & 0 & 0 \\ s_{\theta i} & c_{\theta i} & 0 & 0 \\ 0 & 0 & 1 & 0 \\ 0 & 0 & 0 & 1 \end{bmatrix} \cdot \begin{bmatrix} 1 & 0 & 0 & 0 \\ 0 & 1 & 0 & 0 \\ 0 & 0 & 1 & d_i \\ 0 & 0 & 0 & 1 \end{bmatrix} \cdot \begin{bmatrix} 1 & 0 & 0 & a_i \\ 0 & 1 & 0 & 0 \\ 0 & 0 & 1 & 0 \\ 0 & 0 & 0 & 1 \end{bmatrix} \cdot \begin{bmatrix} 1 & 0 & 0 & 0 \\ 0 & c_{\alpha i} & -s_{\alpha i} & 0 \\ 0 & s_{\alpha i} & c_{\alpha i} & 0 \\ 0 & 0 & 0 & 1 \end{bmatrix}$$

$$T_i = \begin{bmatrix} c_{\theta i} & -s_{\theta i}c_{\alpha i} & s_{\theta i}s_{\alpha i} & a_i c_{\theta i} \\ s_{\theta i} & c_{\theta i}c_{\alpha i} & -c_{\theta i}s_{\alpha i} & a_i s_{\alpha i} \\ 0 & s_{\alpha i} & c_{\alpha i} & d_i \\ 0 & 0 & 0 & 1 \end{bmatrix} \qquad Eq\ 2$$

From Eq 2 $\alpha_i, \theta_i, d_i, a_i$

a_i: The distance between z_i to z_{i+1} along the x_i axis.

α_i: The angle between z_i to z_{i+1} about x_i axis.

d_i: The distance between x_i to x_{i+1} along the z_i axis.

θ_i: The angle between x_i to x_{i+1} about z_i axis.

4.2.1. Homogeneous transformation

$$H = Rot_{x,\alpha}\ \ Trans_{x,a}\ Trans_{\ z,d}\ Rot_{z,\theta}$$

The homogeneous transformation H can be driven throughout rotate α angle about α axis, then translation among x axis then translation among z axis, and finally rotate θ angles about z axis.

$$H = \begin{bmatrix} c_\theta & -s_\theta & 0 & a \\ c_\alpha s_\theta & c_\theta c_\alpha & -s_\alpha & -ds_\alpha \\ s_\alpha s_\theta & s_\alpha c_\theta & c_\alpha & dc_\alpha \\ 0 & 0 & 0 & 1 \end{bmatrix} \qquad Eq\ 3$$

The homogeneous that is given by this matrix is a special status and to generalize it. It should be taken into consideration that the Scale Factor= 1 and Perspective Transformation=[0 0 0].

So, the final matrix will be

$$H = \begin{bmatrix} R_{3x3} & d_{3x1} \\ f_{1x3} & S_{1x1} \end{bmatrix} = \begin{bmatrix} Rotation & Translation \\ Perspective & Scale\ factor \end{bmatrix}$$

$$H = \begin{bmatrix} \mu_x & O_x & \alpha_x & p_x \\ \mu_y & O_y & \alpha_y & p_y \\ \mu_z & O_z & \alpha_z & p_z \\ 0 & 0 & 0 & 1 \end{bmatrix}$$

Then, forward kinematics are given by multiply all transforming matrixes together

$$T_i^j = T_{j+1}^j \dots\dots T_i^{i-1} \qquad Eq\ 4$$

We will use homogeneous transformation T_i^{i-1} which transfer us from i frame to i-1 frame.

$$T_i^{i-1} = T_i^{i-1}(q_i)$$

Depending on previous equation, the matrix $T_i^j (i > j)$

Will transfer us from i frame to j frame given by

$$T_n^0 = \begin{bmatrix} R_n^0 & d_n^0 \\ 0 & 1 \end{bmatrix}$$

the position and direction for the end-effector given by

$$T_n^0(q_1, q_2, \dots, q_n) = T_1^0\ (q_1).T_2^1(q_2).\dots.T_n^{n-1}(q_n)$$

$$T_i^j = T_{j+1}^j \dots T_i^{i-1} = \begin{bmatrix} R_i^j & d_i^j \\ 0 & 1 \end{bmatrix}$$

The following Table below show the derived D-H convention parameters used to create the index finger model; these parameters allow for obtaining the forward kinematics model.

Table 5: DH Parameters (Index finger)

i	θ_{i-1}	d_{i-1}	a_i	α_i
1	θ_1	0	*L*0	0
2	θ_2	0	0	90°
3	θ_3	0	L1	90°
4	θ_4	0	L2	0
5	0	0	L3	0

4.2.2. Hand Kinematic: Forward kinematics

For hand kinematics, we study only the forward kinematics since it is enough for this thesis and project scope. Generally, the difficulty is with the forward kinematics of the robot manipulator and how the tool or end-effector positions and orientations. In other words, the forward kinematics model shows the fingertip positions and orientations once the model provides the known or estimated angles of the finger joints ($\theta_1 . . . \theta_5$). Which are referred to as global coordinates.

Where

a_i: The distance between z_i to z_{i+1} along the x_i Axis.

α_i: The angle between z_i to z_{i+1} about x_i axis.

d_i: The distance between x_i to x_{i+1} along the z_i Axis.

θ_i: The angle between x_i to x_{i+1} about z_i axis.

But applying eq3 and eq4 the matrix for each link

$$A1 = T_1^0 = \begin{bmatrix} cos\,(th1) & -sin\,(th1) & 0 & L0 * cos(th1) \\ sin\,(th1) & cos\,(th1) & 0 & L0 * sin(th1) \\ 0 & 0 & 1 & 0 \\ 0 & 0 & 0 & 1 \end{bmatrix} \quad Eq\ 5$$

$$A2 = T_2^1 = \begin{bmatrix} cos\,(th2) & 0 & sin\,(th2) & 0 \\ sin\,(th2) & 0 & -cos\,(th2) & 0 \\ 0 & 1 & 0 & 0 \\ 0 & 0 & 0 & 1 \end{bmatrix} \quad Eq\ 6$$

$$A3 = T_3^2 = \begin{bmatrix} cos\,(th3) & 0 & sin\,(th3) & L1 * cos(th3) \\ sin\,(th3) & 0 & -cos\,(th3) & L1 * sin(th3) \\ 0 & 1 & 0 & 0 \\ 0 & 0 & 0 & 1 \end{bmatrix} \quad Eq\ 7$$

$$A4 = T_4^3 = \begin{bmatrix} cos\ (th4) & -sin\ (th4) & 0 & L2 * cos(th4) \\ sin\ (th4) & cos\ (th4) & 0 & L2 * sin(th4) \\ 0 & 0 & 1 & 0 \\ 0 & 0 & 0 & 1 \end{bmatrix} \qquad Eq\ 8$$

$$A5 = T_5^4 = \begin{bmatrix} cos\ (th5) & -sin\ (th5) & 0 & L3 * cos(th5) \\ sin\ (th5) & cos\ (th5) & 0 & L3 * sin(th5) \\ 0 & 0 & 1 & 0 \\ 0 & 0 & 0 & 1 \end{bmatrix} \qquad Eq\ 9$$

Forward kinematics is given by multiply all the transform matrixes (Eq 5, 6, 7, 8, and 9) together, which represent a homogenous matrix as shown in Eq 10

$$T_5^0 = T_1^0 . T_2^1 . T_3^2 . T_4^3 . T_5^4 = \begin{bmatrix} \mu_x & O_x & \alpha_x & p_x \\ \mu_y & O_y & \alpha_y & p_y \\ \mu_z & O_z & \alpha_z & p_z \\ 0 & 0 & 0 & 1 \end{bmatrix} \qquad Eq\ 10$$

$$\mu_x = \cos(\text{th5}) * (\sin(\text{th1} + \text{th2}) * \sin(\text{th4}) + \cos(\text{th1} + \text{th2}) * \cos(\text{th3}) * \cos(\text{th4})) + \sin(\text{th5}) * (\sin(\text{th1} + \text{th2}) * \cos(\text{th4}) - \cos(\text{th1} + \text{th2}) * \cos(\text{th3}) * \sin(\text{th4}))$$

$$\mu_y = -\cos(\text{th5}) * (\cos(\text{th1} + \text{th2}) * \sin(\text{th4}) - \sin(\text{th1} + \text{th2}) * \cos(\text{th3}) * \cos(\text{th4})) - \sin(\text{th5}) * (\cos(\text{th1} + \text{th2}) * \cos(\text{th4}) + \sin(\text{th1} + \text{th2}) * \cos(\text{th3}) * \sin(\text{th4}))$$

$$\mu_z = cos(th4 + th5) * sin(th3)$$

$$O_x = cos(th5) * (sin(th1 + th2) * cos(th4) - cos(th1 + th2) * cos(th3) * sin(th4)) - sin(th5) * (sin(th1 + th2) * sin(th4) + cos(th1 + th2) * cos(th3) * cos(th4))$$

$$O_y = \sin(\text{th5}) * (\cos(\text{th1} + \text{th2}) * \sin(\text{th4}) - \sin(\text{th1} + \text{th2}) * \cos(\text{th3}) * \cos(\text{th4})) - \cos(\text{th5}) * (\cos(\text{th1} + \text{th2}) * \cos(\text{th4}) + \sin(\text{th1} + \text{th2}) * \cos(\text{th3}) * \sin(\text{th4}))$$

$$O_z = -\sin(\text{th4} + \text{th5}) * \sin(\text{th3})$$

$$a_x = \cos(\text{th1} + \text{th2}) * \sin(\text{th3})$$

$$a_y = \sin(\text{th1} + \text{th2}) * \sin(\text{th3})$$

$$a_z = -\cos(\text{th3})$$

$$p_x = L0 * cos(th1) + L1 * cos(th1 + th2) * cos(th3) + L2 * sin(th1 + th2) * sin(th4) + L3 * cos(th5) * (sin(th1 + th2) * sin(th4) + cos(th1 + th2) * cos(th3) * cos(th4)) + L3 * sin(th5) * (sin(th1 + th2) * cos(th4) - cos(th1 + th2) * cos(th3) * sin(th4)) + L2 * cos(th1 + th2) * cos(th3) * cos(th4)$$

Eq 11

Eq 11 repersent the ingertip Position on the x axis

$$p_y = L0 * sin(th1) + L1 * sin(th1 + th2) * cos(th3) - L2 * cos(th1 + th2) * sin(th4) - L3 * cos(th5) * (cos(th1 + th2) * sin(th4) - sin(th1 + th2) * cos(th3) * cos(th4)) - L3 * sin(th5) * (cos(th1 + th2) * cos(th4) + sin(th1 + th2) * cos(th3) * sin(th4)) + L2 * sin(th1 + th2) * cos(th3) * cos(th4)$$

Eq 12

Eq 12 repersent Fingertip Position on the y axis

$$p_z = d1 + L1 * sin(th3) + L2 * cos(th4) * sin(th3) + L3 * cos(th4) * cos(th5) * sin(th3) - L3 * sin(th3) * sin(th4) * sin(th5)$$

Eq 13

Eq 13 repersent Fingertip Position on the z axis

4.3. Thumb finger Kinematics modelling

Similarly, the forward kinematics configuration model for the thumb was obtained. From Figure 13, the proposed model considered the thumb as two links. And one active revolute joint (1 DOF for each) and one Universal joint (2DOF). Which associated the natural movements of the thumb including thumb F/E.

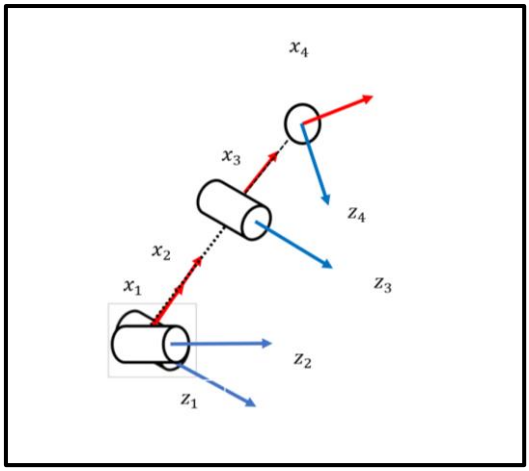

Figure 13: representation the coordinate frame of the two-link thumb

The following Table 6 below shows the derived DH parameters for the thumb by utilising the same index method.

Table 6: DH parameters for the Thumb finger

i	θ_{i-1}	d_{i-1}	a_i	α_i
1	θ_1	0	$L0$	0
2	θ_2	0	0	90°
3	θ_3	0	L1	0
4	θ_4	0	L2	0

These parameters allow for obtaining the forward kinematics model.

$$A1 = T_1^0 = \begin{bmatrix} cos\,(th1) & -sin\,(th1) & 0 & L0 * cos(th1) \\ sin\,(th1) & cos\,(th1) & 0 & L0 * sin(th1) \\ 0 & 0 & 1 & 0 \\ 0 & 0 & 0 & 1 \end{bmatrix} \quad \text{Eq 14}$$

$$A2 = T_2^1 = \begin{bmatrix} cos\,(th2) & 0 & sin\,(th2) & 0 \\ sin\,(th2) & 0 & -cos\,(th2) & 0 \\ 0 & 1 & 0 & 0 \\ 0 & 0 & 0 & 1 \end{bmatrix} \quad \text{Eq 15}$$

$$A3 = T_3^2 = \begin{bmatrix} cos\ (th3) & -sin\ (th3) & 0 & L1 * cos(th3) \\ sin\ (th3) & cos\ (th3) & 0 & L1 * sin(th3) \\ 0 & 1 & 0 & 0 \\ 0 & 0 & 0 & 1 \end{bmatrix} \qquad Eq\ 16$$

$$A4 = T_4^3 = \begin{bmatrix} cos\ (th4) & -sin\ (th4) & 0 & L2 * cos(th4) \\ sin\ (th4) & cos\ (th4) & 0 & L2 * sin(th4) \\ 0 & 0 & 1 & 0 \\ 0 & 0 & 0 & 1 \end{bmatrix} \qquad Eq\ 17$$

Forward kinematics of the thumb is given by multiply all the transform matrixes (Eq 14,15, 16, and 17) together, which represent homogenous matrix as shown in Eq 18

$$T_4^0 = T_1^0 . T_2^1 . T_3^2 . T_4^3 = \begin{bmatrix} \mu_x & O_x & \alpha_x & p_x \\ \mu_y & O_y & \alpha_y & p_y \\ \mu_z & O_z & \alpha_z & p_z \\ 0 & 0 & 0 & 1 \end{bmatrix} \qquad Eq\ 18$$

$$\mu_x = \cos(\text{th1} + \text{th2}) * \cos(\text{th3} + \text{th4})$$

$$\mu_y = \cos(\text{th3} + \text{th4}) * \sin(\text{th1} + \text{th2})$$

$$\mu_z = \sin(\text{th3} + \text{th4})$$

$$O_x = -\cos(\text{th1} + \text{th2}) * \sin(\text{th3} + \text{th4})$$

$$O_y = -\sin(\text{th1} + \text{th2}) * \sin(\text{th3} + \text{th4})$$

$$O_z = cos(th3 + th4)$$

$$a_x = \sin(\text{th1} + \text{th2})$$

$$a_y = -\cos(\text{th1} + \text{th2})$$

$$a_z = 0$$

$$p_x = \text{L0} * \cos(\text{th1}) + \text{L2} * \cos(\text{th1} + \text{th2}) * \cos(\text{th3} + \text{th4}) + \text{L1} * \cos(\text{th1} + \text{th2}) * \cos(\text{th3})$$

$$p_y = \text{L0} * \sin(\text{th1}) + \text{L2} * \cos(\text{th3} + \text{th4}) * \sin(\text{th1} + \text{th2}) + \text{L1} * \sin(\text{th1} + \text{th2}) * \cos(\text{th3})$$

$$p_z = \text{L2} * \sin(\text{th3} + \text{th4}) + \text{L1} * \sin(\text{th3})$$

4.4. Simulation Results and Evaluation

In order to validate the developed index and thumb kinematic models, a simulation of their performance was run using the forward kinematics model. The models and parameter variables, with their respective configurations, are shown above. The hand was initially in a flexed position, as described by q0, and then moved through the simulation to reach the ultimate standard (finger flexing) position q. These hand gestures can be regarded as very close to the actual hand movement. Various simulations were used to track the number of alternative final positions in order to study the system's overall behaviour and the model's performance. In this case, controlling alternative hand openings to grab different-sized objects may be understood as a measure to control alternate hand openings.

Figure 14 illustrate that Several point-to-point motions for the index finger were noted to be possible based on the findings of the simulation tests, starting at the initial position and ending at the final reference position. These movements are a decent approximation of a general finger relaxation movement (case 4), where the initially flexed position gradually transitions to a straightened state (case 1). Similarly, Figure 15 illustrate the simulation result of the 3D kinematic model with 4 cases to represent the thumb F/E approximation model

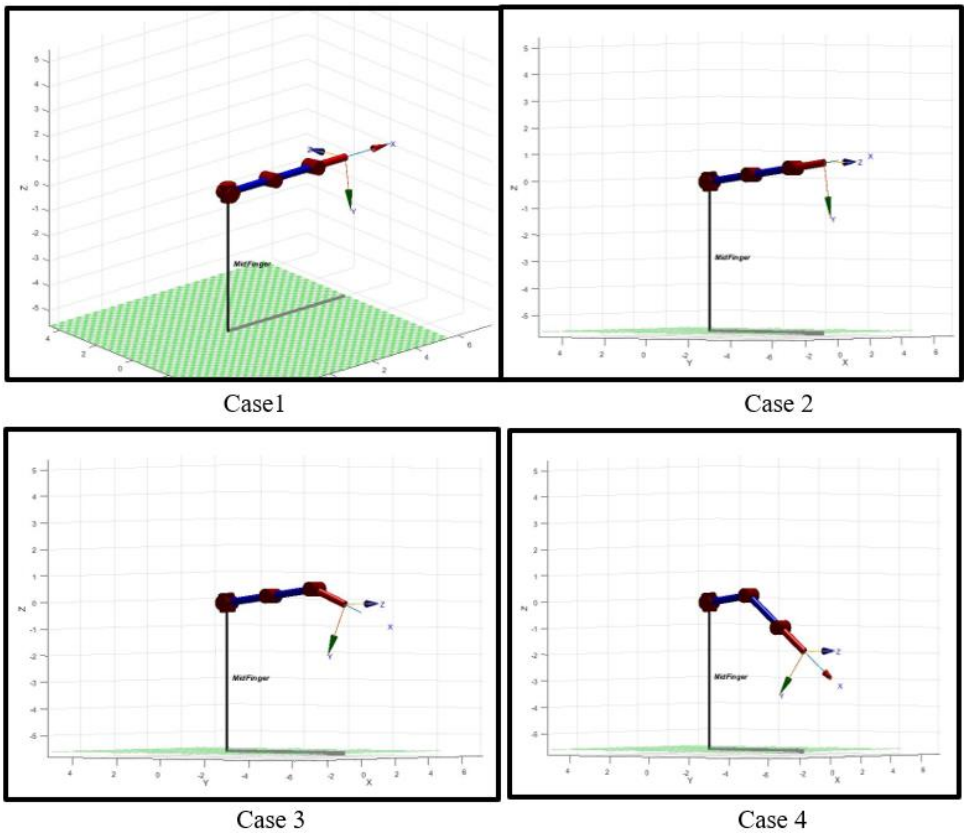

Figure 14: Simulation results for index finger;

case1, where, q1=0, q2=0, q3=0 , q4=0,q5=0. Case2, where q1=0, q2=90, q3=0, q4=0, q5=0. Case3, where q1=0, q2=0, q3=0, q4=0, q5=30. Where case 3, q1=0, q2=90, q3=0, q4=45, q5=0.

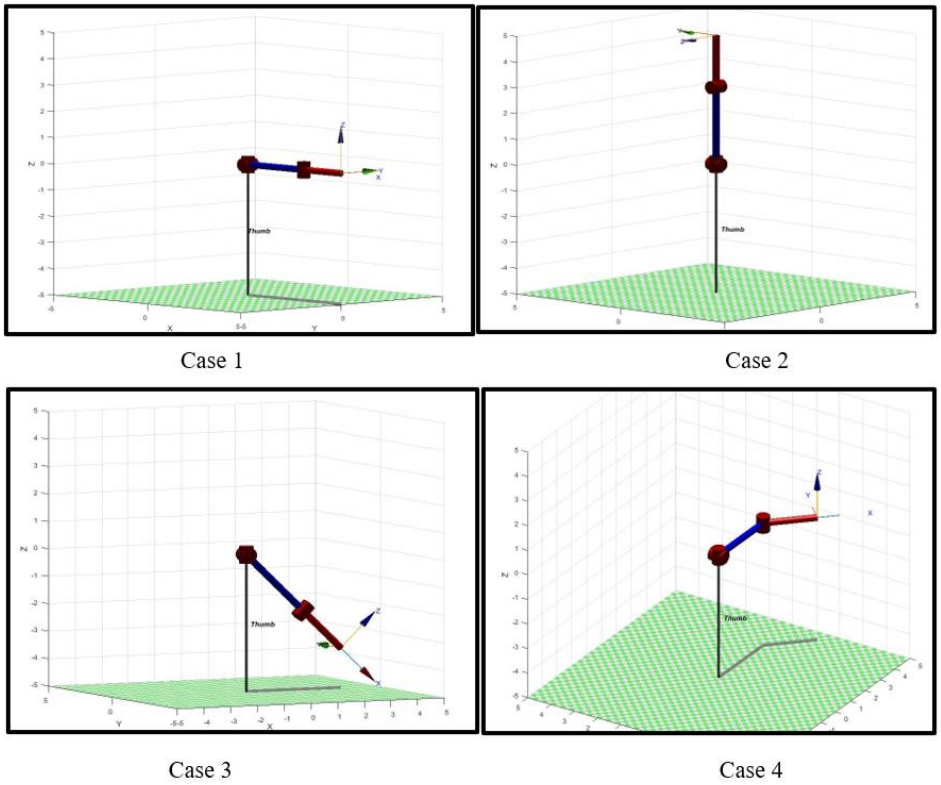

Figure 15: Simulation results for thumb.

case1, where, q1=0, q2=0, q3=0, q4=0. Case2, where q1=0, q2=90, q3=0 , q4=0. Case3, where q1=0, q2=0, q3=45 , q4=0. Where case 3, q1=0, q2=0, q3=0 , q4=-45.

4.4.1. 2D Index finger workspace modelling

Figure 16, exhibits a two-dimensional graph of one finger illustrating the workspace and simulated finger AROM. This is significant since it allows to visually finger F/E and draw the finger trajectory, which can then be compared to the physical measurement trajectories.

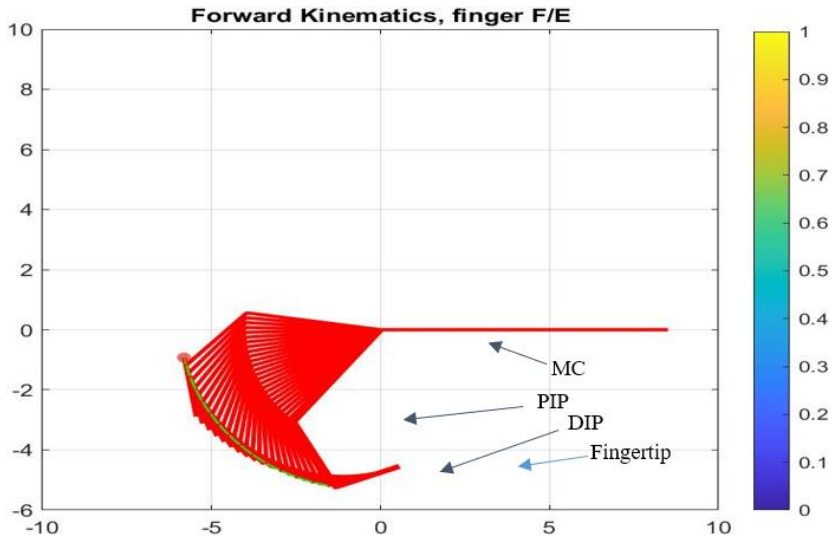

Figure 16: theoretical trajectories and workspace of the finger's F/E

4.1. Finger's Trajectory Planner Mechanism

After studying the hand's natural movement and before designing a hand rehabilitation system, it is crucial to study how a design mechanism can transmit these motions obtained by the motor to the actuated fingers independently. The first challenge is designing finger-machine integration mechanisms by designing an appreciated mechanism that can naturally move the fingers' joints without hurting them. Therefore, many mechanisms were considered and studied to achieve these objectives. Normally, to perform fingers F/E, 12 DOFs must be actuated, divided into three DOFs for each finger joint (MCP, PIP, and DIP joints, respectively). However, to actuate all these joints obviously the number of the needed actuators and power will increase, which clearly leads to an increase in the overall complexity, cost, weight, size, of the system as well as the number of the machines that interact with the joints, which eventually will be uncomfortable to the patient. More importantly, it is unnecessary to actuate three finger joints to obtain a full finger F/E; it would be enough to drive the end-effector of the fingers (distal

phalanx) with only one MC. Therefore, the number of independent DOF can be reduced to one per finger, which leads to reduce the number of the actuated joint and the MCs by 1 to each finger. In other words, the proposed guide each finger individually to the desired trajectories by integrating with the distal phalanx of the targeted finger. The exoskeleton fingertip designed to convert the driven displacement again into rotary motion, which is copying the finger's nature trajectory workspace; in other words, the exoskeleton rotation range will be limited to the patient's fingers ROM; this mechanism assists the patient to move their fingers freely and neutrally. This mechanism's advantage is that the patient places their hand (load) onto the machine, leading to fewer mechanical parts integrations; this is considered a safety and comfort feature, not the opposite, where the mechanical assemblies are placed on the patient's fingers and top palm. This device would be useful for a wider range of patients because it would fit on all hand types, including those with severely spastic symptoms. The mechanism may be placed on the hand for all those individuals who face discomfort while extending their hand or individuals where muscle tone seems to be severe significant.

4.2. Initial Design and Development

This section, present an initial design that can guide the fingers end-effector with a single MC. In this design, the mechanical design of the finger's mover is demonstrated in

Figure 17. From

Figure 17, we can observe the linear dynamic model of the proposed mechanical structure and transmissions mechanism, which is composed of an electrical motor holder, the base, a mechanical coupling, leading screw, nut, supporting bearings, sliders, linear motion ball bearing, a worktable. The initial finger's rehabilitation mechanism design has the following

characteristics: an indirect feed drives with a leading screw and a nut mechanism: the leading screw and the motor's shaft connected through mechanical couplers. The motor's torque operates a rotational angular velocity, which generates a dynamic force between the external thread of the leading screw and the nut's internal thread; at this point, once the revolution is provided, the screw and nut threads convey the thrust. In this design, the nut is positioned then fixed at the button of the worktable. The driven nut then induces a linear displacement to the worktable. Eventually, this mechanism makes the rotational torque convert into translational velocity.

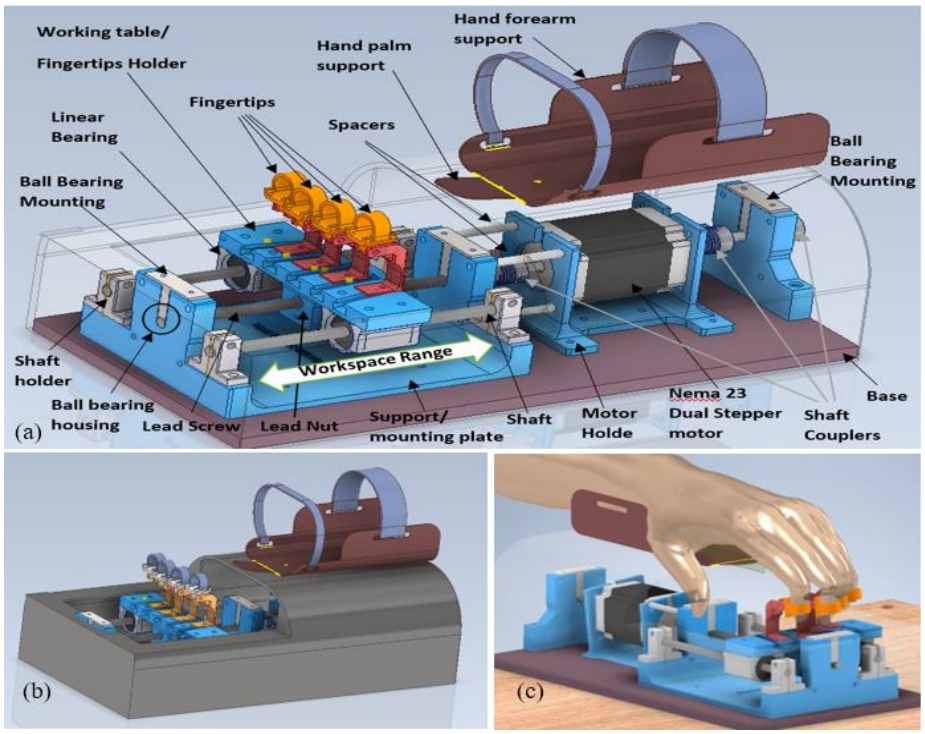

Figure 17**:** The grounded exoskeleton of the finger's rehabilitation *: mechanism design:(a), The Finger rehabilitation indirect feed drive screw and nut mechanism design with all parts; (b) 3D structure of general overview of the proposed prototype; (**c**), 3D structure model of the human finger-robot interaction.*

By taking advantage of produced linear displacement, the exoskeleton fingertips, as demonstrated in

Figure 17 (c), were placed and fixed on the top of the worktable, designed to be the exoskeleton fingertips holder. The same displacement will transfer to each exoskeleton fingertip. Furthermore, the exoskeleton fingertips are designed to convert the driven displacement again into rotary motion, which is copying the finger's nature trajectory workspace; in other words, the exoskeleton rotation range will be limited to the patient's fingers ROM; this mechanism assists the patient to move their fingers freely and neutrally. This mechanism's advantage is that the patient places their hand (load) onto the machine, leading to fewer mechanical parts integrations; this is considered a safety and comfort feature, not the opposite, where the mechanical assemblies are placed on the patient's fingers and top palm. Moreover, the fingertip's holder is adjustable to fit different hand sizes and lengths for either right or left hand, as demonstrated in

Figure 17 (b). Additionally, since the exoskeleton fingertip is the integration part between the patient's fingers and the proposed mechanism, they are designed to be removable, changeable, and more hygienic. Moreover, the base limits the worktable's mechanical structure and exoskeleton fingertips to limit driven displacement with respect to the finger's workspace.

However, It is crucial to define a starting position, which considers as a safety position. Therefore, before and after any therapy session, the exoskeleton fingertips return to their starting position (zero position). Figure 18 demonstrates the summarized block diagram of the control working flow. The actuator starts spinning until it reaches the worktable's maximum workspace physically clicks the first limit (+LS) switch. Once the +LS signals are registered, the controller disables the motor's driver's pulse signal. Eventually, that leads to stop the stepper motor, then return to the motor start spinning

again in the opposite direction till the worktable reaches the other limit switch (-LS); once the -LS signal is confirmed, the motor driver provides the stepper motor with the required pules till it reaches the predefined zero-position.

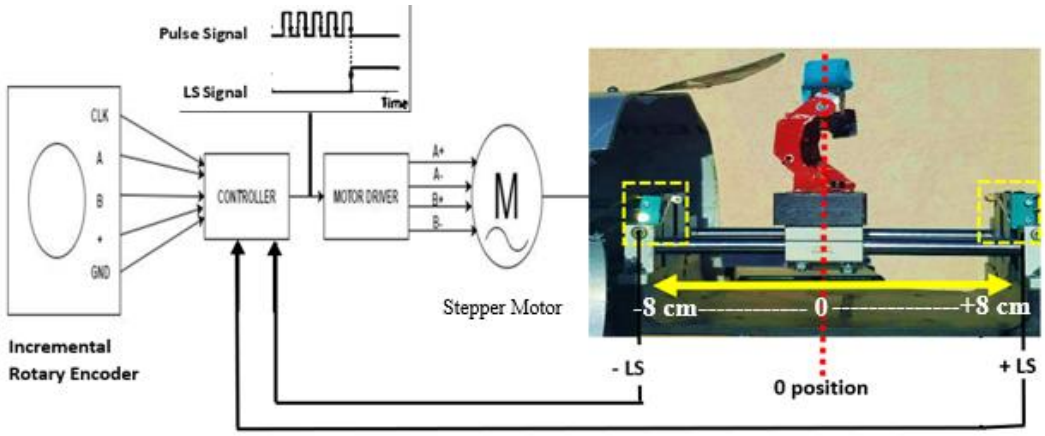

Figure 18:. Block diagram of the actuation system workflow

Eventually, regarding the finger's rehabilitation, the end-users arm should be fixed and appropriately fastened from the lower side of the forearm by using woven belts throughout the therapy process. The hand forearm cuff support is presented in Figure 19 (a); ultimately, Figure 19 (c, d) shows the 3D structure of the proposed fingers grounded-exoskeleton design machine and end-user hand and fingertips integration.

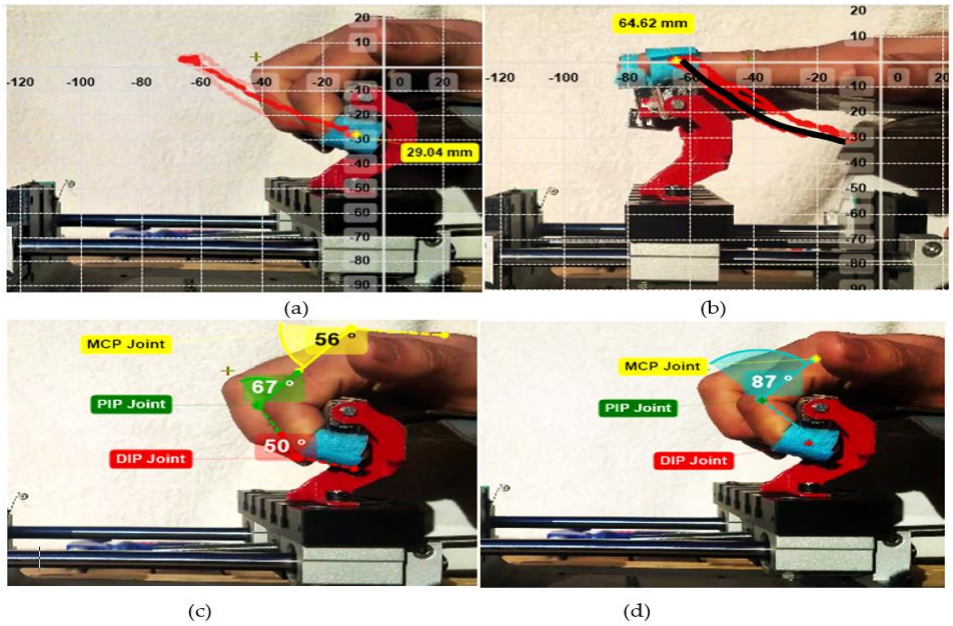

Figure 19: A real-time experimental setup of the index finger's workspace trajectories measurement:

(a) Index finger fixation actual range of motion (ROM) angle, workspace trajectory, and position caused by FWRMS. (b) index finger extension actual (black curve) and desired (black curve) workspace trajectory. (c) Index finger joints (MCP, PIP, and DIP) grasping ROM. (d) the overall grasping angle of the index finger.

Although the initial system could provide a sufficient ROM and trajectory guidance to four fingers, it could not provide a full extending range. Moreover, all the fingers had to move together, not individually, which made the design not compactable for spastic patients. Additionally, the indirect leading screw mechanism generates a high vibration which could influence the therapy. Therefore, a major improvement needed to be taken.

Chapter 5: Mechanical System and Mechanism Design

5.1. Design overview

This chapter presents the mechanical structure and mechanism of the proposed system and its most significant side i.e., design of training components incremental sieve and active mechanisms. It presents a new five-fingered mechanism that integrates with the patient-user through a single phalange. The proposed mechanical structure provides active and passive motion to fulfil the demands of various rehabilitation stages for both rights and left hand's fingers individually. Besides the four finger's rehabilitation mechanism, a new and straightforward thumb rehabilitation design is presented for either right or left thumb. Moreover, the proposed structure also presents a rightist joints mechanism that is structured to provide active and passive treatment. The overall structure of the proposed system can be defined as a mixture of end-effector and grounded-exoskeleton mechatronics systems. At the mechanical mechanism design phase, the number of mechanical connections (MCs) with the finger's phalanges, the number of DOFs that can be controlled, and the exoskeleton mechanism structure were considered. To accomplish one DOF for each single finger F/E individually, including the thumb, two DOFs for wrist F/E, R/U, and one DOF for forearm P/S, the designed mechanism for finger extension should have the facility positioned on the hand. A mechanical modelling and mechanism simulation method was required to understand then minimize the complexities of the electrical and mechanical structure between fingers. The proposed system was designed and assembled using Autodesk® Inventor® Professional software (2020, Autodesk, Inc, San Rafael, CA, USA, 2020), while the 3D hand model was developed using Autodesk® Maya® (2020, Autodesk, Inc San Rafael, CA , USA, 2020). Most of the designed components were printed 3D, and each part was manufactured with the easy to use and bio-degradable polylactic acid (PLA) filament. In accordance with

the physiological configurations of the trainable joints by the proposed system, both the grounded-exoskeleton, end-effector structures, and the total number of degrees of freedom (DOFs) are constructed. Each trainable joint is activated by DC servo engine, which provides a rotating motion then transformed into a linear displacement using a mechanism of a customized rack-pinion, which enables the fingers to open and close. The proposed prototype's overall exterior dimensions are 40 × 25 × 20 cm with a total mass (including the actuator, the driver, and attachments) of 12 kg.

5.2. Actuation Unit

For this project, electric servo motors were selected as the best choice. This type of engine is vastly employed on the robotics field and RC (Radio Control) applications. RC type servo motors are a low-price, small size, different choices with sufficient power and speed in order to provide the requirements for driving the orthotic device, also all these points represent one of their main pros when compared to other sorts of motors. As well as They were available in markets with different capacities, torque, sizes, as well operating voltages, and currents. A basic RC servo is made up of four aspects: a gear reduction unit, a DC (Direct Current) motor, a position sensor (usually a potentiometer), and an internal control circuit. In the market there are several brands, however, a brand called LD-3015MG were selected to fit the requirement of the project based on the technical specifications. This metal-geared servo motor it capable to rotate 270-degree and provides 17kg large torque when it supplies with 7.4 DCV, which is robust enough to move to ensure smooth working of the machine to move the linear rack-pinion mechanism and the attached fingers forward and backwards in the passive therapy, besides it is sufficiently strong to protect the servo's gear mechanism from damage, as a result, the external forces that act on the opposite direction of motion in case of the active therapy.

The external dimension of this motor is 54.5mm*20mm*47.5mm which is small enough to be used to fit the idea of this project. In total nine motors were used including 4 motors for the index, middle, little, and pinkie fingers F/E respectively, 1 motor for the right thumb F/E, one motor for left thumb F/E, one motor for wrist F/E, one motor for wrist U/R, and one motor for forearm S/P.

5.3. Four Fingers Design Description

This section illustrates the various design characteristics of the four fingers rehabilitation mechanism, including the whole structure of the proposed solution, Transmission and Driving mechanism, Exoskeleton fingertip mechanism design, and finger-robot integration. These aspects and more will be detailed discussed.

5.3.1. Transmission and Driving mechanism

The transmission technique to transform the motor's rotational movement to a linear displacement had to be determined once the initial concept of flexing and extending the fingers has been demonstrated. At the initial design, an indirect drive screw-nut mechanism was employed to drive a linear displacement to four fingers at the same time however, to drive fingers independently using the indirect drive screw-nut mechanism would increase the system complexity, vibration, noise, and cost. Therefore, the new finger's rehabilitation transmission mechanism design has the following characteristics: adopting the rack-pinion mechanism to transmit the angular positions derived by the actuator to linear displacement to drive the desired joints.

5.3.2. Rack and Pinion Mechanism

As part of a simple linear actuator, combinations between rack and pinion are frequently utilized; it is a mechanism that put together two gears with a set of teeth that equally spaced, one is a circular gear which called a pinion that engages and moves along the flat rectangular, toothed bar which called a rack. This mechanism operates to change the rotational movement to a linear movement at a fixed axis moving on a straight path. When the pinion is rotated, the rack is driven linearly. However, the pinion will be forced into the rotation if the rack is driven linearly.

Figure 20, describe part of the employed mechanism, in which we can observe the linear dynamic model of the proposed mechanical structure and transmissions mechanism. It is composed of a Servomotor and its holder, rack, pinion, and supporting rack home

The servomotor, fixed at the motor holder then directly mounted with the pinion. A spline, small grooves along the shaft, and screw holes for firmly mounting servo horns make up the output shaft of the used servomotor. The Servomotor horns are attachments that are appropriate to the output shaft, can be mechanically connected to the servo's output shaft then can be secured with a screw. Therefore, the pinion was designed to be home to the motor horns, then manually and carefully attached and mounted to the motor horns. While the driven pinion grooves are supplied to guide the movement of the rack. The rack is securely mounted into a rigid body at a fixed axis.

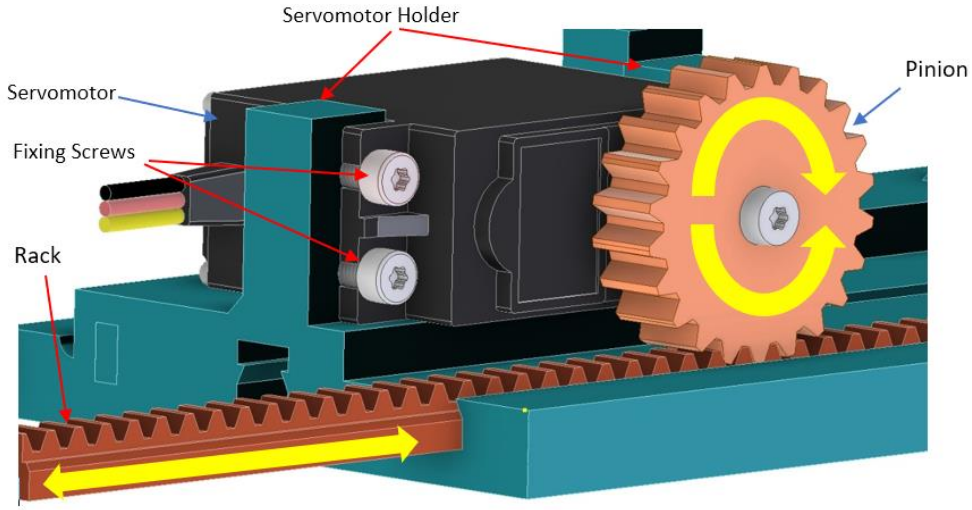

Figure 20: 3D structure of the employed Driving mechanism

Figure 21 (a), present the developed two-linear driving mechanism, in this mechanism, as soon as the motor's torque operates a rotational angular velocity, it generates a dynamic force between the teeth of the pinion and the rack, which leads to moving the rack at fixed axis with predetermined displacement at either forward or backward direction, depending on the motor's rotation direction. At this point, once the mechanism was approved, the diving mechanism was expanded with the same mechanism by adding another motor with a rack-pinion mechanism to actuate with a fixed axis; each one will later be used to move a single finger.

Additionally, to properly take the advantage of the driven linear motion, the pinion was extended then mounted with, 8mm diameter, smooth circular shaft. The shaft and the rack are connected and fixed by a screw as can be seen in Figure 21 (c). The lightweight shaft plays the role of leading support to the driven displacement of the rack. Moreover, the leading shaft is also supported with a linear guide bearing. The employed supporting bearing can be seen in Figure 21 (b), which also call linear slide bearing, which is designed to provide free motion in a linear direction. There are cylindrical balls situated between

the inner and the outer rings of the bearing. This makes the inner ring rotate while the outer ring remains stationary. With an inner diameter of 8 mm. Moreover, the rack also houses the Force sensor, which measures the amount of force exerted by the finger; this novelty designed mechanism can be seen in Figure 21 (d).

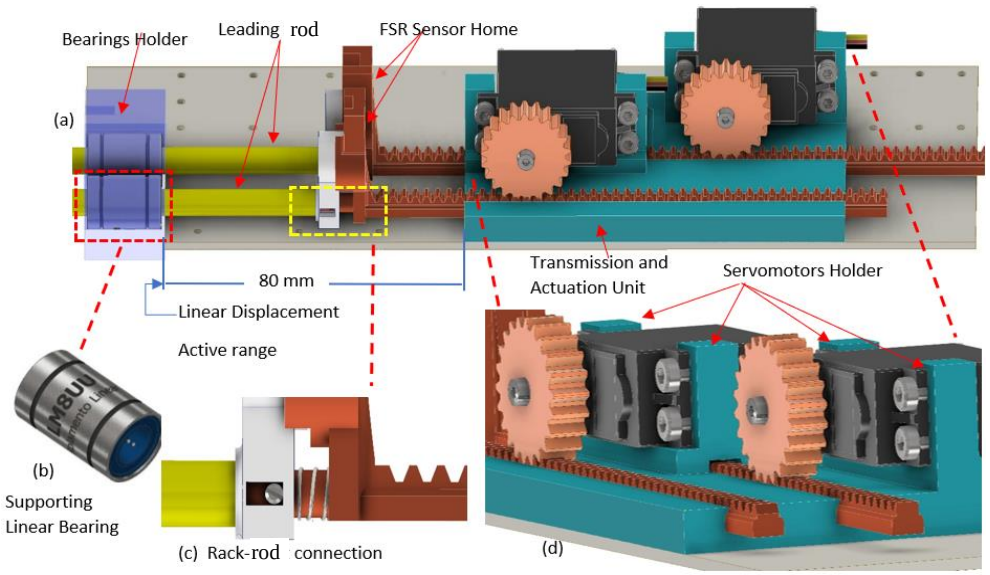

Figure 21: the proposed linear guide mechanism:

(a), the proposed two linear drive mechanism; (b) supporting linear bearing; (c) rack-guiding shaft connection point; (d) servomotor with its holder and rack-pinion mechanism

Ultimately, Figure 22 (a) demonstrates the 3D design of the final driving and transmission mechanism unit, which is structured to be driven by four servomotors. The same previously explained rack and pinion mechanism were employed to convert the rotary motion to a linear displacement. The whole rack and pinion mechanism were mounted and rigidly fixed onto the design body. Figure 22 (b) present the dimensions of the custom-designed rack and the distance between each rack's centre, and another, which is 24mm, rack-

based width is 7mm, and the rack's teeth 5mm; this customize rack, designed to be fit and secured into the rigid transmission and actuation unit. Moreover, it is worth mentioning, the distance between one rack and another was determined based on the premeasured anthropometry data of the average human fingers size. Therefore, the motors were arranged to meet that regard. Additionally, from Figure 22, the first rack from the top and the third rack is longer than the other two with few centimetres due to different locations of the motors that drive these racks. Figure 22 (c) shows the supporting linear guide assembly encloser, which consists of; the bearing home, which was designed to fix the bearings inside. The leading shaft is placed inside the bearing. The bearing is used to hold the driver in place and to facilitate its rotation. The bearing is enclosed and secured by a screw. The whole supporting linear guide assembly, driving, and transmission mechanism are mounted and fixed on a 300 x 204 mm aluminium plate. The overall proposed structure represents the driving mechanism capable of providing a linear displacement for four guiding shafts, which are used to transfer these displacements to four fingers except the thumb.

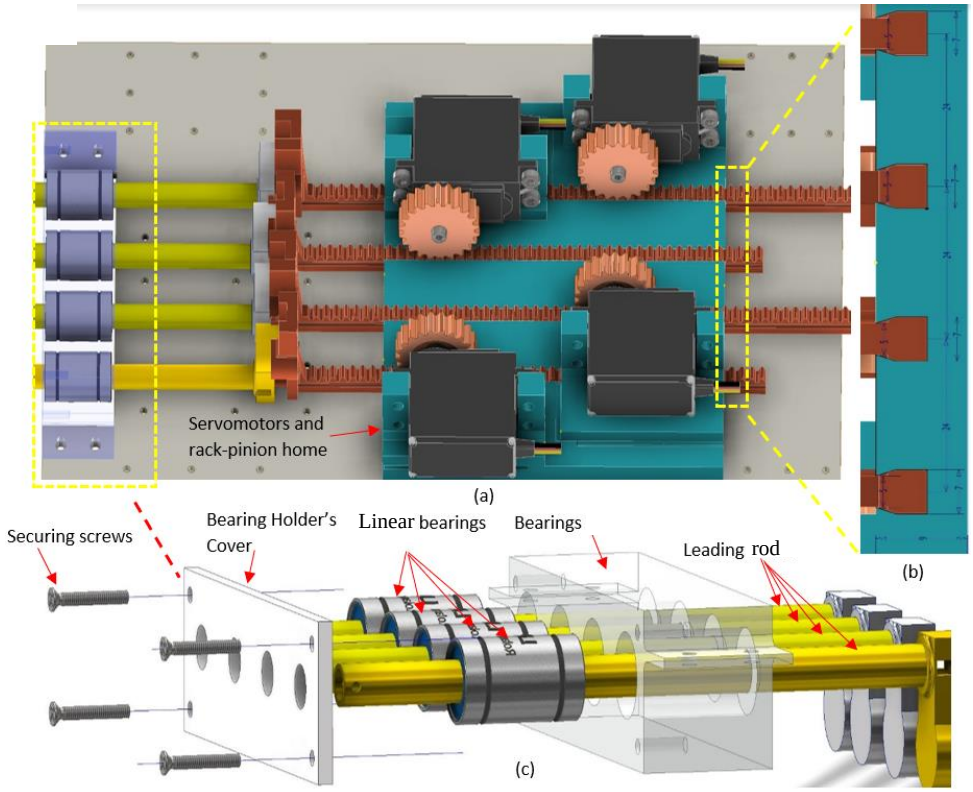

Figure 22: Ultimate 3D design of four-driving mechanism assembly:

(a) the total driving and transmission mechanism; (c) back view of the rack housing; (b) supporting linear guide assembly

5.3.3. Exoskoleten fingertip holder design

As briefly explained in section (Finger's trajectory planner mechanism) in the initial design, the exoskeleton fingertips holder is designed to be integrated with the human finger with on MC, more specifically at the finger's end-effector (distal phalanx). j guiding shaft moved backwards and forward, which guide the fingers to achieve full finger's F/E. for the final design, a few improvements are needed to meet the new system design requirements. The whole fingertips holder assembly was split into two parts: the distal fingertip

holder and the primary finger support. Figure 23 presents the 3D model structure of the fingertip support mechanism assembly was designed to house the fingertip then fasten it from the lower side of the distal fingertip by using a Velcro strap fixed to one of its ends. This strap would create a ring around the finger and end on the opposite side. The exoskeleton distal fingertips holder and the primary finger support are joined together through a set screw to hold them together at a fixed axis and enable the exoskeleton distal fingertips holder to rotate around 180 degrees at the fixed axis. The area of the distal fingertip holder was designed based on an anthropometry study of the designer and the participants' fingertips distal area.

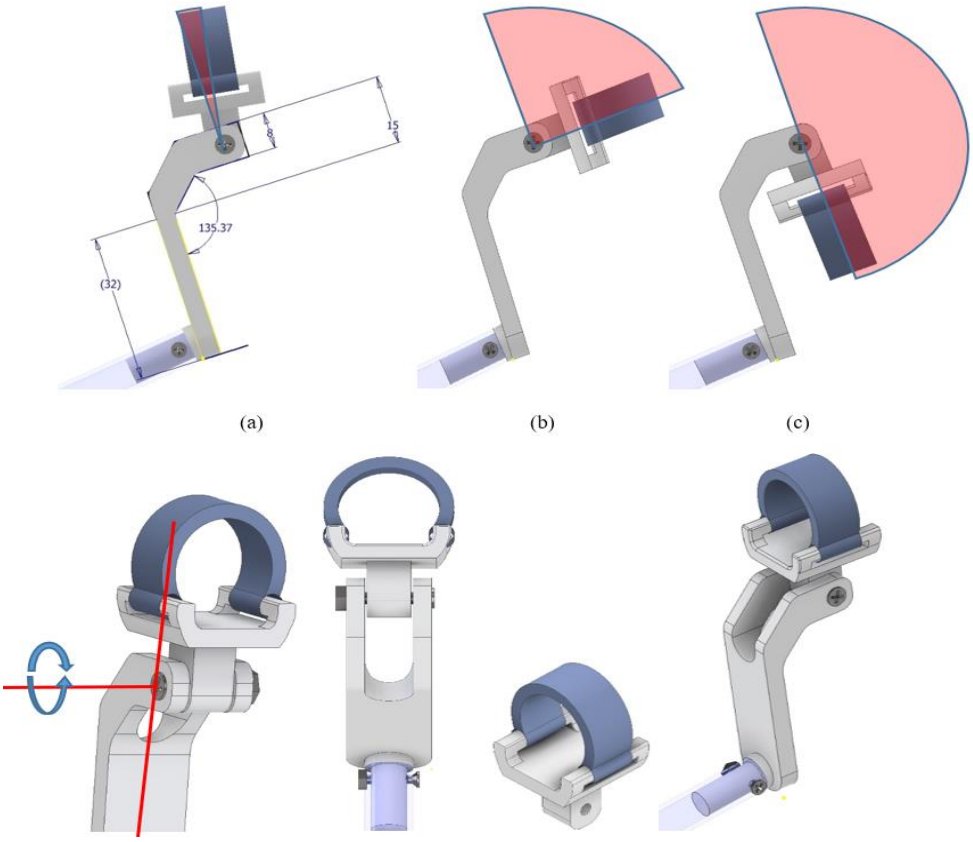

Figure 23: 3D model of the distal fingertip's holder assembly:

(a) extending position of the fingertip holder with the dimensions in millimetres; (b) 90-degree flexing range of the fingertip holder assembly (c) 180-degree flexing range of the fingertip holder assembly; (d) front-side view; (e) back view of the proposed fingertip holder; (j) 3D model of the distal fingertip support fasten by Velcro strap; (k) back-side view

Like the described method, four different parts (Figure 24) were designed to provide figure F/E movement with 6 mm space between fingers; all parts were 3D printed using PLA filament. Eventually, the entire fingertips holder mechanism assembly is connected to the other side of the guiding shaft using a set screw and nut. As can be observed in Figure 25.

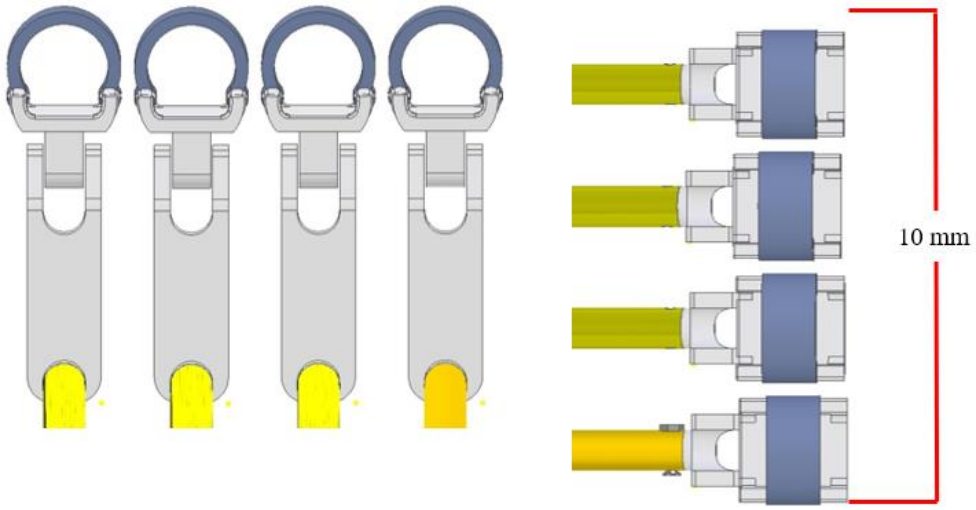

Figure 24: 3D assembly of four fingertips holder and support that connected with the guiding shaft.

5.3.4. The mechanism for (extension and flexion) of the fingers

Figure 25 demonstrates a 3D model of the novel proposed mechanical structure and its mechanism of four fingers F/E, which consist of integrating the actuation and driving unit plus the transmission mechanism unit, linear guide mechanism, supporting linear bearing encloser and distal fingertip

holder assembly. The whole system is mounted over a rigid body supported by aluminium shafts within a 25 degrees angle; this angle was decided to improve the ROM provided by the proposed system and enhance the maximum extending and flexing range.

The same displacement driven mechanism produced by the driver unit will transfer to each exoskeleton fingertip through the guiding shaft. The exoskeleton fingertips are designed to convert the driven displacement again into rotary motion, which is copying the finger's nature trajectory workspace; in other words, the mechanism's advantage is the exoskeleton rotation range will be limited to the patient's fingers ROM; which actively assists the patient's fingers to perform F/E without any discomfort by following the nature ROM of attached fingers.

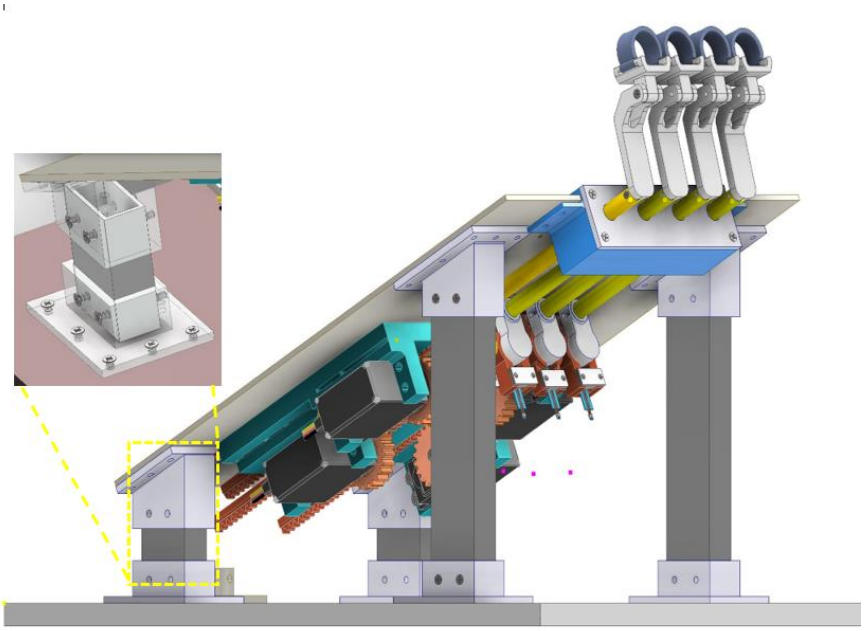

Figure 25: 3D structure assembly model of the proposed system concept's integrations

The proposed mechanical structure and mechanism are able to perform both active and passive training. Active therapy the device to move the patient fingers throughout one mechanical integration point (the exoskeleton fingertips) mechanically, this means the servomotor-pinion assembly produces a rotational angular velocity that will be converted into a linear displacement throughout the rack-shaft which will guide the attached fingers onto the fingertips holder to perform F/E for going and coming back relying on the orientation of the rotation engine shaft.

While in passive therapy training, on the other hand, the fasten fingers onto the fingertips holder needs to apply a particular grasping force to move the exoskeleton fingertips mechanism assembly leading to drive a linear displacement to the guiding rack-shaft assembly, which will drive a rotational angular velocity to the servomotor-pinion assembly. In other words, the fingers move to act as an actuator that led the servomotor-pinion assembly to produce a rotational angular velocity, and the system ensures the fingers movement directions.

5.4. Thumb Rehabilitation Mechanism Design

Thumbs are a critical element of human hands as they facilitate dexterity when humans grasp small objects. In general, combination movements involving the thumb and other fingers cover 40% of complete hand movements [131]. Consequently, patients who lose thumb movement functionality find it challenging to perform daily life activities. Owing to their functional importance, the rehabilitation and grafting of thumbs are of high priority. Generally, with small space, the thumb exhibits five movements: abduction, adduction (palmar and radial), flexion, extension, and opposition. Therefore, the thumb has a very complex structure and unique way of trajectory motion and ROM compared to other fingers, which is the truly challenging part of designing a hand rehabilitation robot. Mostly, in literature the rehabilitation

robotics advancements, most of the existing prototypes failed to involve the thumb mover mechanism in their designs for the hand rehabilitation robotics, and they present the only mechanism enough for only four fingers without the thumb.

Moreover, those who include the thumb rehabilitation in their designed a considerable number of them load the entire mechanism onto the thumb, leading to conflicts between the fingers and the mechanism, discomfort, and limiting the fingers natural trajectories movement. Conflicts also might lead to damage to the attached finger. Therefore, unique and particular requirements and considerations should be taken into mind when designing a thumb rehabilitation mover more focused on the hand attachment parts and the placement of the actuators. Besides, avoiding conflicts is essential to consider in the design process. Alongside the mentioned requirements, the interaction between the mechanism and the thumb is one of the most important keys. As a result, the thumb needs a deeper study and technical and clinical considerations, and the functioning prototypes need a certain investigation; otherwise, the design will not fit and function well and might even harm the end-users.

With that in mind, in this section, present and describe a novel solution design and mechanism targeting both rights and left thumbs. Generally, the proposed mechanism will guide the thumbs to perform thumb flexion/extension. However, to perform normal thumb F/E, the three joints of the thumb (IP, MCP and CMC joints) need to flex and extend within a certain angle as presented in Figure 26. Figure 26 (a) shows the Radial Abduction position at 60 degrees, which the best position to start performing thumb F/E, while Figure 26 (b) shows the IP and MCP joints flexion ROMs. The proposed thumb rehabilitation mechanism is capable of guiding the thumb to move these joints that are needed to perform thumb F/E to with limited and controllable

ROM by using only one actuator placed on a rigid body, not over the thumb. The proposed mechanism is based on a combination of end-effector and grounded-exoskeleton structures. It integrates with the thumb with only one MC at the thumb tip when the thumb is at around 60 degrees of its Radial Abduction position (Figure 26 (a)); This position helps to have smooth thumb F/E. Moreover, the proposed thumb rehabilitation design is not to perform such motion across the CMC joint. Eventually, for prototyping purposes, most of the mechanical structure of the intended system was fabricated using 3D printer (Prusa) and printed using PLA filaments.

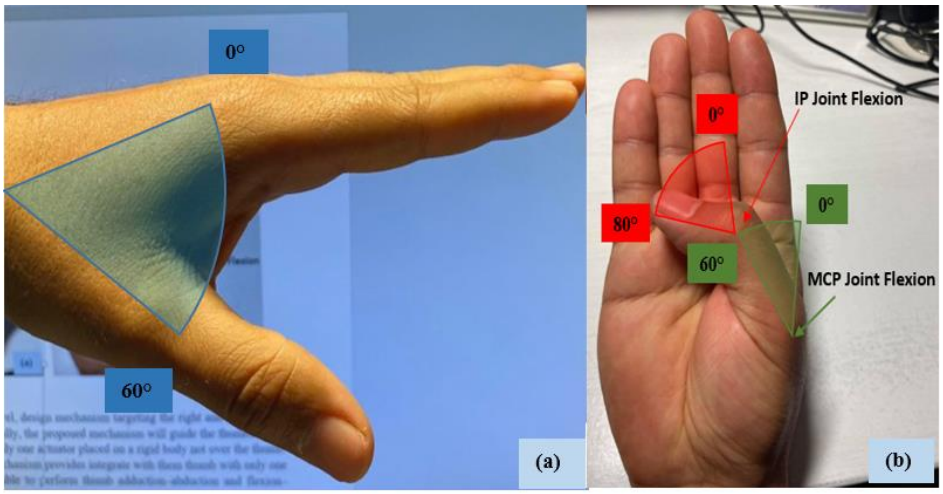

Figure 26: Thumb range of motion;

(a) Thumb Radial Abduction position; (b) thumb flexion, IP and MCP joints trainable ROM

5.4.1. Thumb rehabilitation mechanism Design process

In this section, the overall design process of the proposed prototype is described. Figure 27 shows a side view of the thumb rehabilitation prototype's 3D CAD assembly model, which mainly consists of servo motor, motor holder, motion transmission mechanism, and thumb tip holder. The whole thumb rehabilitation design was secure and carefully mounted onto the same

rigid aluminium base that used to hold the other four fingers entire mechanism from the other side. The thumb rehabilitation design and its mechanism were constructed to integrate three parts with three revolute joints (A, B, and C joints, respectively); these help adjust mechanism length to match various hand sizes and naturally provide and/or follow the thumb motions. From (Figure 27, Figure 27) it is observable that the motor is inserted and fixed into a specially designed motor house, and the other three parts are called the motor-link part, base part, thumb tip holder part, respectively. The motor-link part, from one side, is directly connected to the motor's output shaft through flexor revolute joint connection (A joint) able to perform a 1 rotary DoF, and from the other side is connected on top of fixed axis with the thumb base part. The thumb base and motor-link parts are connected through the rotator revolute joint (B joint, one Dof) within an adjustable angle between them. Moreover, the thumb base part is mounted under the motor-link part within a certain distance which was made attentionally to keep the whole mechanism away from the dorsal side of the hand palm. This help to avert any conflicts between the mechanism and the hand. Depending on the adjustable angle between the motor-link part and the thumb-based part, the thumb mechanism can be shorter or longer, which means it can adopt small and big size thumbs. The thumb tip holder part is passively linked into the base part through a passive hinge revolute joint at fix axis with limited ROM that matches the thumb's ROM.

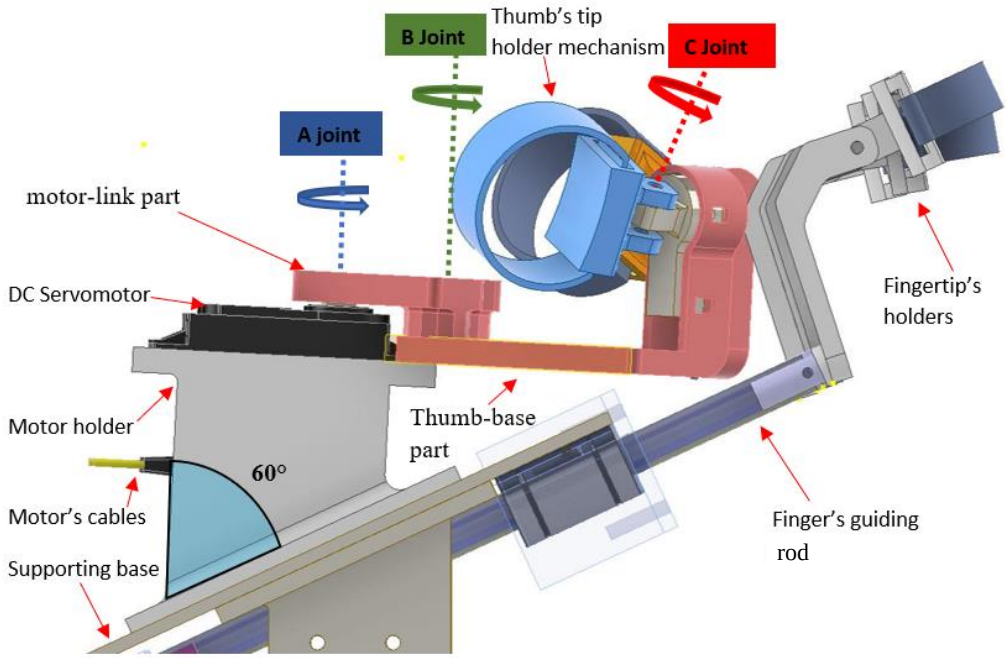

Figure 27: 3D CAD structure model of the proposed thumb rehabilitation mechanism with its implementation.

It is observable from (Figure 27, Figure 27), that the thumb holder at C joint is a little bit curved with a specific angle which is attentionally made to be more comfortable to the thumb tip. Through this structure, the entire mechanism will meet with the thumb with only one mechanical connection, with the thumb tip is considered an advantage as it reduces the mechanical connections between the machine and the patients. Figure 28 demonstrate the possible workspace of each mechanical part with the joints of the proposed mechanism, starting from the motor-link part with its A joint. This link transfers the motion generated by the servomotor to other joints, and it was limited to rotate within a range of 0-50 degrees which is enough to open and close the thumb fully. The thumb-link joint should be manually changed and fixed depend on the hand size. The thumb holder and its joint can freely rotate and fully the thumb IP joint ROM within 80 degrees.

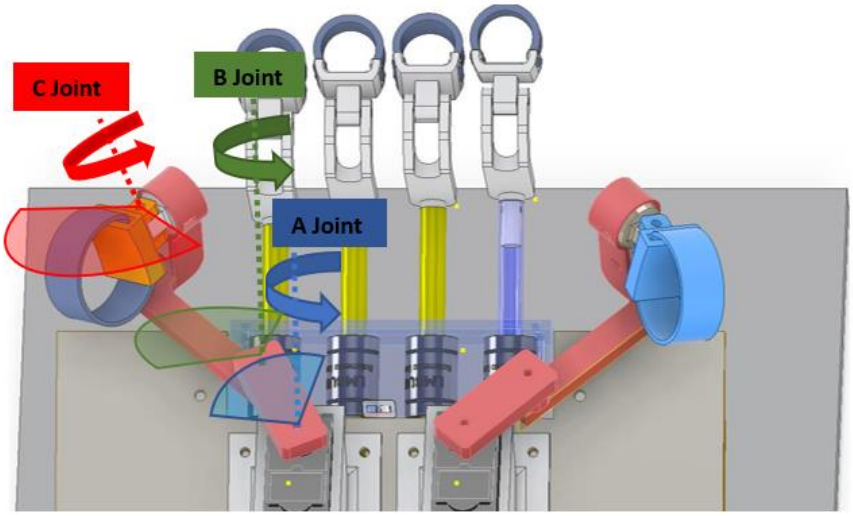

Figure 28: 3D CAD assembly top view, demonstrate the active ROM of the proposed system's links.

Additionally, the thumb tip holder was designed to house the thumb and fix it using a Velcro strap, as shown in (Figure 27, Figure 27, Figure 28) Similarly, using the described method two thumb rehabilitation were designed for both right and left thumbs as present in (Figure 28, Figure 28).

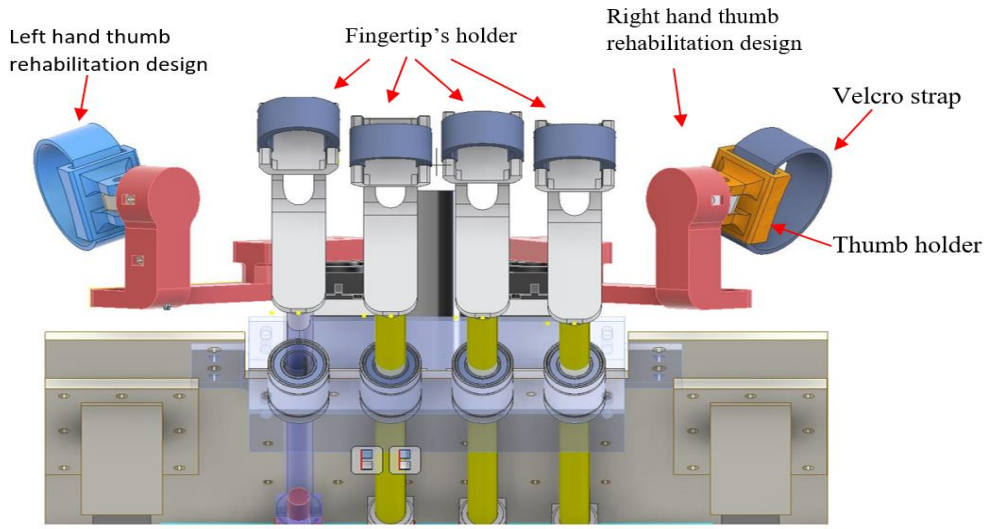

Figure 29: 3D CAD assembly front view demonstrate the proposed thumb rehabilitation mechanism for both right and left hands.

5.5. Forearm Support and Cover Design

A modified aluminium composite panel covers the proposed system. As shown in Figure 30, the cover is properly fixed onto the device base and then supported by a supporting shaft. Generally, the cover is used to house the entire device mechanism, driving unit and to be base to the patient forearm support. On Top Of the cover, the forearm supporting structure and mechanism is fixed correctly. The forearm support cuff is used to hold and fasten the end-users arm and keep it properly mounted by fastened hand forearm by using woven belts throughout the
therapy process.

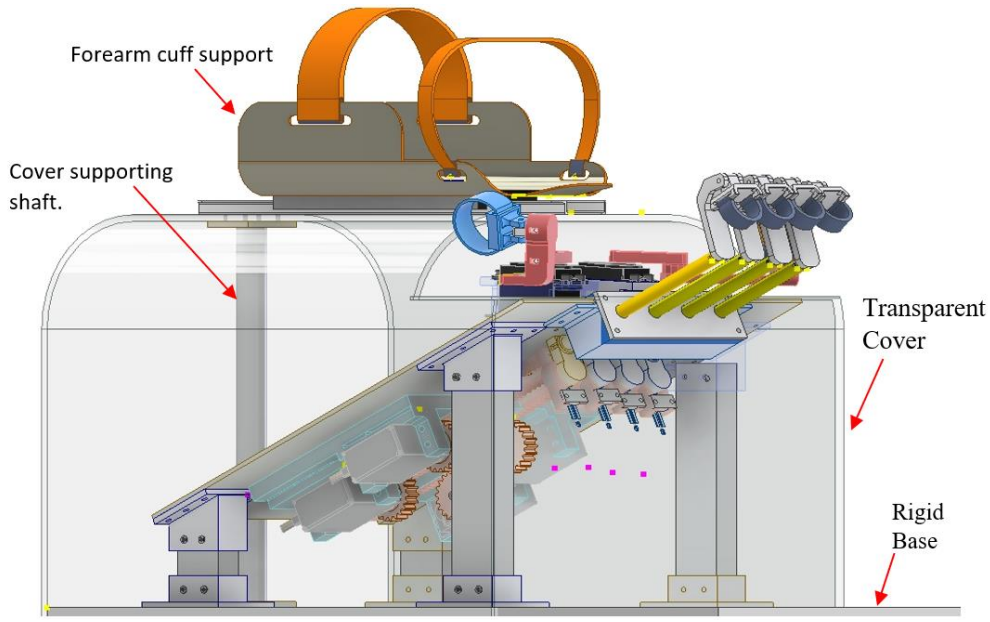

Figure 30: the proposed system with its cover and forearm support design

To properly transmit forces and torques to the target joints by the proposed system without a considerable amount of positional error, the arm should

properly place and fix. In other words, the arm for the forearm rest should be well set and fix; this would restrict any unnecessary movements that might affect the desired movement.

Also, the forearm support cuff was created to give extra support to the dorsal side of the hand palm. Eventually, the whole forearm and palm support base is part of the mechanical slider; the advantage of the slider is to move the forearm support backwards and forward based on the hand size. This feature makes the proposed system more adaptable and adjustable to be fit to different hand sizes. Moreover, Figure 31 demonstrate the hand forearm cuff support

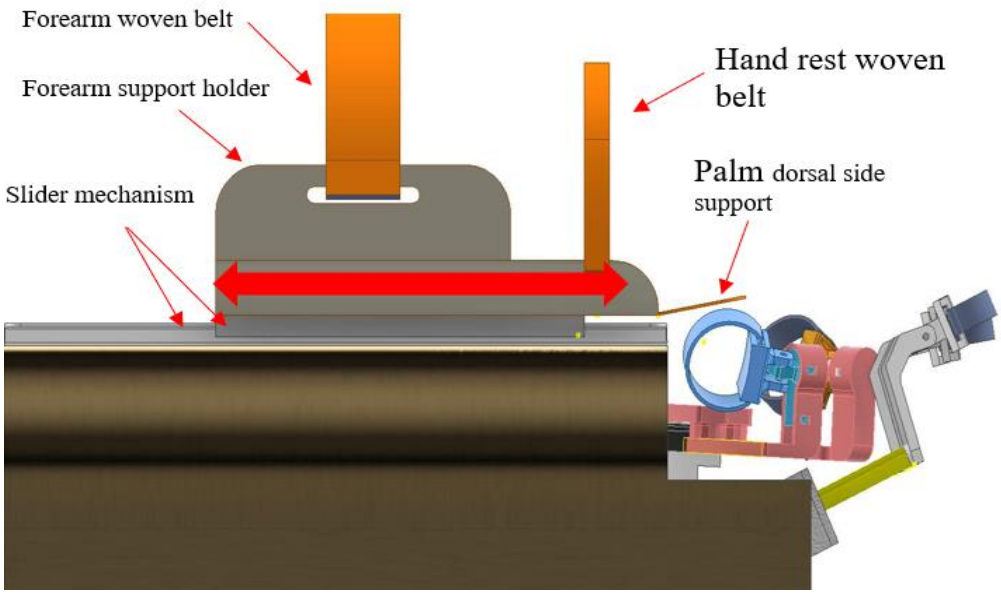

Figure 31: 3D structure implementation of the cover and forearm support design woven belts

5.6. Assembly

A 3D design for a human arm was formed by using AUTODESK Maya 2020. To generate the human arm model, the rescuers had to rescale it according to the size of the 3D structure of the proposed system. The Hand design was positioned in the armrest, and the fingers were fixed to the Finger holders.

Figure 32, demonstrates the arm-robot integration 3D CAD models. In which the hand fingertips model is integrated with the fingertip's holder and fastened to it, it is also observable that the arm forearm is rest on top of the proposed forearm cuff design

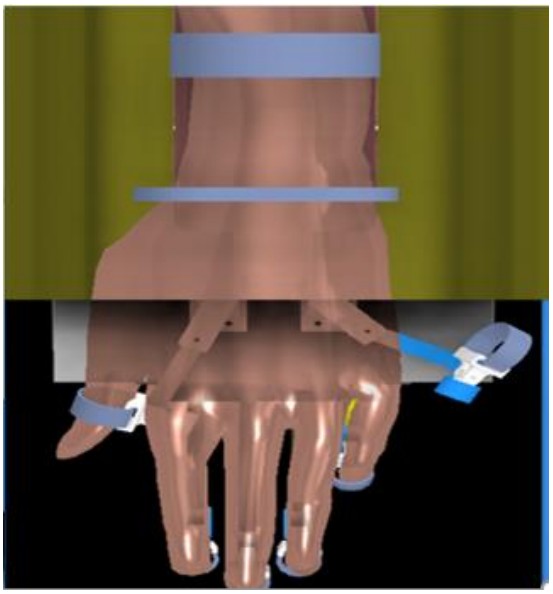

Figure 32: 3D CAD model of the arm-robot models;

5.7. Wrist and Forearm Mechanism Design

The wrist joint links the hand and the forearm together, the wrist formed by a series of eight carpal bones and a soft tissue wrapping them, basically the wrist important small joint anatomic planar structure. The wrist joint performs one DOF for wrist flexion/extension and one DOF for wrist radial/ulnar deviation [132], [133]. One DOF by the forearm joint process of supination/pronation (S/P), thanks to the elbow joint [134].

The proposed approach provides an active, passive and continuous passive motion to the wrist joint movement (F/E, R/U) and forearm (P/S). The proposed system utilizes in total three servomotors to power these joint movements, as shown in Figure 33.

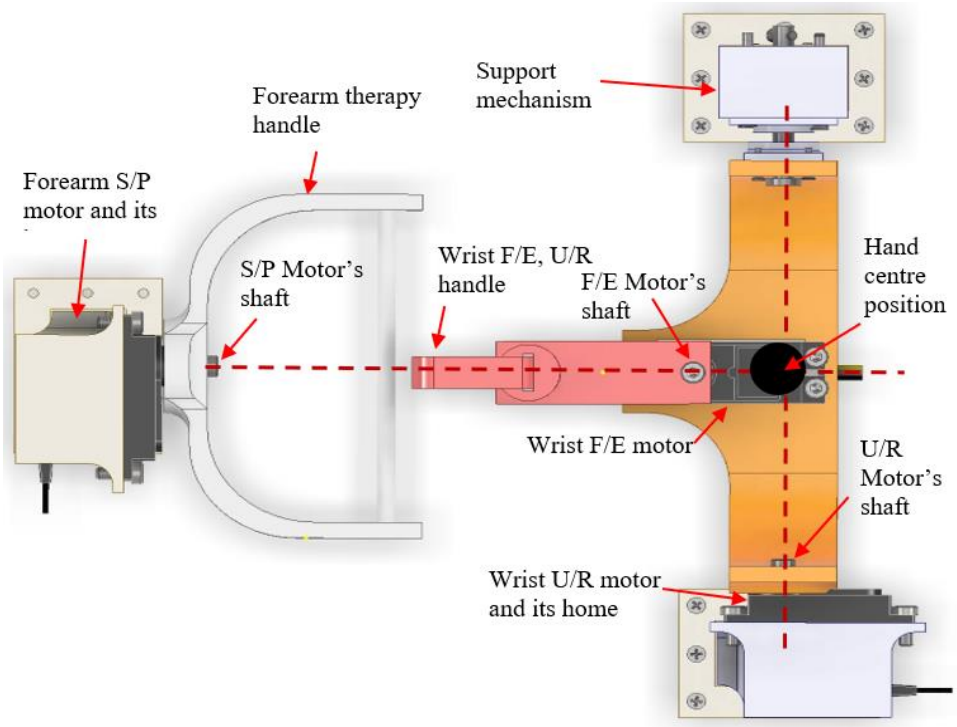

Figure 33: 3D structure of the proposed wrist and forearm rehabilitation system

The Whole wrist and forearm proposed mechanism is connected into the same base of the fingers and thumb mechanism and it uses the same forearm support and control with the same controller and UI. This would keep the whole mechanism more compact and straightforward, and accessible.

5.7.1. Wrist F/E and R/U Mechanism

To achieve the natural movement of wrist's joints movements such as F/E and R/U and considering the requirement and objective of this project, by providing an active and passive motion to these joints. Therefore, the proposed mechanism actuates each joint with a single actuator but with one handle, as this means the end-user needs to have the grabbing capabilities to hold the handle through the therapy sessions. As shown in Figure 34, the wrist F/E

actuator is mounted in the middle of the arc, the F/E actuator's output shaft is connected to the handle mechanism. While the wrist R/U actuator is mounted into a specially designed holder, then is its output shaft is connected to one edge side of the arc. Perpendicularly, form the other edge side of the arc is connected into an arc supporting mechanism through an arc supporting shaft. As shown in Figure 34 (b), the arc supporting mechanism consists of an arc supporting shaft, one rotating ball bearing and two bearings holder with their covers in which the bearing was secured. The reason of it to provide support to the other side of the arc and smoothing the motion provided by the R/U actuator. Eventually, the whole wrist F/E and R/U rehabilitation mechanisms were supported and fixed from each side with an aluminium supporting shaft.

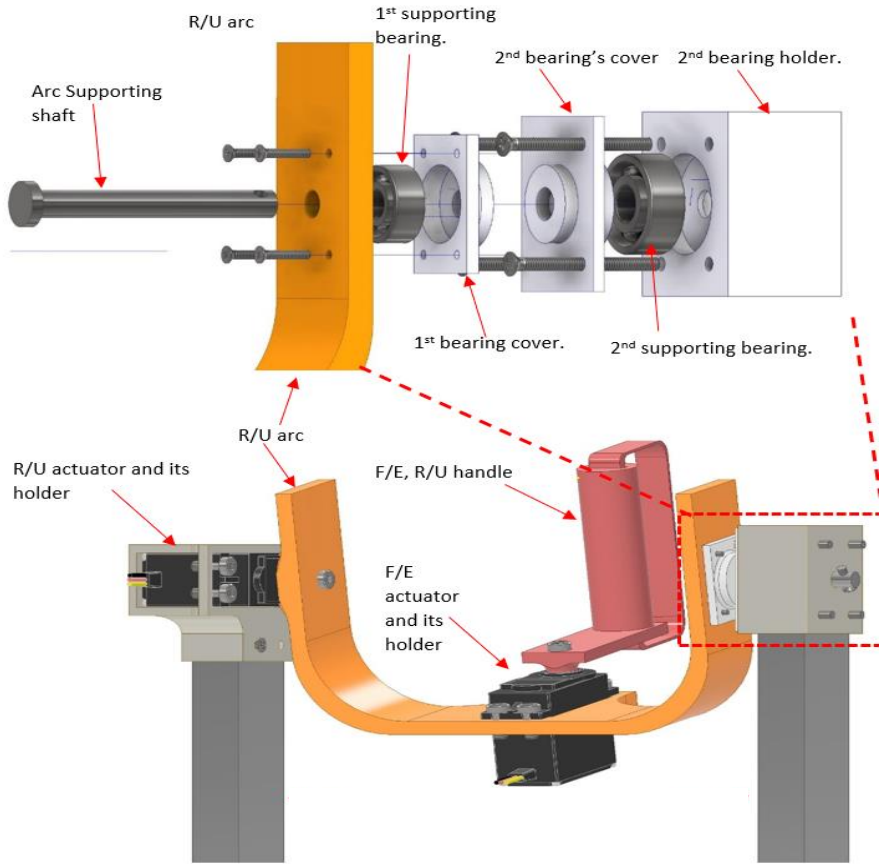

Figure 34: 3D CAD assembly model of the wrist F/E and R/U mechanism:

(a) the entire structure; (b), arc supporting mechanism.

5.7.2. Wrist F/E Mechanism

Wrist flexion involves a movement of the wrist so that the palm faces the hand's orientation, while the extension is a move away from the palm. There has only been one DOF involved with this activity. This can be accomplished by only making sure the actuator's rotation shaft is parallel with the wrist. This mechanism in Figure 35 shows the way the device executes and establishes the Dynamic Range of Motion (ROM). The system could move the wrist through complete ROM of flexion/extension, with no restrictions.

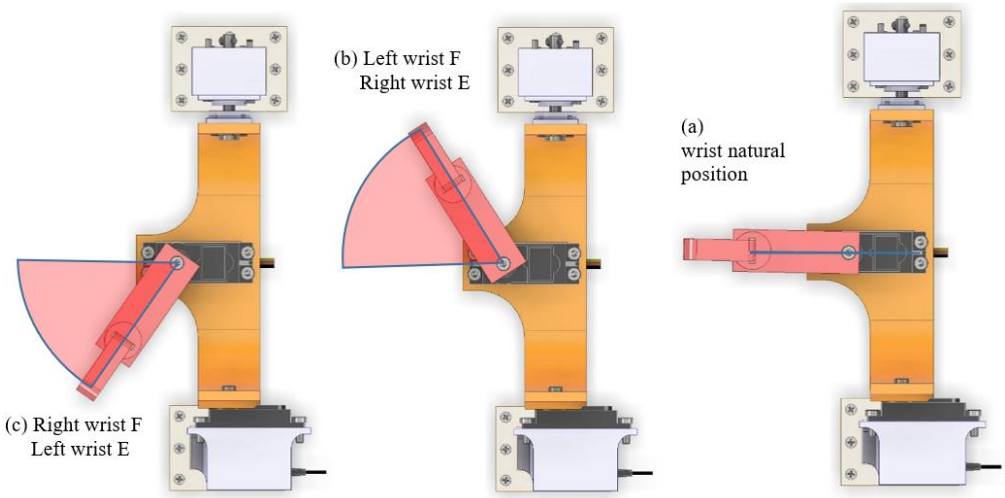

Figure 35: 3D CAD assembly of the proposed system F/E ROM:

(a) wrist zero position; (b) Left wrist F and proper wrist E range from the zero position; (c) Right wrist F and left wrist E range from the zero position.

5.7.3. Wrist-Robot Assembly Integration

A 3D assembly model of the proposed wrist F/E rehabilitation system is shown in Figure 36, together with a 3D model of the human hand. In order to conduct the passive wrist movement, the arm and forearm must be manually tied to the arm support part, precisely as it was stated for the finger. To begin, the patients

fasten the wristband on their forearms, then adjust the pressure. This helps prevent the brace from slipping during exercising.

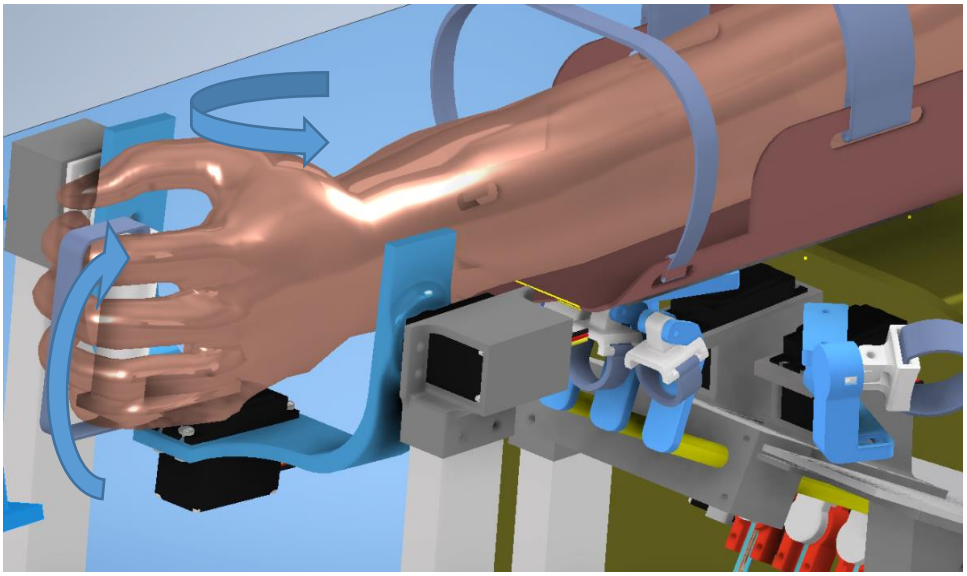

Figure 36: 3D model assembly of human-robot integration for the wrist

Additionally, as previously stated, the wrist and forearm mechanism uses the same forearm support cuff, which is already part of a sliding mechanism that enables it to move forward and backwards. The operator needs physically to move the forearm support cuff to cover the fingertip holders to protect them and be closer to the wrist handle as presented in Figure 37Figure 37.

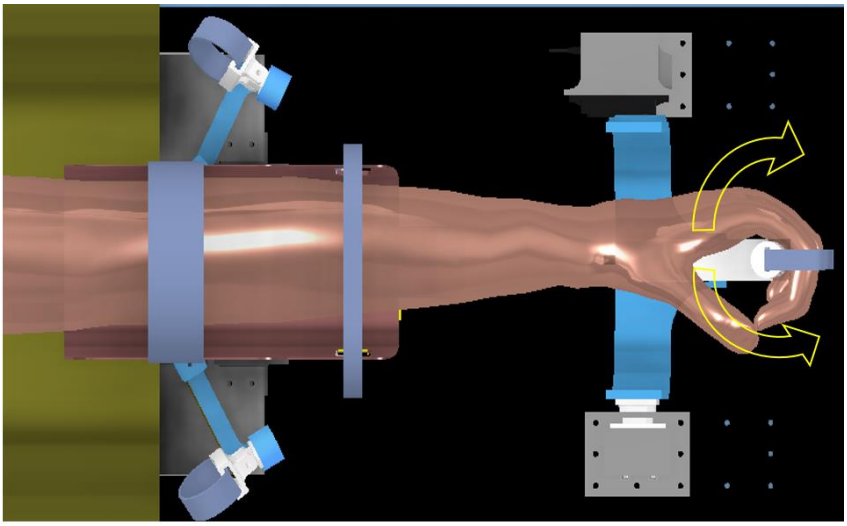

Figure 37: 3D model assembly of human-robot integration for the wrist

5.7.4. Wrist Ulnar/Radial Deviation Mechanism Design

An individual who exhibits radial deviation is when they bend their wrist towards the direction of their thumb (on the palm side of the hand). The opposite of that is the wrist ulnar deviation when an individual moves their little finger downward on their wrist. Figure 38Figure 38 demonstrate 3D structure assembly the possible ROM of wrist R/U deviation that the proposed mechanism can perform

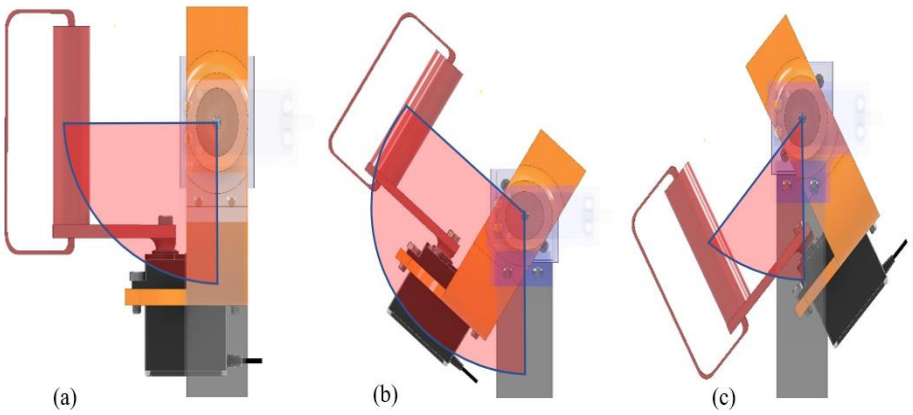

Figure 38: 3D CAD assembly of the proposed system F/E ROM:

(a) wrist zero position; (b) suitable wrist R and left wrist U deviation range from the zero position; (c) Right wrist U and left wrist R deviation range from the zero position.

Figure 39 demonstrates the 3D structure model, the entire proposed system assembly and integrations

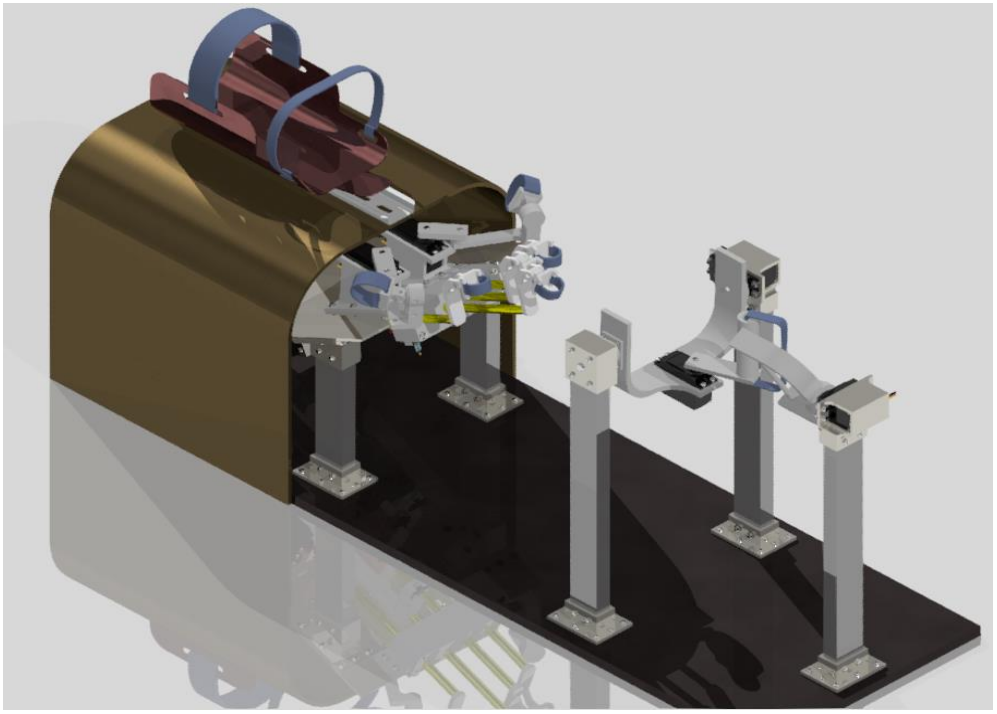

Figure 39: final 3D structure design assembly

5.8. kinematic modelling and simulation

This section presents and describes some analyses over the proposed mechanical system for deeper investigation and test the system behaviour in such conditions as the maximum stress that can be applied on the mechanical parts and simulation of the trajectories, velocities, and workspaces of the system's end-effectors. TO achieve these objectives, several methods and software's were used, mainly the Autodesk Inventor® to derive the stress

analysis, and MATLAB® with Simulink® and Peter Croke to drive dynamic and Forward kinematics.

5.8.1. Forward Kinematic model of the proposed system.

A forward kinematic model was constructed and simulated for further investigations, mathematically represent the proposed system, and test and validate the kinematic behaviour of the proposed mechanical system. While the proposed robot with an end-effector may have several kinematic features indices, these are all connected to the robot's motions, not the device's design or implementation. For the finger rehabilitation process, the requisite coordinate systems must be constructed. The developed kinematic model with its reference frames is shown in Figure 40Figure 40.

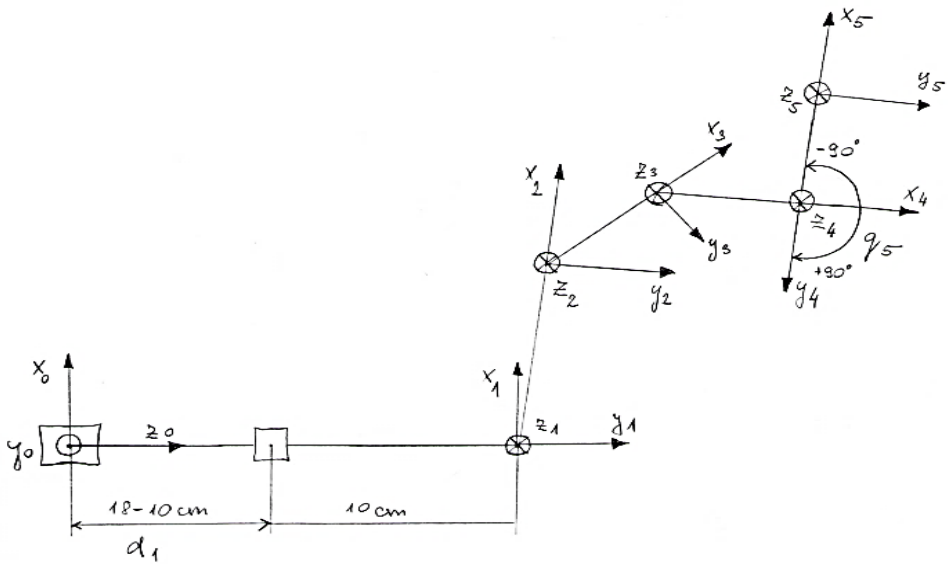

Figure 40: Coordinate frame of the proposed finger rehabilitation system.

For the sake of visibility and to keep the image legible, the axis names $(x_0, x_1, ..)$ were omitted. Instead, the Reference Frame (RF) was indicated, i.e., Reference Frame 02 is RF02 in the pictures. The colour for each axis can also be seen.

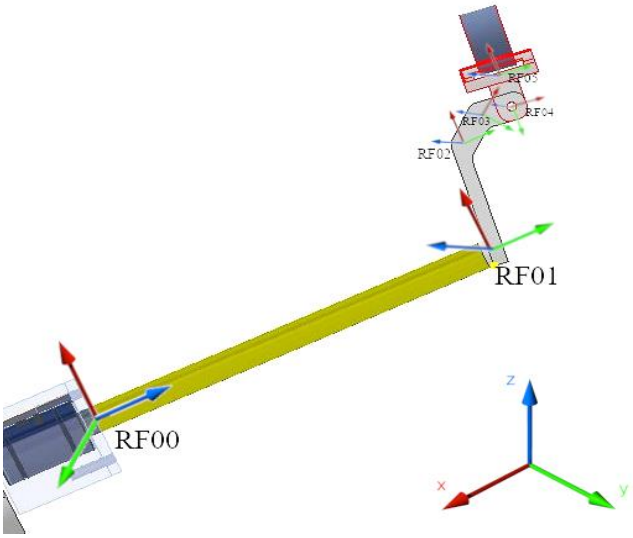

Figure 41: Detailed view of the robotic arm

The Denavit–Hartenberg parameters shown on Table *7* was defined considering the actual mechanical design of the driving and transmission mechanism with the end effector (fingertip holder).

Table 7: DH Parameters

θ_i	a_i	d_i	α_i
0	0	100-180	90°
5°	30	0	0
30°	13	0	0
45°	10	0	0
θ_5	6	0	0

Then, the reference frames were defined based on the following drawing.

Workspace

For the workspace plot, it is not necessary to install or use any third-party toolbox or software; just MATLAB will be enough.

All the values from the DH-table are defined as constant but two: d1 and Theta 5 since they will be the changing variables.

Then, it is vital to notice that the transformation matrix for a prismatic joint is slightly different from a rotational joint.

$$T_{10} = \begin{pmatrix} cos\,(\theta_1) & -sin(\theta_1)cos\,(\alpha_1) & sin(\theta_1)sin\,(\alpha_1) & 0 \\ sin(\theta_1) & cos(\theta_1)cos(\alpha_1) & -cos(\theta_1)sin(\alpha_1) & 0 \\ 0 & sin\,(\alpha_1) & cos\,(\alpha_1) & d_1 \\ 0 & 0 & 0 & 1 \end{pmatrix} \textit{Eq 19}$$

$$T_{21} = \begin{pmatrix} cos\,(\theta_2) & -sin(\theta_2)cos\,(\alpha_2) & sin(\theta_2)sin\,(\alpha_2) & a_2cos(\theta_2) \\ sin(\theta_2) & cos(\theta_2)cos(\alpha_2) & -cos(\theta_2)sin(\alpha_2) & a_2sin(\theta_2) \\ 0 & sin\,(\alpha_2) & cos\,(\alpha_2) & d_2 \\ 0 & 0 & 0 & 1 \end{pmatrix} \textit{Eq 20}$$

For joints 3, 4 and 5 the matrix will be the same, just changing indices.

The final transformation matrix will be given by:

T50 = T10 * T21 * T32 * T43 * T54;

At this point, it is essential to notice that the variable $T10$ in the Matlab code refers to the Transformation Matrix ${}^{0}T_{1,}$ which refers to the homogeneous transformation from reference frame 1 to reference frame 0. The same happens for T21, T32 and so on.

To get the end-effector position:

reference = [0; 0 ;0; 1];

position = T50 * reference.

So, the coordinates will be stored in x, y and z variables.

x = position(1);

y = position(2);

z = position(3);

Then, the angle limits for joint5 and linear limit for joint 1 is defined. The ngrid command is used to “prepare” Matlab to calculate all possible values for the workspace.

% Angle restrictions for rotational joint

% q5 from -90deg to +90deg and divide into 90 units

theta5=linspace(0, pi,90);

% Length restriction for prismatic joint

d1 = linspace(100,180,90);

%implementing the output from DH convention

[D1,Q5]=ndgrid(d1,theta5);

After this point, change every occurrence of d1 in x, y and z to D1 and every occurrence of theta5 to Q5. It can be done using a text editor with “Search and Replace” tool. Then a new X, Y and Z are defined with this replacement.

plot(Z(:),X(:),'.');

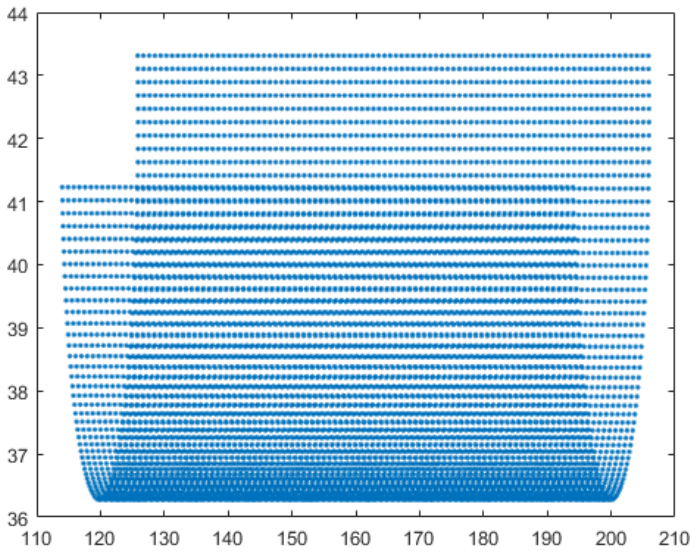

Figure 42: Robot’s end-effector workspace plot

a) Trajectory

To build the robot model using Peter's Corke toolbox, the following links were created, respecting the DH-table.

```
L(1) = Link ([0 L1 0 pi/2 1],'standard'); %The "1" parameter indicates that this is a prismatic joint
%Joints 2 to 4 have a fixed theta
L(2) = Link ([pi/32 0 L2 0]);
L(3) = Link ([pi/6 0 L3 0]);
L(4) = Link ([pi/4 0 L4 0]);
% The last Joint is rotational, theta=0
L(5) = Link ([0 0 L5 0]);
% The prismatic Joint can have from 100 to 180mm
L(1).qlim = [100 180];
```

Initial and final states should be defined as a vector with 5 dimensions, for prismatic joints the dimension will be the length, and for rotational joints will be the angle:

```
%This is the initial state for the robot, theta = 0, to visually verify how
%the robotic arm will stay at this orientation.
q0 = ([100 pi/32 pi/6 pi/4 -pi/2]);
%This is the final state, so the trajectory can be plotted.
qf = ([180 pi/32 pi/6 pi/4 pi/2]);
```

The function jtraj from the toolbox is used to get the trajectory from one point to another.

Then, the homogeneous transform is obtained.

```
%Get the trajectory from q0 to qf
q = jtraj(q0,qf,t);
%Then the homogeneous transform for each set of joint coordinates is given by
```

T = Rob.fkine(q);

%where T is a vector of SE3 objects.For example, the first point is T(1)

%the translational part of this can be extracted using the transl method

To plot the trajectory, the simulation considered the initial state as $\theta_5 = 0\,°$ and the final state as $\theta_5 = 180\,°$ and the prismatic joint varying from 180 to 100mm.

But, considering the Peter Corke Robotics Toolbox, the simulation will go from -90 to

90 (always in radians).

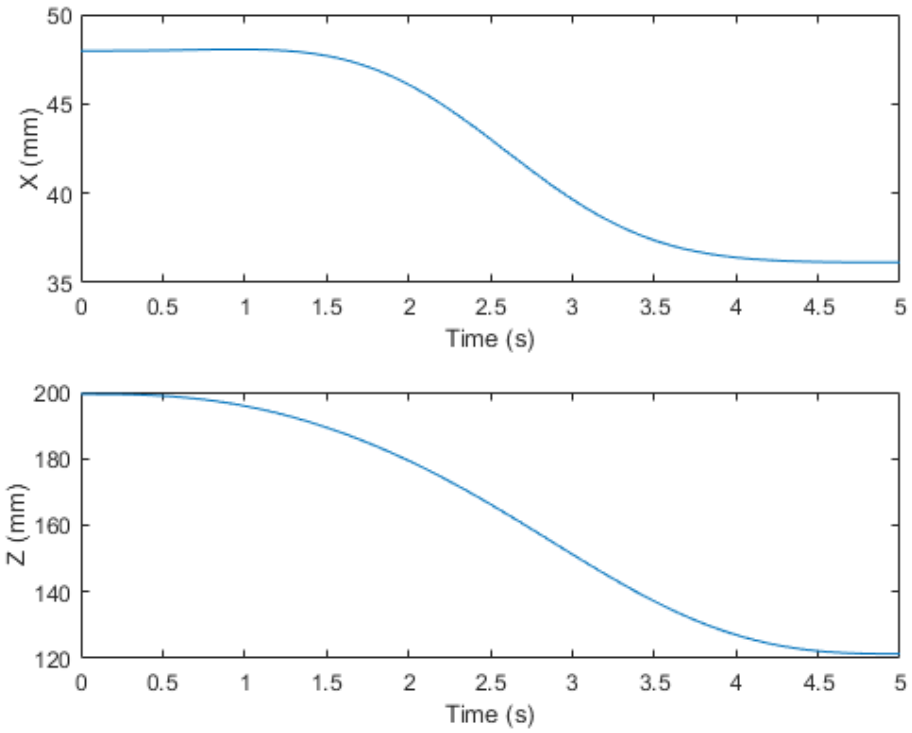

Figure 43: X and Z position for the end-effector

(When the joint 5 goes from -90 to 90 degrees.)

For visual verification, the robot was plotted in both positions theta5=-90 and theta5=90

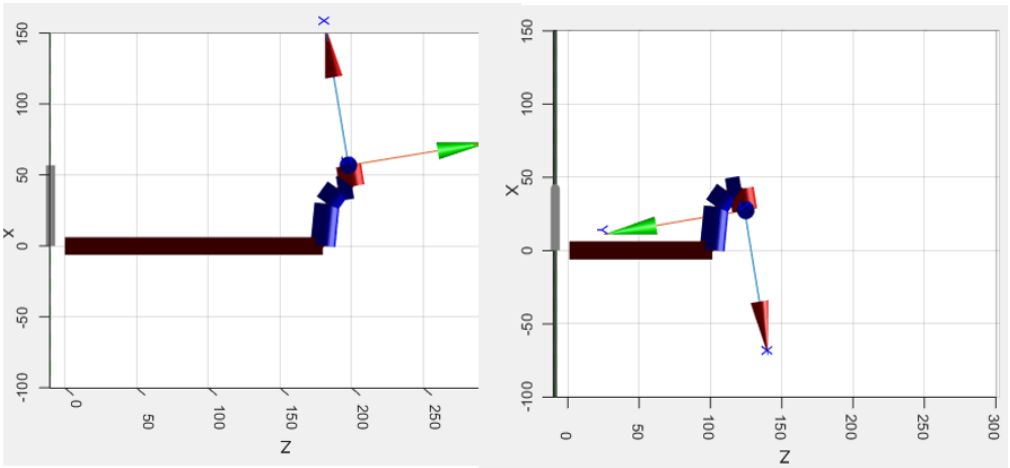

Figure 44: Driving transmission mechanism of the proposed system end-effector:

(a) Theta5 equals to -pi/2; (b) Theta5 equals to pi/2

Chapter 6: Hardware and Software Development

This chapter describes the technical and functional design and development of embedded hardware and software to control and mechanical structure and provide sufficient power to control motions and read the ROM and force of the end-users. The proposed system employs nine servomotors at the hardware level, six for fingers and two for wrist motions, and one for a forearm. Additionally, six force-sensitive resistors were used to extract the grabbing force of the patients. Besides, eight-position sensors were used to read the performed ROM of the patients. Generally, everything is controlled by a Raspberry Pi 3B+. in the software level, a user-friendly embedded graphical user interface GUI and logic were developed using Python programming language. For database, MongoDB is used for storing patient and therapist information as well as the results and graphs. As previously stated, the robot's purpose is to automate repetitive tasks, make therapies less human labour intensive, and keep track of patient’s progress in a systematic way. Moreover, a novel 2D game was developed for motivating patients for more practising by giving them small and fast achievable goals, such as winning completing a game level. Additional to these features, the device is portable, and the application is independent of the operating system.

6.1. Electrical System Design

The primary objective in building the motherboard was to provide a structure to support 9 DC actuators and enable the reading of 6 force feedback, 6 angular position feedback. the hardware design handles data integration and signal gathering and processing. Figure 45 demonstrated a 3D model of developed embedded electronic system components; the proposed circuit was developed using Kicad software. In picking materials, it was decided to minimize the overall costs while adhering to the project's specifications. Their data

processing and visualization abilities were essential, too. Besides the previously describe servomotor, figure1. Shows the 3D assembly of the proposed electric and electronic schematic circuit. Which consists of the rest of the used components is presented as a bill of materials (BOM) which includes:

1. **Embedded Microcomputer**: Raspberry pi 3B+ [135]. it is a single board, compact, and low-cost computer. It is a little capable device that capable of processing anything just as a traditional computer. Technically, Raspberry pi 3B+ required 5V/2.5A DC via micro-USB as input power it is also possible to power throughout GPIO. Other features are Power over Ethernet (PoE) (with the add-on PoE HAT). Moreover, it comes with a 64-bit quad-core processor CPU running at 1.4GHz, with 1GB RAM. In addition, it has a built-in dual-band 2.4GHz and 5GHz wireless LAN, Bluetooth 4.2/BLE, and a speedier Ethernet network. The device also supports 802.3at Power over Ethernet (PoE). The dual-band wireless LAN is equipped with modular compliance certification, which helps decrease both cost and time to market [136]. Additionally, it consists of 40 pin headers (26 GPIOs), one HDMI port, which can connect it to HD monitors, 3.5mm analogue audio-video jack; Four USB 2.0 ports are sufficient to link the machine to a keyboard and mouse, as well as to the CSI, DSI, and the screen itself. Besides, it consists of a microSD card socket. a Linux based operating system called Raspbian is the most popular OS compatible for Raspberry pi [137]. The most used programming language for projects in raspberry pi is Python because it has lots of libraries specifically for GPIO pins and the modules for raspberry pi [138].
2. **Adafruit servo driver- PCA968** [139]. you should not copy the references and figures numbers. There are 16 output ports. Each port

contains three pins: a "V" (positive voltage), a "GND" (ground) and a "PWM" (pulse-width modulation) output. The PWM frequency must be the same for all PWM's. Technically, PCA968 module has two power pins VCC this power logic ranged 3 - 5VDC, while V+ optional power pin can be supplied within 5-6VDC power range. Additionally, PCA968 module has three control pins, including SCL - I2C clock pin, SDA - I2C data pin, and OE - Output enable which use to instantly deactivate all outputs

3. **ADC converter**: because Raspberry pi is a microprocessor-based which cannot process the analogue inputs. Therefore, MCP3424 [140] A/D an analogue to digital is integrated module converter were used. MCP3424 module has a 4-channel differential input operation. However, its resolution can be set to 12, 14, 16, and 18 bits, representing the accuracy of data conversion. Technically, MCP3432 A/D converter chip operating voltage ranging 2.7 - 5.5VDC, Onboard programmable gain amplifier (PGA): x1, x2, x4, x8. The differential input full-scale range is -2.048V on the PGA. Output Interface I2C is used.
4. **Force Sensor:** Force Sensitive Resistor (FSR) branded CP24 FSR, technically it has a force measurement range of range 0.2...100N, Nominal operating voltage 1..5 VDC, Operating temperature -40...75°C, Typical activation resistance range 1 MW > RL > 2 kW, CP24 FSR self-adhesive property with External dimensions 18.3 x 54.15 x 0.34mm
5. **OPAMP LM324** [141]**:** The LM324 operates with a single source and has four operating amplifiers. 1.5 V to 16 V, dual supplies: ±1.5 V to ±16 V. It is affected by Common-Mode the entire input voltage range is included. With the ground allowed direct sensing nearby, the open-

loop differential voltage amplification is 100 volts per millivolt. Typical, which is 7mV at 25C with each channel having 0.175IQ and 35nV/rtHz at 1kHz; typical, which is 7mV at 25C with each channel having 0.175IQ and 35nV/rtHz at 1kHz; typical, which is 7mV at 25C with each channel having 0.175IQ and 35nV/rtHz at 1kHz.

6. **Electronically Cooling system**: the cooling system was designed and implemented to protect the microprocessor from overheating. For that purpose, a DC FAN 12V DC 120x120x38 / 10W, Airflow: 234 m^3 / h (3.90m^3 / min), with ball bearings, which has the feature of robust, high performance, long-lasting for ventilation in microprocessor,
7. **Olimex SHIELD- EKG /EMG** [142]: The ECG shield was built to gather ECG signals from the Arduino. New ways to learn about biofeedback are created because of the shield. The muscles' movements can be tracked by monitoring and recording their The ECG/EMG potentials generated by muscles are sent to the CH1 IN+/CH1 IN- inputs, where they are transformed into a single stream of data.
8. **Relay board**: The relay consists of three pins: an open pin, a closed pin, and a standard pin that is attached to a coil. A status indicator LED is connected to the standard pin. This appliance has a Contact voltage of 10A, 30VDC. Every channel has an LED that shows that the current is flowing. This relay supplies 3.75 to 6 VDC. with a Contact Current of 10 A
9. **Monitor, keyboard, and mouse**: these read and write hardware devices are used in the proposed system to input data and display data.

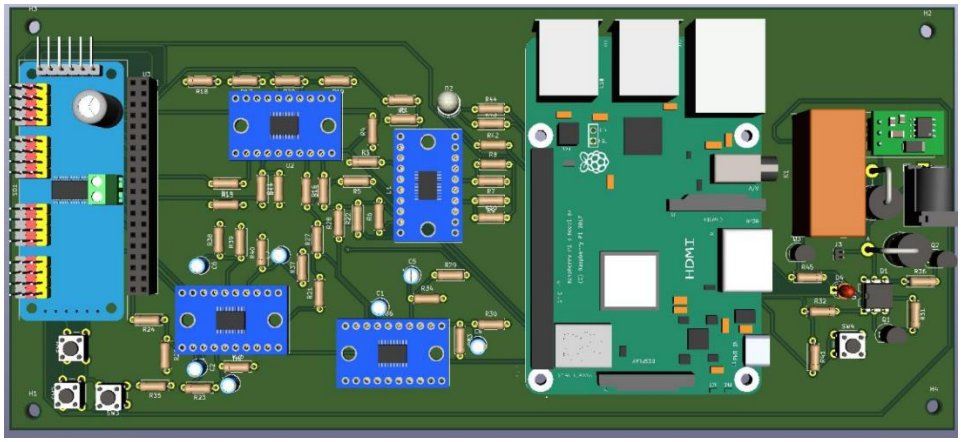

Figure 45: 3D assembly of the proposed electric and electronic schematic circuit.

6.2. Servo motor speed and position control

The controls for eight servo motors will be shown in this section. Most servomotors have the functionality to be commanded with high precision as to rotational and angular positions [143]. This kind of servo motor is further distinguished by the fact that the control signal isn't used to keep the servo fixed in position but rather as an indication of the rotational direction and speed [144]. However, the one big issue with servo motors is they do not support the speed control. The correlation between the position of a servo motor and the duty cycle of the PWM signal that is supplied to the servo motor is positive. The speed control can be achieved by changing the duty cycle gradually. The step size and the time between steps will determine the speed of the servo motor. Figure 46 the control method can be replaced with any control method.

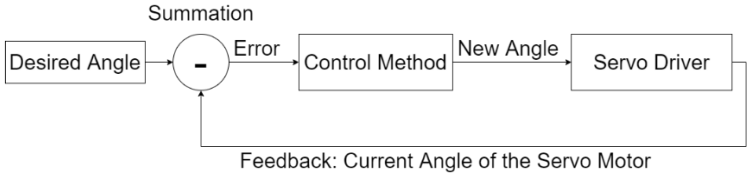

Figure 46: Servo motor position control

In Figure 46, the control method block is modular, which means it can be replaced with any controlling method. In Figure 47, the control method is replaced with Proportional Derivate (PD) controller and saturation block. Step and delay determine the speed of the servo motor. PD controller calculates the required step to reach the desired angle, but the output step can also be big, making the speed bigger. Because of security concerns, the step should be limited between maximum and minimum. That is why the saturation block is used. The servo motor is calculated and sent to the servo driver based on the limited step new angle of the servo motor. After sending, the application waits for a pre-defined time.

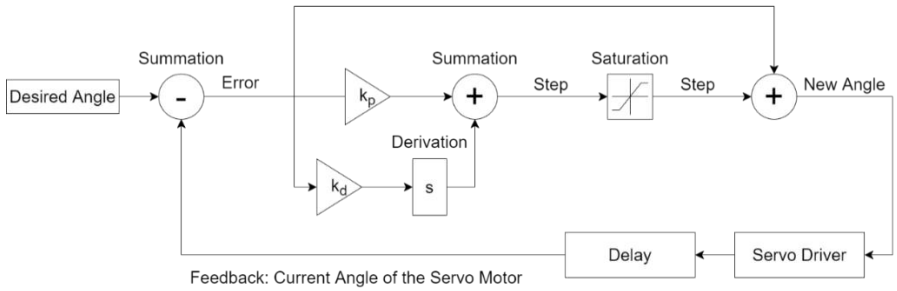

Figure 47: Servo motor speed and position control block diagram

On the other hand Figure 48 demonstrate the motors implementation onto the developed driving unit's rigid body

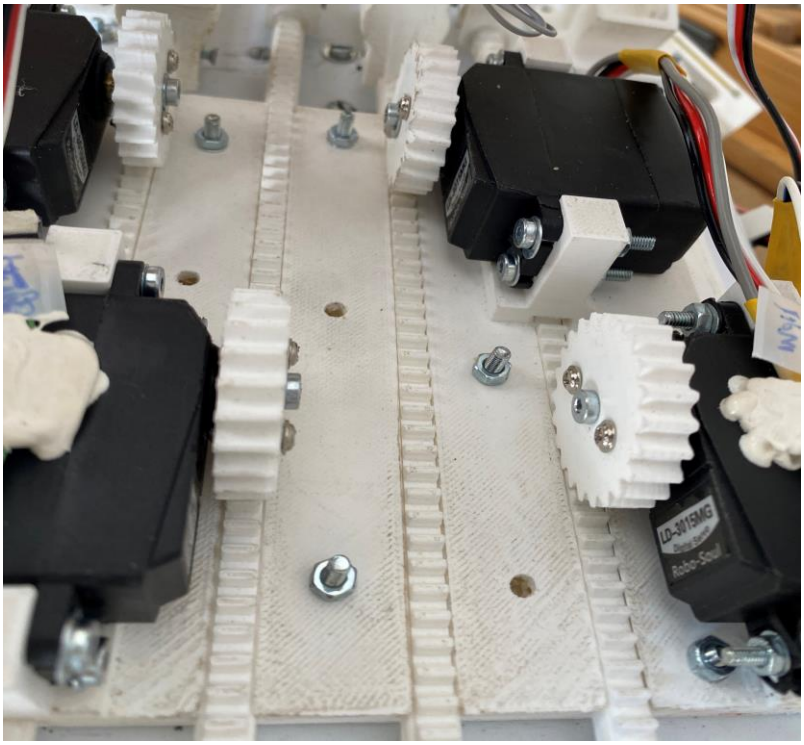

Figure 48: Motors connected to the 3D printed parts

6.3. Design And Development an Integrative Grabbing Force Sensing Unit

In rehabilitation, measuring and evaluating the fingers grabbing force and strength has been routinely checked to in which the outcomes of the rehabilitation progress can be evaluated of stroke patients. Developing a practical and affordable hand grasping force sensor is still challenging since various limits should be addressed. Therefore, most of the existing rehabilitation robotics that researchers and institutes developed are not equipped with any way to evaluate the user's progress.

This section described a novel development and implementation of a self-assessment approach to measure fingers grasping and strength of the proposed system users. A piezoresistive sensor (FSR) sensors were embedded on the device to serve as a force sensor, and the grabbing force data will be collected

and shown in real-time during the therapy through the developed GUI, and the collected data will be stored for later evaluation. The developed algorithm will analyse the input forces and store it in a local database and show them as a graph. The proposed design helps the therapist and the patient easily monitor the improvement process by monitoring the grabbing force after each therapy session or group of sessions.

6.3.1. Design Of the Integrative Force Sensing and Working Principle

the modular grasping force sensing's entire mechanical structure is illustrated in Figure 49 (a, b). The proposed structure mainly consists of a sensor base, FSR sensor, sensor contacting cover, spring. As it can be observed, the whole structure of the force-sensing mechanism is part of the motion driving mechanism, it plays the role of the rack-guiding shaft connection point. The sensor base is part of the rack mechanism; however, it was uniquely designed it was designed to be a house for the FSR sensor, and the utilized sensor is equipped with backing adhesive to stick it at the sensor base. The sensor base follows the structure of the FSR sensor, so part of the flexible substrate of the FSR is secured with a cover to avoid any later vibration that can affect the sensitive area of the sensor. Additionally, At the top front of the sensor base, a small shaft designs. On the other side, the sensor cover is mounted into the guiding shaft, facing the sensor base; the guiding shaft is like a tube, empty from inside, so the sensor base male shaft go es inside the guiding shaft and then screwed into it with 5mm limited movement, so that hold the rack and guiding shaft together which obviously hold the sensor base and the sensor cover together with 5 mm linear motion. Besides housing the FSR, the sensor base also houses the sensor cover, making the whole mechanism has a sandwich structure. The FSR is a slot in between the cover and sensor base.

A solid round tactile pad was applied into the face FSR cover, with the portion of the force sensor that is sensitive to variations in sensitivity glued to the pad.

As shown in Figure 49 (b), the contact pad has a size of 5mm, which suits the susceptible region of a force sensor. the sensor contacting cover.

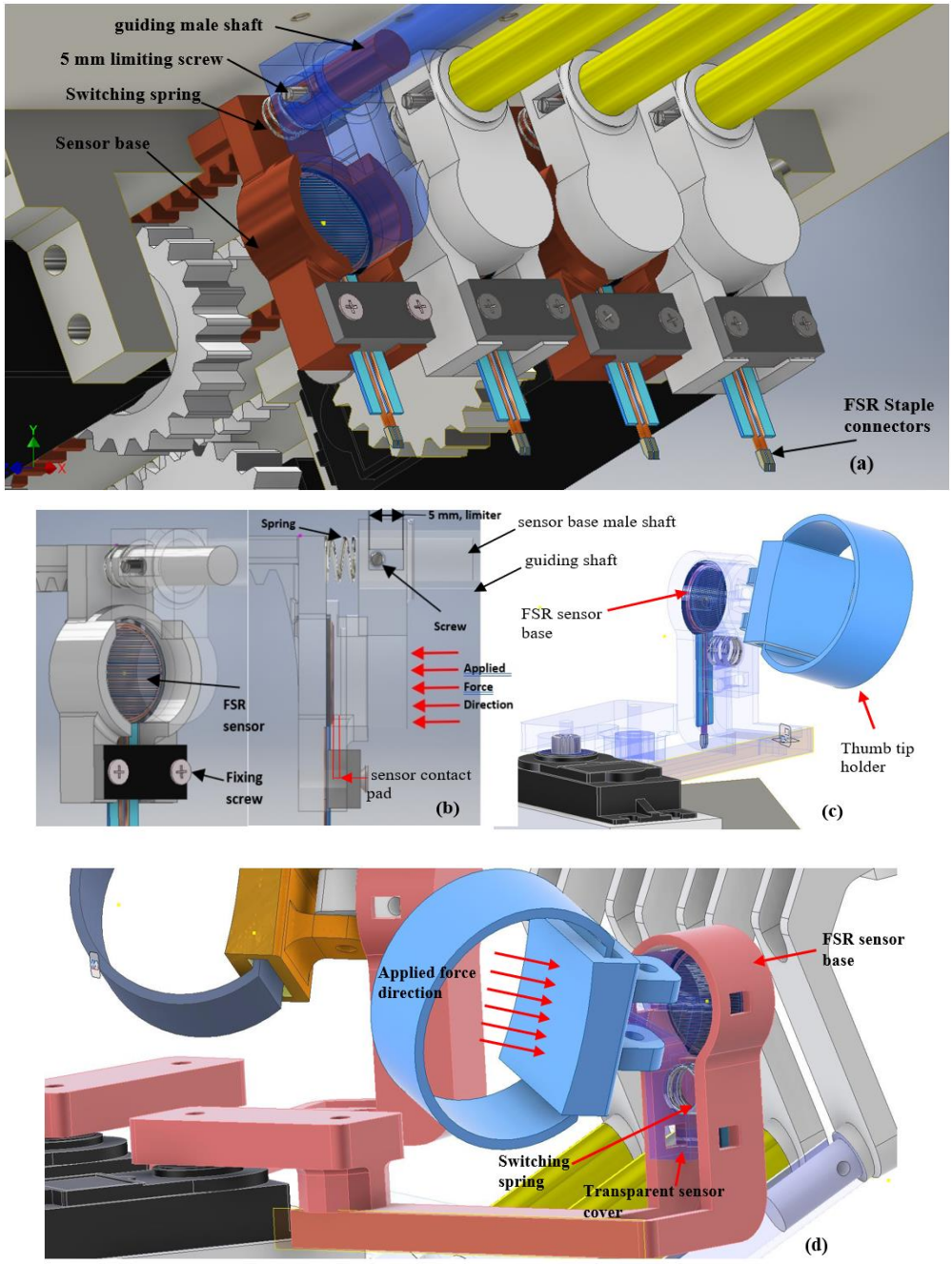

Figure 49: Force-sensing resistor:

(a) 3D CAD structure of the proposed grabbing force mechanism which consists of four integrative force sensing units for four fingers. (b) The detailed structure of the FSR sensor module, in which the contact pad is used to improve the sensitivity and stability of the FSR sensor and switch spring to avoid undesired contacts. (c, d) the thumb tip proposed an integrative force-sensing measurement approach. Which mainly consists of, FSR sensor, Sensor base, sensor cover with contact pad, and switching spring.

Moreover, to avoid constant contact between the sensor cover pad and the sensitive area of the FSR sensor, a spring is added between the sensor cover and the sensor base. The advantage of adding the sensor it makes the whole integrative force sensing mechanism like a normally open switch, which means the sensor and will contact point of the sensor cover will be integrated just when there is an external force pushing the sensor cover towards the FSR sensor. Since the sensor cover is part of the guiding shaft and the fingertips holder is part of the guiding shaft, this means when the patient applies a small amount of force on the fingertip holder that force will be transmitted to the sensor cover forcing the spring to be compressed and make contact over the FSR sensor within 5mm limited linear distance.

As shown in Figure 49 (c, d), the same concept with minor modification was applied on the thumb holder mechanism. However, it is a little more direct since there is no rack and guiding shaft mechanism is needed.

6.3.2. Electromechanical Implementation

In this section, the physical implementation of the structure of the proposed design. Figure 50 (a) demonstrates the physical integration of the proposed design main complement, including the FSR sensor, guiding shaft, sensor cover, and sensor base. Figure 50 (b, c) illustrate the working principle of the proposed design,

1. Figure 50 (b) shows an external force acting on the fingertip holder that transferred to the sensor cover. This force makes contact between the sensor sensitive area and sensor cover contact surface; it is observable that the spring was compressed because of the applied force.
2. While in Figure 50 (c), shows when the force was released from the fingertip holder, which is the natural state. In this case, the spring-applied force in the opposite direction releases the contact between the FSR sensor sensitive area and the senor cover connected surface.

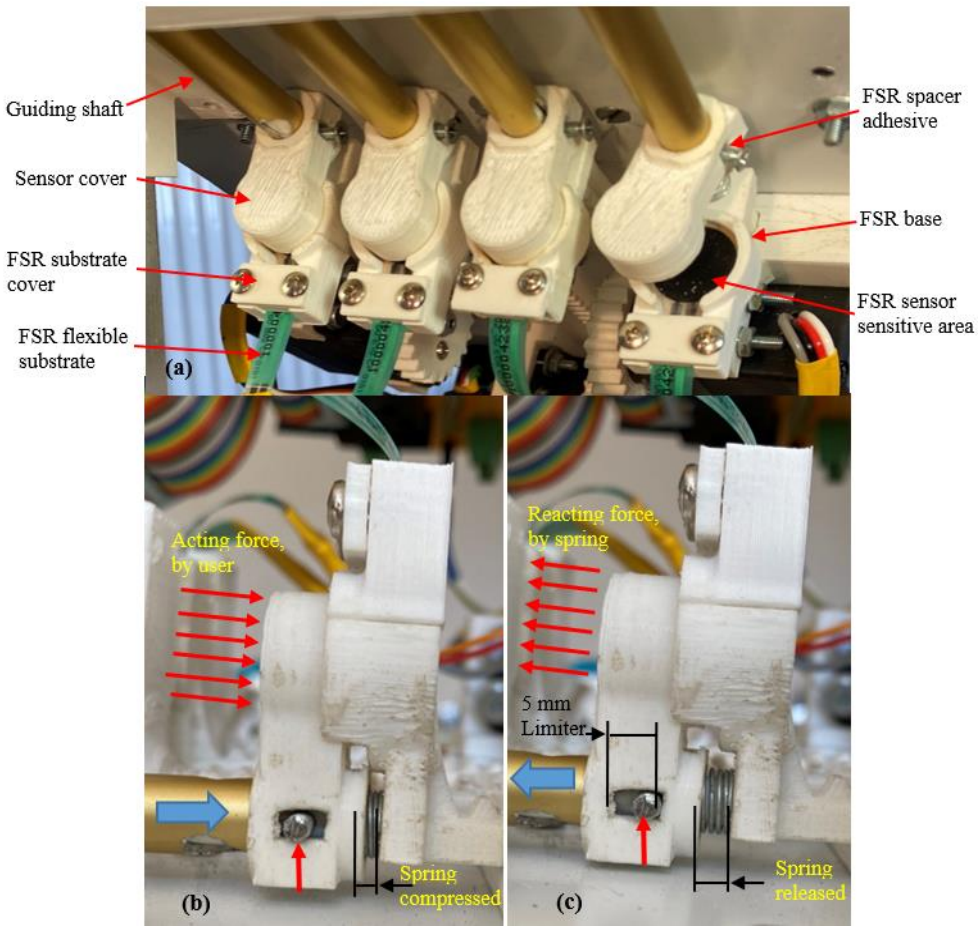

Figure 50: Electromechanical Implementation.

(a), physical integration of proposed integrative design main complement. (b, c) the two cases when there is, and there is not grabbing force applied onto the sensor sensitive area.

Figure 51 illustrates the thumb rehabilitation mechanism and the force-sensing design; the thumb integrative force sense follows the same described working principle. However, the whole mechanism of the four fingers and two thumbs (right, and left) was tested and showed promising results. However, to get the best readings, calibration and signal to condition, including filtering and amplifying the FSR readings were needed.

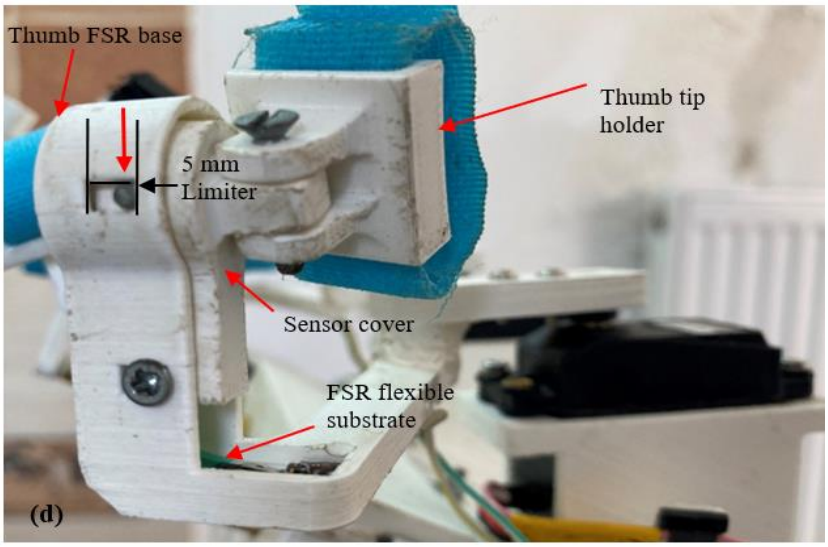

Figure 51: The proposed integrative force for the thumb.

6.3.3. Force-sensitive resistors

Force-sensitive resistors (FSR) is a piezoresistive sensing technology, they are made from plastic, and the connection tab is crimped on delicate material. When force is applied or released, the FSR changes and makes it act as a variable resistor based on pressure change [145]. It's been proven that robotics and biomechanics applications frequently use FSR detectors [146]. Especially for robots that interface with the outside world [147]. The

resistance of FSR can be calculated as below, where l is length, A is cross section and ρ is the resistivity of FSR [148]:

$$R = \rho \frac{l}{A} \tag{1.}$$

When stress is applied to the FSR longitudinally, change of resistance can be calculated as follows[148]:

$$\frac{dR}{R} = \frac{d\rho}{\rho} + \frac{dl}{l} - \frac{dA}{A} \tag{2.}$$

Since these sensors act like variable resistors, a voltage divider circuit should be used to measure the sensor output [149], and the resistor named R1 can be replaced with an FSR, Figure 52. To calculate the output voltage, the following equation can be used[150]:

$$V_{out} = \frac{R_2}{FSR + R_2} V_{in} \tag{3.}$$

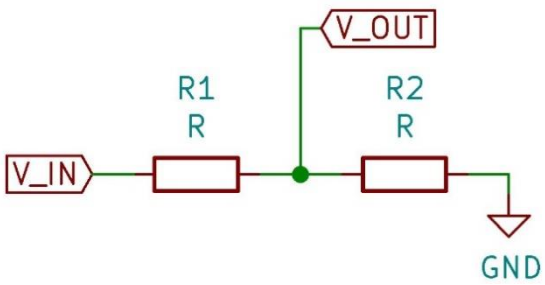

Figure 52: Voltage divider circuit

A. Signal conditioning for sensors

The noise in the circuit can easily mislead us when using analogue sensors. That is why analogue sensors' outputs need signal conditioning. For this project, force-sensitive resistors are suitable since we are trying to measure the grabbing force. To reduce the noise in the circuit, I used a second order low

pass filter. The best part of this filter is its operational amplifier; the output voltage can be changed by modifying the gain of the amplifier, and also higher-order filters can also be created by chaining this filter. After measuring the frequency of the noise in the circuit, we can calculate the required resistance and capacitance for the second-order active low pass filter (1).

$$f_c = \frac{1}{2\pi\sqrt{(R_1 \times R_2 \times C_1 \times C_2)}} \qquad (4.)$$

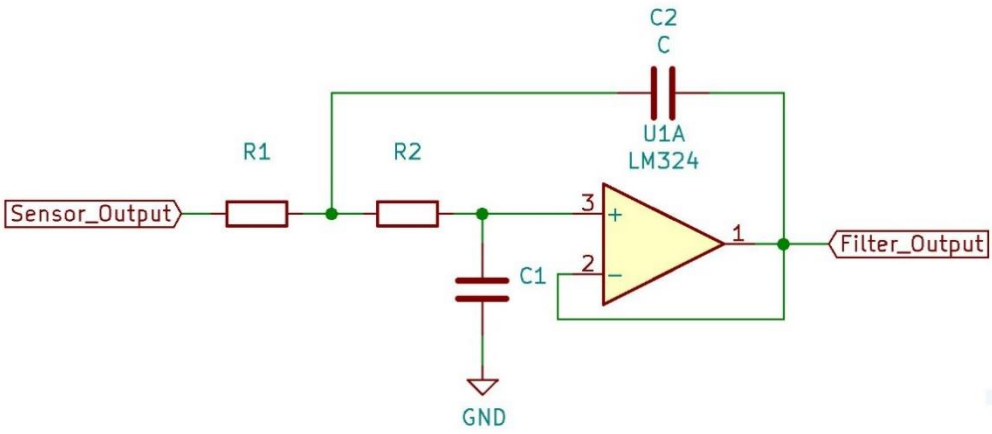

Figure 53: Second order active low pass filter

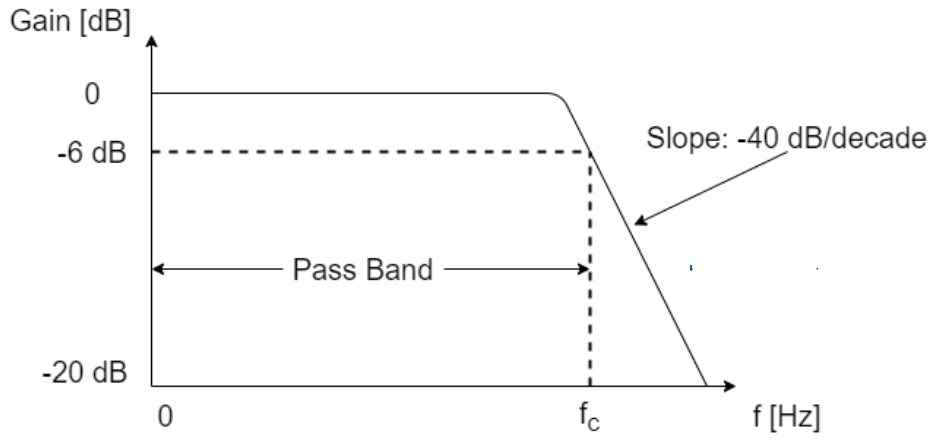

Figure 54: Bode plot of second-order active low pass filter.

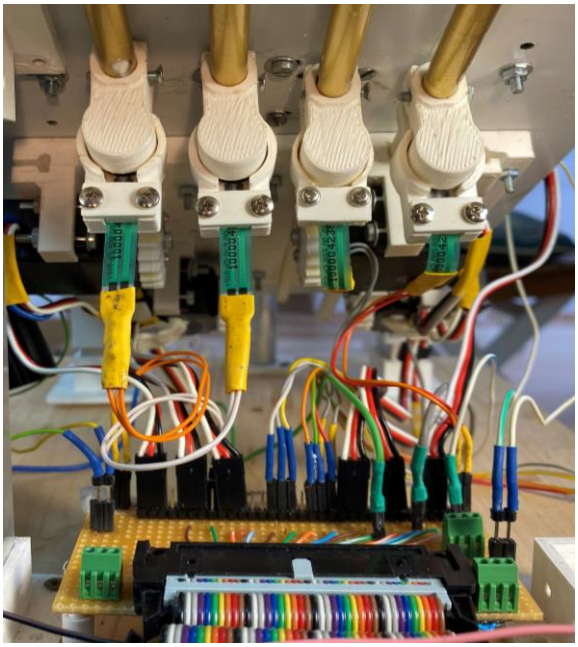

Figure 55:Connections

6.3.4. Analogue to digital converters

Most of the signals in the environment are analogue, but microcontrollers can only understand digital signals [151]. That is why analogue signals should be converted to digital ones. A comparator is the primary part of an analogue to digital converter (ADC). 1bit ADC works as follows, and the microcontroller converts the read data to decimal based on reference voltage:

$$1^{st}\ bit = \begin{cases} 0, V_{in} < \dfrac{V_{ref}}{2} \\ 1, V_{in} > \dfrac{V_{ref}}{2} \end{cases} \quad (5.)$$

The resolution of an ADC is equal to the number of bits and determines the smallest voltage increment that can be recognized. Each bit of *N* bit ADC can be set by using the formula below [152]:

$$n-th\ bit = \begin{cases} 0, V_{in} < \frac{V_{ref}}{2^N}\sum_{i=n}^{N} 2^i \\ 1, V_{in} > \frac{V_{ref}}{2^N}\sum_{i=n}^{N} 2^i \end{cases} \text{ where } 1 \leq n < N \qquad (6.)$$

One of the common ADC architectures is delta-sigma (ΔΣ)[152].

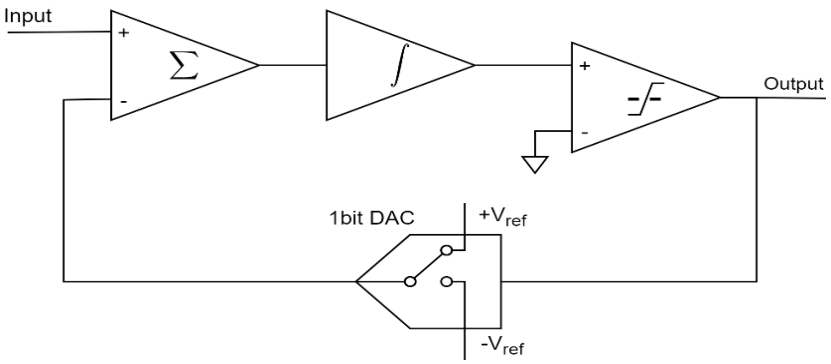

Figure 56: Delta-sigma ADC architecture

6.3.5. Inter-Integrated Circuit Communication Protocol

I2C is a serial communication protocol interconnecting integrated circuits, which makes transferring data in between multiple devices using only two wires, namely Serial Clock (SCL) and Serial Data (SDA)[153]. This protocol supports half-duplex communication, which means only reading from or writing to a device is possible at a time[154]. The devices which are connected to SDA and SCL busses are named master and slave. The master controls the SCL bus, and by using the SDA line, it can read from or write to the slaves. A slave can be identified by their address which can be configured by connecting the address pins to ground or supply voltage. A master device can handle 128 or 1024 different addressed slaves depending on whether the master uses a 7bit or 10bit when communicating. 10bit master devices are not used widely compared to 7bit devices. All slaves should be connected to SDA and SCL busses in parallel,

I2C transfers data in a stream of 8bits and data exchange happens in the following sequence[155]:

1. The master starts by pulling low first SDA and then SCL.
2. Sends the address of the slave and whether wants to read or write.
3. Waits for an acknowledgement (ACK) / negative acknowledgement (NACK) bit.
4. Transfer of data happens in chunks of 8bits, and after every chunk, the receiver has to reply with ACK/NACK bit. This repeats until the data is transferred fully.
5. To stop the transfer, the master switches first SCL and then SDA high.

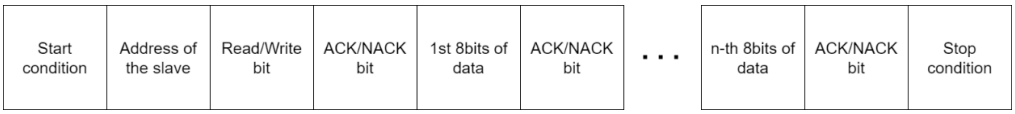

Figure 57: I2C Message

6.4. The Power Supply Unit Design and Hardware Implementation

Concerning power management of the proposed system, to supply a stable voltage and sufficient required current for different electronic components that required a different voltage level. The employed LD-3015MG servomotor requires 7.4VDC, while Raspberry Pi 3B+ consumes 5VDC[135], whereas the cooling fan requires 12 VDC. Therefore, to meet these needs, the utilized power supply unit includes: an AC/DC converter, which takes AC 110-260v as input, and gives 24 VDC, and is able of driving a 6A load with a high-efficiency current. This 6A is sufficient to power 5 servomotors running simultaneously in case of active fingers therapy. Additionally, two buck converters were used to regulate the 24 VDC. the first-named CN4015-3,

which has an input voltage range between 4V and 40V, and adjustable output voltage can be from 1.5V to 35V [156] was used to step down the 24 VDC to 7.4VDC which was used to supply the servomotors through its motor driver. The second buck convertor, named MF-6402402, with adjustable output voltage, was employed to step down the 24 VDC into 12 VDC, which was used to power the cooling fan circuit. In addition, both buck converters include built-in current limit features, which also include an internal MOSFET over current protection mechanism. Whereas, the Raspberry Pi used an A-type female USB connection to obtain power from an external power converter.

The proposed comprehensive electrical and electronics system is shown in Figure 58. This figure presents the developed embedded motherboard, which consists of the essential parts such as, microprocessor, power supply units, relay switching unit, cooling unit, motor driving unit, ADCs unit, and filtering unit.

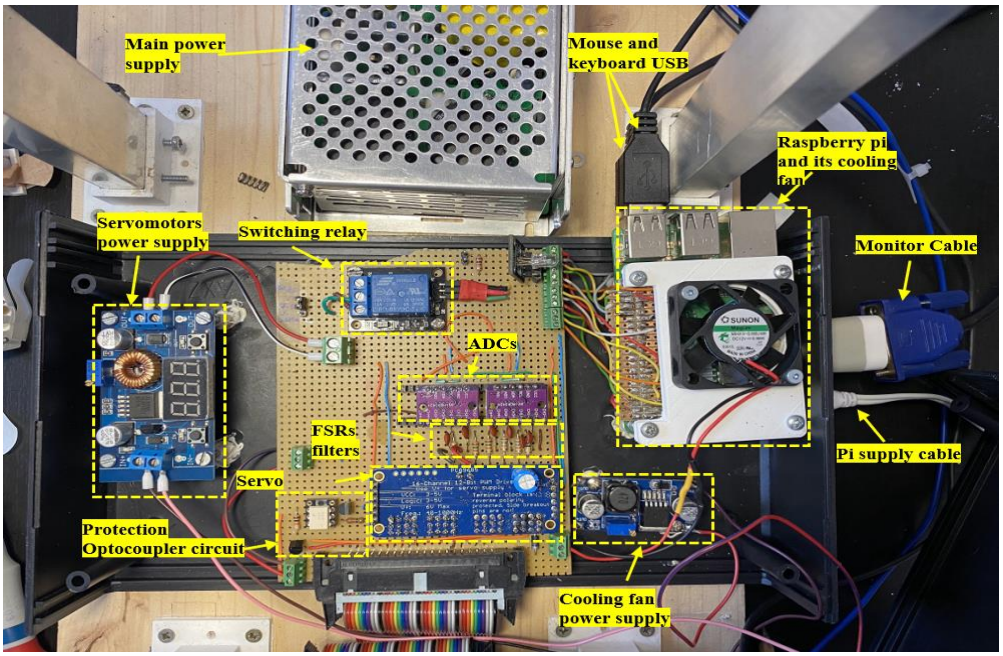

Figure 58: A low power consumption. illustrates the hardware composition and relationship.

6.5. Software: Back-End and Front-End Development

The Graphical User Interface (GUI) allows patients to interact with a developed user-friendly dashboard used in conjunction with the rehabilitation hardware and proposed control method. The specially developed UI was developed based on therapists suggestions; it provides an interactive and motivating training environment with feedback, based on measuring selected quantitative features of hand function such as ROM tracking and grabbing force. The developed software, also equipped with a specially developed integrative game and a diagnostic therapy assessment, was developed to provide an adjustable evaluation UI to check the therapy and patient progress. As can be seen in Figure 59, the front-end of the developed UI consists of multiple tabs: patient information, session information, hand parameters, therapy, and evaluation. It simply works; when a patient comes, the therapist starts by writing the health insurance number of the patient or any ID number. Because this number is unique, the patient who is new or who came before can be checked easily by searching for the number in the database. If it is the patient's first time for therapy, fields can be filled, and a new patient file can be created by clicking the save button. And if the patient is someone who already came before. All his/her data can be loaded with the help of the load button. This data is store in a MongoDB database collection named patients. This tab contains data about both patient personal and stroke information.

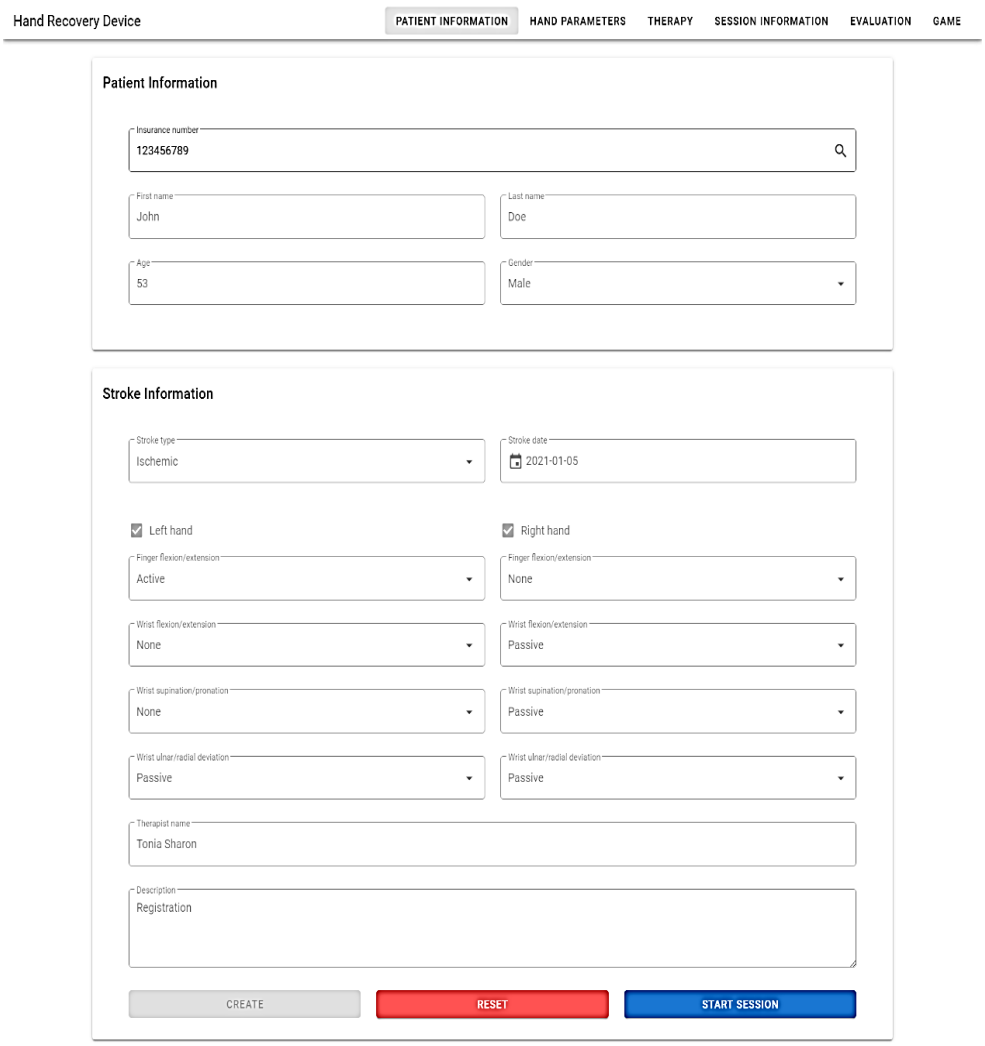

Figure 59: Front-end of a specially developed (Patient information tab on GUI)

One of the most used programming languages in the world is JavaScript. JavaScript is an implicitly typed language, which means the programmer does not need to define the type of variables. Interpreter manages the types for low-level languages [157]. JavaScript, alongside HTML and CSS, is mainly used for creating web applications. Many open-source JavaScript libraries/frameworks that help build web applications more accessible and

Vue.js can be shown as an example. One of the benefits of this framework is the structure of the project. The structure of a page written in HTML, CSS, which is used to make the page look prettier, and the logic that determines how the page should react to different interactions written in JavaScript can be in the same file and makes component-based coding much more manageable. The variables that are used in components are reactive, which means when they have been modified the UI changes accordingly.

With the help of a framework called Electron, websites can be converted into standalone desktop applications, and these applications are cross-platform, which means with one source code, the application can be used in different operating systems, such as Windows, Mac and Linux.

6.5.1. State Management System

Handling globally accessible variables becomes more demanding as the application gets bigger. When these variables are modified from everywhere in the code, the other components will not know about the new values of the variables unless they try to read them. To make the application reactive to changes, these kinds of variables can be stored in a state management system, and when these variables are modified, it can notify other components. To achieve this, a plugin of Vue.js called Vuex can be used. When using Vuex, components can dispatch actions; these actions can communicate with backend application programmable interfaces (API); based on the received response, they change the state by committing mutations and new states take effect on the UI.

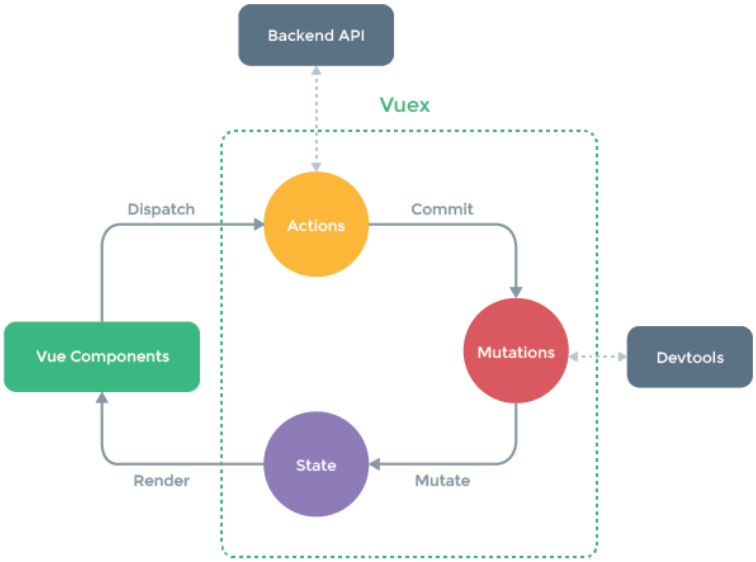

Figure 60: Flow chart of Flux architecture [158]

6.5.2. UI – Servo and UI – ADC Controller Communication

The servo and ADC controller logic are written in Python programming language, but the UI is created with web technologies. As a result, they cannot communicate with each other natively. That is why the controllers written in Python are served as a server and the UI connects to those controllers using the Socket.io library. The difference between Socket.io and traditional HTTP protocol is the connection type. When using HTTP, the client sends a request to the server and gets a response back. The problem with this method is when there is a change in the data, the server cannot send it to the client. On the other hand, when using Socket.io server authenticates the client during connection, and it is called handshaking. After a handshake, if the client is authenticated, the connection between the client and the server stays open, unless one of them closes it. Because the connection is not closed, the server can send data to the client without any request.

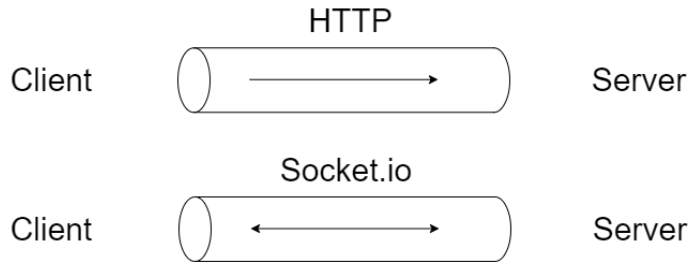

Figure 61: HTTP vs Socket.io

6.5.3. Data collection development and storage

The proposed system collects data from different sources such as position feedback to collect the ROMs from either active, passive and/or gaming; additionally, the force feedback collects the grabbing forces and the manually added data by the therapist such as the patient information's. The system maps these data in real-time as the patient is conducting the therapy or offline to check the therapy sessions later. As well as computing the predefined measurements and their statistics, the system also analyzes the metrics defined in this model and makes instantaneous graphs to visualize these results. Technically, the database is one of the most important parts of an application because it helps store and retrieve any information. While there are other data storage methods for databases, the most prevalent is structured query language SQL, and not only structured query language NoSQL [159]. MySQL, PostgreSQL can be shown as an example for SQL databases. These databases are also known as relational database management systems (RDBMS)[159]. SQL databases store data in tables, which means a column should be handled even if that column is empty. On the other hand, NoSQL databases have four different storage models: graph databases, key-value pairs, column-based databases, and document-oriented stores [160]. When the displayed data is linked to each other, a graph database is the best option. As the name suggests, key-value pairs database stores as a set of keys and values, and another name

for this data structure is hash tables[161]. Storage of column-based databases is very similar to RDBMS; when the data is retrieved, the data includes related data too [162]. And lastly, document-oriented store saves information in extensible markup language (XML) or javascript object notation (JSON) format[162].

MongoDB is a document-oriented NoSQL database[163]. The database has multiple collections. Collections are similar to tables in RDBMS and the documents that serve the same purpose are stored in the collection[164]. Documents can have multiple fields, there is not a requirement for having the same fields in different documents if a field is not useful in one of the documents. When creating a document, a unique ID is created automatically. For more deeply created documents, an embedded document field can be used [164]. The difference from a normal document is, it is inside another document.

MongoDB supports most of the programming languages. But the official packages do not support object-relational mapping (ORM). ORM helps to apply the code in object-oriented programming (OOP), which manages the software design about objects instead of functions and logic[165]. Using an additional ORM library built on top of the MongoDB library, the database part of the application can be easily created.

A. Constants

Constants consist of variables that could be changed neither before launching nor during usage of the application. Spelling mistakes can mislead the behaviour of the application without throwing errors during the runtime. Thus, constants are used to pre-define text and numbers that will be used across the application. As a result, these variables prevent typographical mistakes by throwing errors before the application starts.

B. Settings

Settings are like constants in a way that they cannot be modified during application runtime. These variables hold information such as the channel number of the servo motor corresponding to fingers and wrist for each hand, ADC address, and channel number of fingers. They also store information about limits and servo motors' initial position, which have been implemented as security features. As a result, these variables help to use the same application for different robots by changing some settings.

C. Environment Variables

These variables consist of sensitive information about the application and must be kept a secret. Database host, port and credentials, programmable application interface (API) keys, and application keys which are used for hashing passwords, can be shown as an example to environment variables.

D. GUI and sensor communication

For the measurements, CP151, which is a force sensitive resistor, is used. The sensor's resistance varies between 3kOhm and 30kOhm when activated; the pressure range is from 0.5N/cm2 to 100N/cm2. Since raspberry pi does not support analogue input, an ADC should be used, in this case, it is MCP3424. This ADC has 4 channels and 4 different resolutions (12, 14, 16, and 18 bit) [140]. ADC and raspberry pi communicate using I2C protocol, and one of 4 different addresses can be assigned to the ADC by setting address pins to high or low [140] . The converted reading of the sensor is between 0 and 2.048. Because this range does not make much sense, the range can be changed with the help of the range function as below. After mapping, the range will be between 0 and 100 which is the force that can be measured by the sensor.

$$M = (X - I_{\min}) \times \frac{(O_{max} - O_{\min})}{(I_{max} - I_{min})} + O_{min} \qquad (7.)$$

X – Reading of the ADC

I_{max}, I_{min} – maximum and minimum output of the ADC

O_{max}, O_{min} – resulting range

Since 100N is such a big force and it is not usual to see that much force being exerted by a finger, the mapped reading should be clamped in between more realistic values, which is in this case, between 0 and 10.

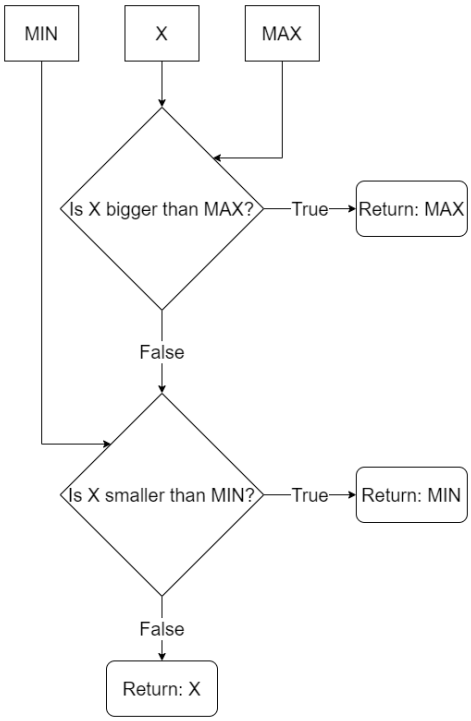

Figure 62: Clamping function

There are two ways of reading the sensor data. The first is the UI requests new data when it is required. The second is the UI requests for starting a stream, and the ADC controller send the new data in real-time until the UI does not need it anymore.

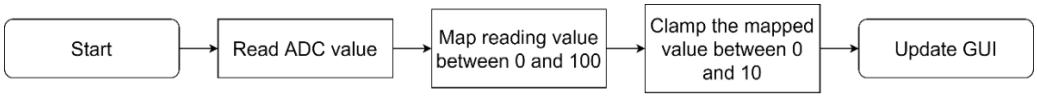

Figure 63: Updating GUI based on the sensor reading.

E. GUI and servo controller communication

Since servo motors do not support speed control by default. To achieve speed control, the angle of the servo motor can be changed gradually, which means, the angle will be incremented/decremented by step and there will be a delay in between steps. The speed control can be achieved by modifying steps and delays.

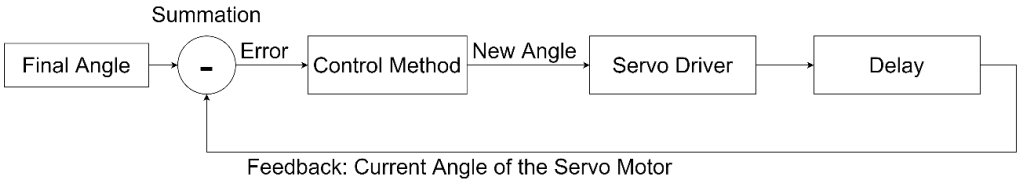

Figure 64: Servo position and speed control

The method for controlling servo motors and updating GUI based on sensor reading happens as below.

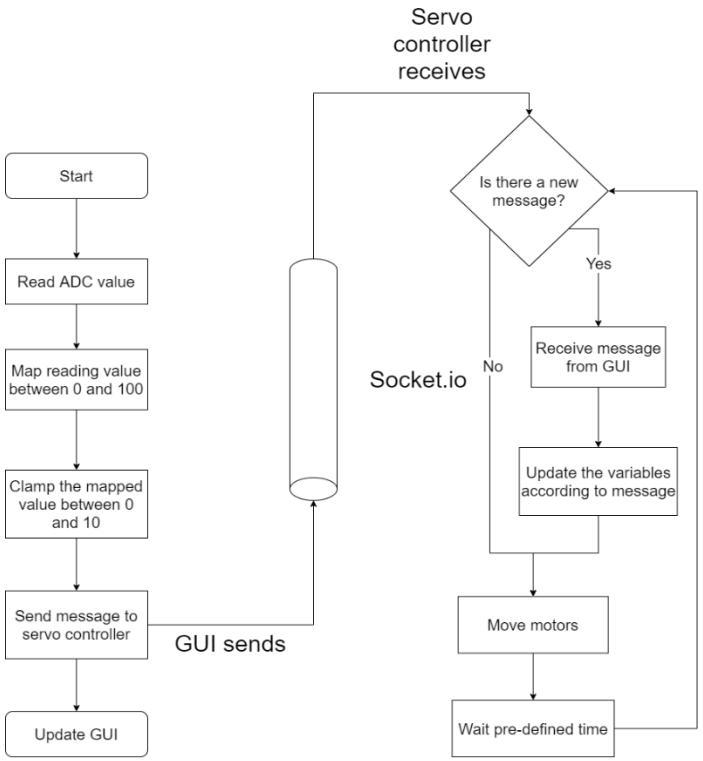

Figure 65: Controlling servo motors and updating GUI based on the sensor reading.

6.6. Interactive based Game Rehabilitation

This section illustrates a patient-tailored approach to assist with and invigorate the neurorehabilitation technique by implementing game mechanics. In recent years, a large number of assistive games was adopted in modern hand neurorehabilitation. The game-based recovery programs allow patients to undergo physical rehabilitation services using an interaction between person and computer, a supporting mechanism to track treatment and healing progress [166]. Generally, there are certain advantages of employing gaming development with the hand recovery process since it allows patients to participate in personalized, entertaining, motivational, and challengeable sessions while performing a repeatable exercise. For this stage of the proposed

system, the proposed games are compactable for wrist rehabilitation only, for those who suffer from stroke and spasticity. The analogue feedback of the servomotor's potentiometer was used as analogue feedback to an integrative developed game. Initially, to design a game that is compatible to be run using Raspberry PI. A game of catching falling multicoloured balls (red, blue, and grey, respectively) was developed using Python programming by calling PiGame, a python-based game library. In this game, different difficulty stages were adapted by adjusting the ball's number and speed, which the end-user has to open a sliding gate. Each gate was assigned with the same colours assigned for the balls once the ball fell and the patient opened the same ball coloured gate. When the falling balls are dropped into the baskets, the baskets must be moved to catch them. The game did not influence parameters within the therapist's control, as shown in Figure 66. Which shows the user-friendly developed game, in which it is observable the patient scored 6 points.

Figure 66: the proposed 2D game development which was used for the hand rehabilitation interactive game

Although, most of the excessing recommended PiGame, library to develop simple gaming compactable with raspberry pi. However, the disadvantages of using PiGame is that: non-resizable window and low FPS on the PI when using more complicated graphics elements. The graphics elements such as .jpg and .png files are used for the character, background, and other similar contents.

Although PiGame supports jpg and png, it still does not support Scalable Vector Graphics (svg). Therefore, using HTML and JavaScript (JS) to develop the game solves both the resizable window problem and the .svg support problem. Since these are the languages of the web, they support every file format, have great support for all kinds of screen sizes and have a fantastic performance. The abbreviation HTML is an abbreviation for HyperText Markup Language. It's more accurately classified as a markup language and not a programming language [167]. It includes all the elements, text, images, etc. It uses tags (opening and closing tags) to store the elements. A multi-coloured boat and containers game was developed using HTML and JS.

Chapter 7: Experimental Results and discussion

7.1 Experimental Procedure

As previously stated, the proposed hand rehabilitation system (Figure 67) can be characterized as is a desktop upper limb rehabilitation robot that adopts the combination of grounded-exoskeleton and end-effector mechanism to drive and assist the patient's four fingers, thumb and wrist to the desired trajectories and ROMs. To test and evaluate the passive and active, interactive therapies that produced by the proposed system, six participants; five men and one woman were involved in the experimental tests; however, only one participant will be discus for simplicity reason. The participant was a healthy man with no noticeable neurological or mental disabilities. The selected participant was 30 years old, 168 cm tall, and weighed 78 kg, and we hypothesized that the participant's right hand was the affected side.

This chapter discusses and describes the different levels of experimental tests and analysis to check and validate the proposed system performance and stability. For passive therapy, this analysis compares the experimental joint trajectories and ROM acquired during freehand movements (without the proposed system) and sets them as desired trajectories and ROMs. On the other hand, the actual trajectories, positions, and ROMs are caused by the proposed system (with the proposed system). While in active therapy, the patient's ROM and trajectories will be compared with the integration force between the patient's fingertips and fingertips holders. As well as, needed ROMs and trajectories to perform an interactive game was tracked and demonstrated.

Figure 67:The proposed System implementation

A motion capture acquisition system was used to capture the workspace trajectories, ROM angles, and displacements, which can validate motions caused by the proposed prototype. For that purpose, HD camera, computer and motion capture analysis software called Kinovea® v0.9.3 [168]). Kinovea® is based on 2D motion analysis software. It is a reliable system that can measure kinematic parameters. It was approved as a method to evaluate criteria related to time [169], [170], used for various fields, including clinical therapeutic analysis [169]–[172]. For advanced analyses, objective and quantitative evidence may be given.

Moreover, it is used as a diagnostic technique and an instrument for assessing the outcomes of under test intervention [173]. The quantitative and objective findings would help understand the proposed system openness. A timestamped evaluation of distinct motions that the patient makes across multiple sessions to evaluate the progress performance of the therapy sessions over time.

Eventually, a subjective study was conducted based on the user's feedback to test the proposed system usability and comfortability.

7.2 Passive Therapy: Experimental Test

In stroke therapy, passive rehabilitation is one of the initial steps to be taken. These exercises are considered passive because the patient does not exert any effort. Instead, the therapist and the rehabilitation-based robot helps to move the muscles and joints. Additionally, the therapist is required to aid the patient in flexion and extension motions of all phalanges.

7.2.1 Experimental human-robot integration and software setup

A primary configuration was carried out to test and capture the desired and the actual trajectories and then superimpose them in the finger's F/E experiment. First, as presented in Figure 68, the proposed system was installed and fixed onto a table; then, the participant was guided to sit on a chair, place his right arm over the developed forearm support, and then fix it using a Velcro strap, then the fingers were also placed and properly fastened onto the fingertips holder.

Figure 68: human-robot integration setup

To start the passive therapy, the therapy parameters and configurations must be set from the developed dashboard. The passive therapy can be selected to the desired joints as was shown in Figure 59. Once, the session starts with measuring the hand parameters of the patient. This tab has sub-tabs that correspond to joints and movement types, and these tabs should have windows for hands that are chosen as an impaired side. There are two types of measurement methods: active and passive. Measurement type is active, or passive determines whether servo motors are controlled by sensor input or via sliders on the UI. With the help of this tab, the maximum and minimum angles and displacements for movements are measured. For security, when measurement starts for any joint, everything on the UI is disabled except the one that has been started. This prevents starting multiple measurements by mistake and locks the GUI. As a result, other tabs cannot be selected.

At this point, before starting the passive training by the proposed system the therapist must determine the spasticity level of the patients. In other words, the therapist must determine the active ROM of the patients before starting any robot movement assistance to avoid broke the hand bones. Therefore, to aid in a thorough assessment, therapists must first conduct a test of the phalangeal range in each finger, with particular attention paid to the joints that allow flexion and extension. To meet these requirements, The proposed system enables the therapist to select the fingers extension and flexion ROM, to be generated towards each finger individually, through the developed sliders. Each slider corresponds to a finger as can be seen in Figure 69.

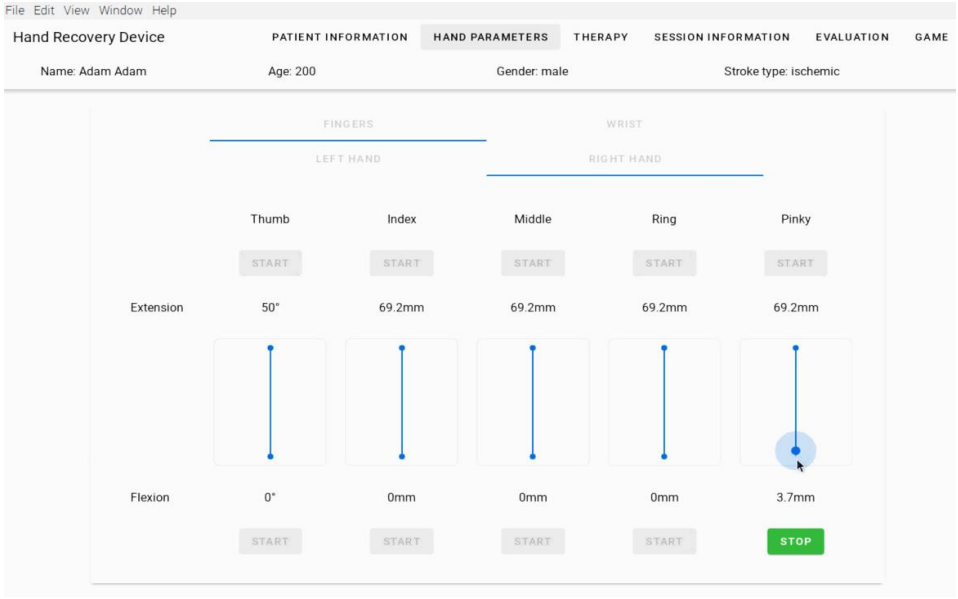

Figure 69: Hand parameters tab on UI

the passive therapy's motions ranges were selected and set depended on the spasticity and contraction level. Once these parameters are set, is stored in the developed database and can be recalled later. The session continues with configuring settings for the therapy. This includes the side and the joint to be trained, and how long the therapy will be, as shown in Figure 70.

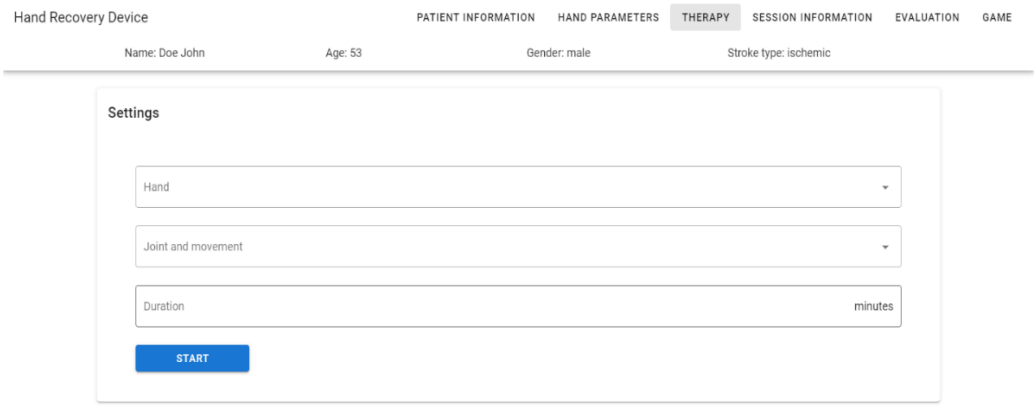

Figure 70: Therapy settings tab on UI

When the therapy is initiated from the dashboard, a repeating movement in the range previously selected begins to assist the patient's fingers in gradually increasing the range of movements. After the therapy settings are set, the session continues with therapy. The therapy tab, patient information, remaining therapy duration, live graph of the servo motor, working, and visual emergency stop buttons can be seen. The joint was selected when the therapy settings were configured. Servo controlling methods are the same as measurement methods in hand parameters. The only difference is that the motor rotates between the minimum and maximum measured value of the joint instead of being controlled by sliders on UI. The therapy can be paused and resumed after it started and if the stop button is clicked, therapy finishes and asks if the therapist wants to save the data to the database. Saved data contain maximum and minimum angles reached and the maximum force applied by the patient during therapy.

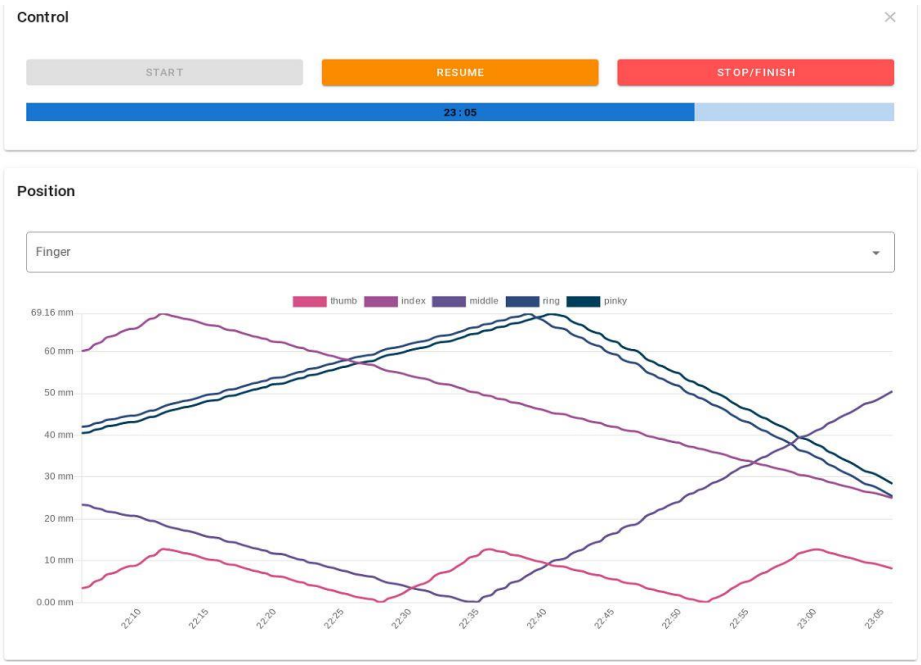

Figure 71: Real-time, passive finger F/E therapy training.

First and end-users can observe a real-time graphing of the selected ROM, which encourages and psychological feedback to the patients about their abilities to perform active motion later. From the presented real-time graph data, it is observable that all fingers are moving independently from one other with different ranges of motions with low rpm; this result indicates the ability of the proposed system to guide the attached fingers and move them smoothly and repeatably.

7.2.2 Motion Capture System Setup

To collect more quantitative and objective results, a motion capture data acquisition system was set using Kinovea® software. Parallel to the participant's fingers and the proposed device, an HD camera was fixed in a particular position to capture and track the finger's movement and capture the fingers ROM and trajectories caused by the proposed system.

Initially, before linking up the participant's fingers to the developed fingertips holder, the participant performed a fingers F/E (without the proposed system); these gestures were video recorded, then temporarily, the camera recording was paused. Afterwards, as it was described earlier, the participant was then instructed to place his fingertips to the top of the developed exoskeleton fingertip template and fix it with single-use injury tape plaster or a small Velcro strap, as shown in Figure 72 (a, b, c, and d) which illustrate fingers–robot integration of fingers F/E experiment. Following selecting the therapy's control parameters and starting the device, as described in (Experimental human-robot integration and software setup), the exoskeleton fingertip moved to the home position. Then the device starts moving accords the preselected F/E ROM degrees with a slow-motion used to extend the finger and flex it back. At the same time, we resume the video recording to capture the finger motion induced by FWRMS. Subsequently, the captured video data were analysed using the Kinovea®. However, since all fingers follow the same

phalanx trajectories, we have decided to track only the index finger for simplicity.

For the first part of the video, in which the participant performed a freehanded finger F/E (without the proposed system), a placed a tracking passive marker was placed onto the finger distal phalange (fingertip) to acquire the finger's end-effector natural workspace trajectory with respect to the coordinate frame to execute a Cartesian trajectory. These gestures were video-recorded; then temporarily, the camera recording was paused. Following the second part of the same captured video, another passive tracking marker was placed onto the actuated finger's end-effector driven by the proposed system. Ultimately, as a result, we obtain the desired trajectory superimposed to the actual trajectories that were induced using the proposed system.

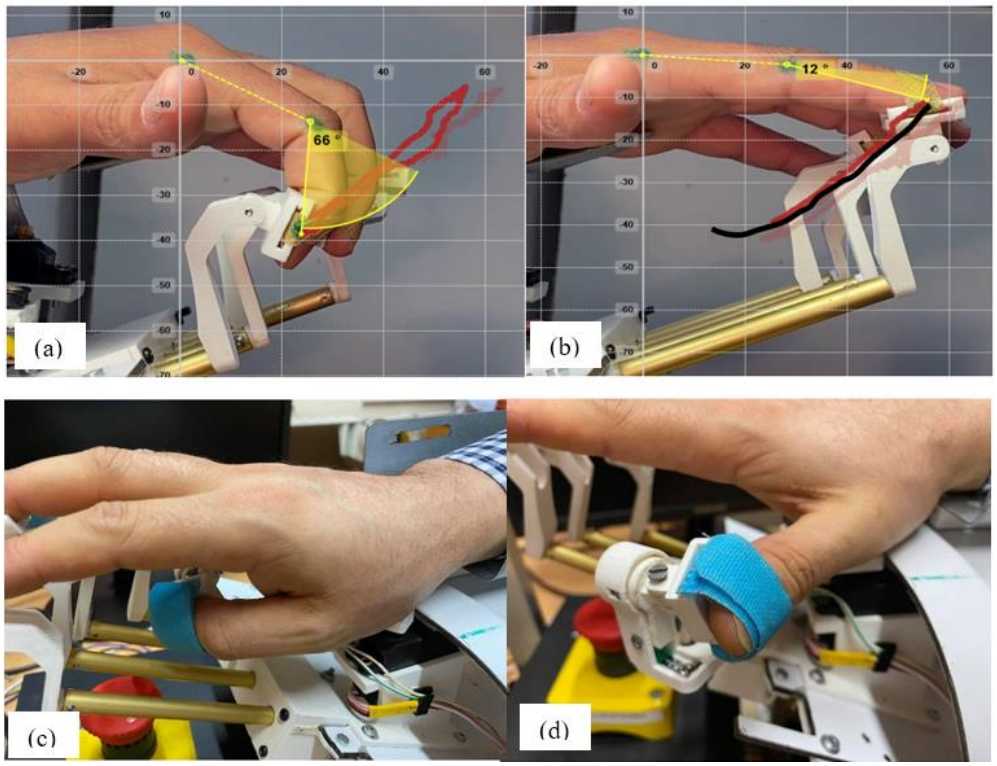

Figure 72: A real-time experimental setup of fingers-robot integration and the index finger's workspace trajectories measurement:

*(**a**) Index finger extension actual ROM angle and workspace trajectory caused by the proposed system; these ranges are considered within the normal functional grasping range of motion of the index finger. (**b**) index finger flexion actual (red curve) and desired (black curve) workspace trajectory. (**c**) thumb finger flexion induced by the proposed thumb mechanism. (**d**) thumb finger extension induced by the proposed thumb mechanism*

7.2.3 Passive Fingers F/E Experimental Results and Discussion

Figure 74 (a, b) elucidates the experimental implementation performing a continuous passive motion of the finger F/E. The solid red curve demonstrates the fingertip workspace trajectory caused by the proposed system, and the solid black curve again illustrates the fingertip trajectory workspace without the proposed system. In contrast, the yellow highlighted angles tracker presents the finger ROM of opening and closing the index finger in the set coordinate frame. It is easy to confirm that the actuated finger phalanx movement caused by the proposed system is within the natural functional trajectory workspace of the index finger phalanx. And both trajectories are closely associated with each other.

Besides, graphical descriptions were accomplished by analyzing the video data used for both the index finger opening and closing phases. Figure 73 (a, b) shows a comparative analysis between; (1) the desired fingertip displacement, which plotted a solid blue curve; (2) the actual fingertip displacement induced by the proposed system, which is plotted by solid orange. It is straightforward to understand that the participant performed a finger flexion and extension two times, and the plotted displacements are in both vertical and horizontal orientation, respectively. Figure 73 (a) plots the horizontal X-axis, while Figure 73 (b) describes the vertical displacement in the Y-axis.

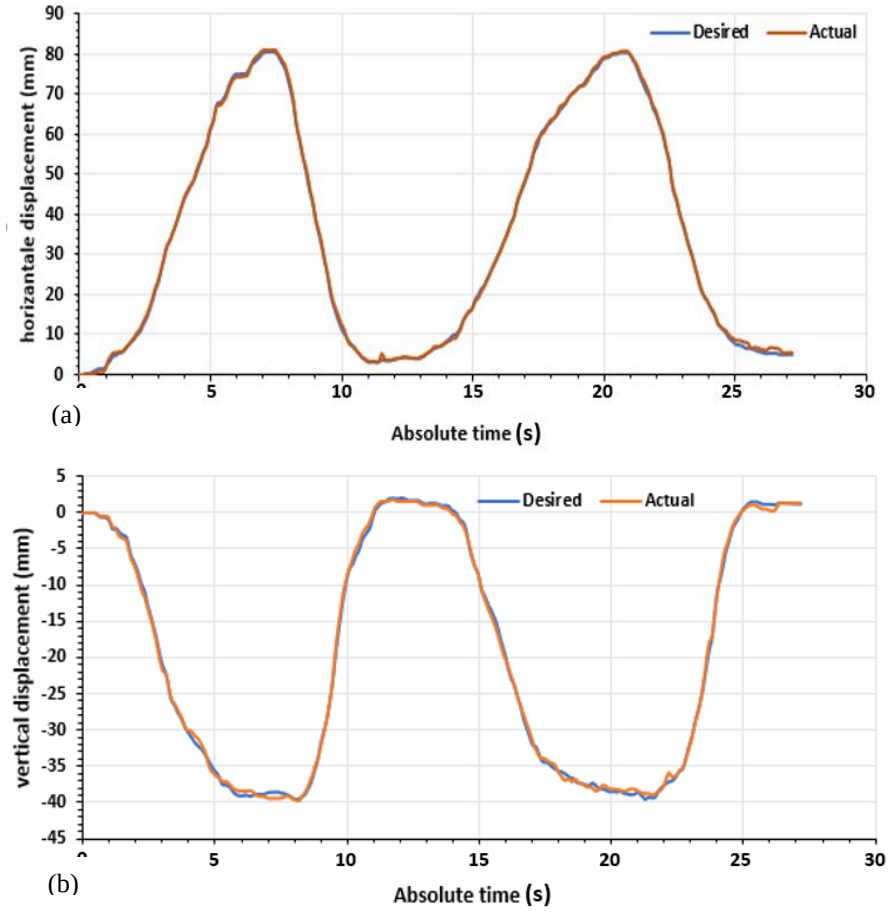

Figure 73: Continuous passive motion rehabilitation experiment of s typical finger flexion and extension displacement.

(a), the fingertip displacement in horizontal; (b), the fingertip displacement in the vertical axis.

Moreover, we can also observe that the proposed system drives 80 mm of total displacement at the horizontal axis to open and close the index finger and −39 mm displacement at the vertical axis; these displacements values are considered within the normal functional range of the index finger. Besides, the actual guided trajectory corresponds to the planned desired trajectory, and all the finger joints (DIP, PIP, and MCP) travelled concurrently without any movement discomfort. Accordingly, the results indicate that the motion of the

finger rehabilitation design is stable. However, it can be observed that the actual and desired displacements of the DIP phalanx have a small percentage of error during the execution of the movement. It is worth noting an error percentage, about 0.874% error at the vertical axis and 1.257% error at the horizontal axis. The error rates are limited mainly by the friction between the external threads of the rack and the external threads of the pinion, and the vibration caused by the movement. However, these minor errors do not influence the continuous passive motion (CPM) rehabilitation characteristics and the proposed device's performance.

7.3 Active Therapy with Assistance

In the active therapy, the patient is supposed to have enough grabbing force to actively move their fingers or wrist; however, it is possible that they can move their fingers actively but do not have enough grabbing force to move the robot's end-effector. Therefore, the proposed system first measures the grasping force capabilities force, and once the patient applies a small amount f force within the 5N stress range, the proposed system will passively move the fingers whenever the patients apply an active force. With this in place, end-user with neuroplasticity will be more motivated to perform out with the proposed system's support; the control logic behind this concept is known as the assist-as-needed (AAN) control strategy. By having the patient perform the movement themselves, they have to invest a considerable amount of effort. Hence the AAN technique prioritizes minimizing the use of robotic aid for this purpose. The proposed system motion's support is discontinued if somehow the user can do the required operation. The assistance is provided just as much as is necessary.

From the control dashboard, the active therapy can be selected; then, the patient is asked to apply an active force to move the guiding mechanism. Initially, the applied forces will be measured in real-time, and the motors will

be moving within a limited range; that range will be selected depend on the patient case, which means the grasping force abilities and the AROM that patient can perform. Once these ranges have been registered and stored, the therapy can be started and limited to these ranges that have been predefined. This considers as a safety feature to product the patients with limited AROM due to spasticity.

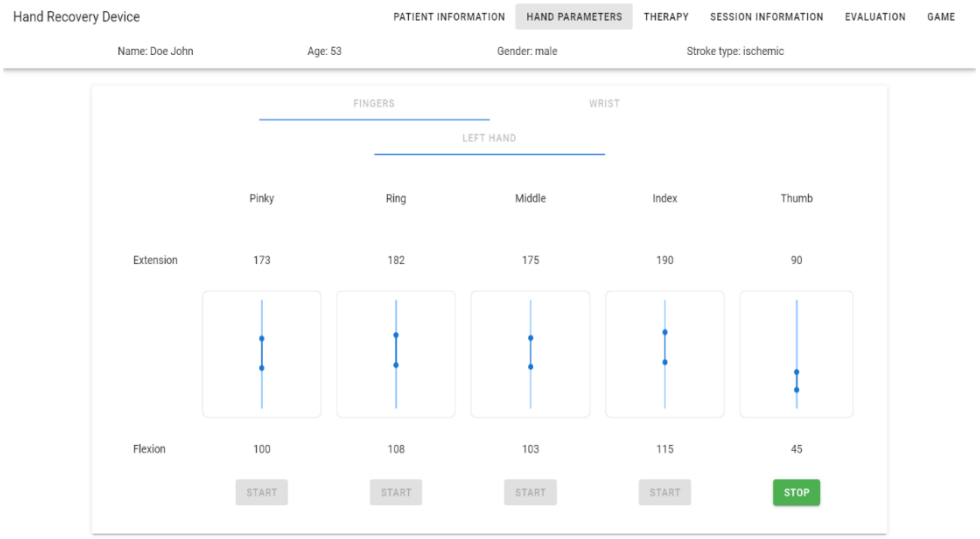

Figure 74: The developed control dashboard: hand parameters selection

According to the experimental results, the system waits for the patient to apply an active force; when this state condition is approved, the fingertip holder starts to flex the finger with slow-motion till it reaches the maximum predetermined range, if the patient keeps applying force, the fingertips holder will maintain the maximum predetermined position, and once the patient released the applied force, the device will passively move the fingers to the predetermined extension position.

Figure 75 indicates a real-time experiment in which the fingers perform an active therapy with assistance, Figure 75 (a), shows the performed ROM displacement in X-axis, for four fingers; it is observable that each finger

performed three times finger F/E with different ROM. It can also indicate the muscle activation recorded throughout an EMG sensor to show the muscle activities while the participant performs an active therapy through the fingers opening and closing, as shown in Figure 75 (b). In order to assess the signal detected from the bare hand when it is clutching the fingertips' holder, the EMG signal analysis is performed. While the ranges of the interaction force between the participants and the robot's fingertips holder are within the range 0- 5N, as demonstrated in Figure 75 (c). The middle finger applied the maximum interaction force, and that it is why it reaches the highest ROM, which can be explained that the middle finger is the bigger and stronger among the other fingers. Follows by the index, ring and pinkie fingers. From Figure 75Figure 75, the red highlighted to represent the fingers flexion phase, in which the interaction force is applied, while the green highlighted represents the extending phase in the interaction forces released

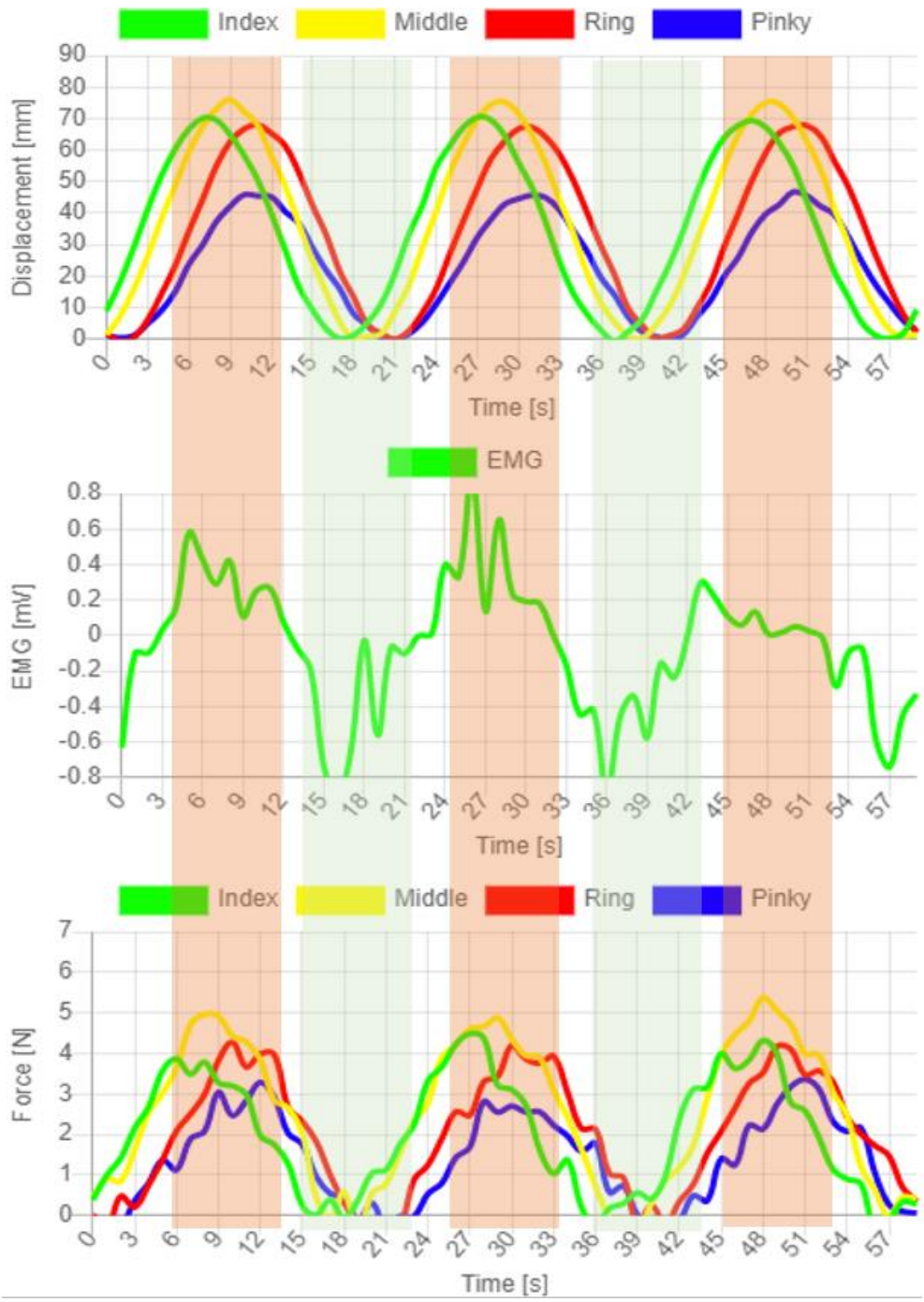

Figure 75: illustrates the real-time performance of active therapy with assistance.

(a) four fingers ROM displacements. (b) shows the EMG signal analysis of a human during the active therapy with assistance with high muscular effort is during grasping periods. (c), the grasping force applied onto the fingertip's holder to perform active therapy.

7.3.1 The Force Measurement and Evaluation

in addition to delivering the force-feedback, the proposed system was also constructed to aid the patients in their self-managed rehabilitation exercises. This increase the usability of the proposed system to help self-managed rehabilitation exercises be as simple and cost-effective as possible. in order to determine how much grabbing force the patients were capable of applying, a force measurement diagnostic feature was designed. Though this was conceivable, it was also conceivable to create an instrument to evaluate tip-pinch power, which is a component of hand functions examined on stroke patients regularly to evaluate their functional results [174]. Owning FSR sensors in the proposed system, it was also programmed to be used for the. Figure 76 present the developed force integration UI and the results of the five fingers. Moreover, this system can be used for either the right and left hand's fingers.

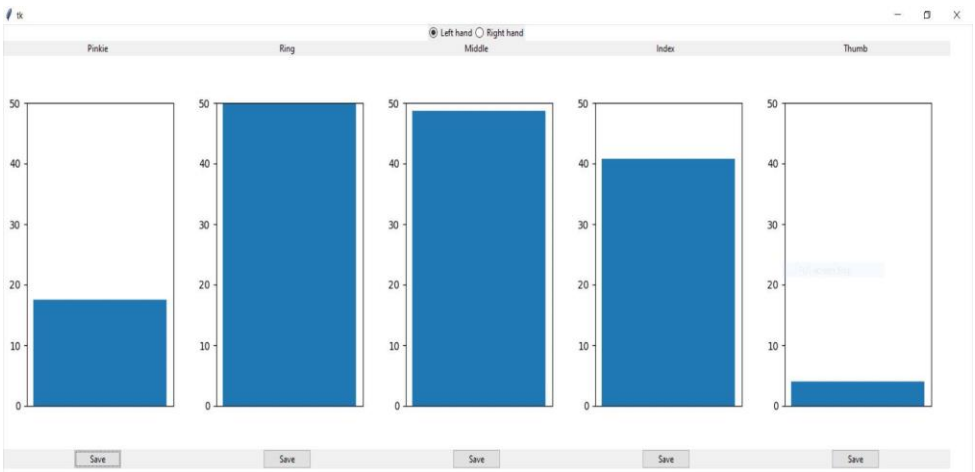

Figure 76: the developed force integration UI of fingertip-pinch force evaluator

7.4 Wrist Rehabilitation Experimental Results

Similar to the previous method of the finger's F/E, the initial setup was applied in the case of wrist F/E, and R/U. The proposed wrist rehabilitation system adopt passive, active and interactive control mode therapies. To start a wrist therapy, the same finger initial setup was applied in the case of wrist F/E and R/U. However, the patients need at least to have to grab the ability to start the wrist rehabilitation sessions and hold the wrist handle, as briefly explained in (Wrist and Forearm Mechanism Design) sections. To be able to compare the nature wrist motion (without any passive assistance) with the wrist motion that guiding or induced by the proposed system. The nature wrist motions were studied and analyzed with and without the proposed device, then later it will be compared with wrist motion caused by the proposed. In this experiment, we selected the desired ROM for wrist F/E to be (0°–45°/0°–25°); these degrees were chosen to be within the wrist's normal. Using the motion capture system, passive markers and angle measurement markers were located on the targeted joint to acquire these ROM angles and trajectories; After the therapy started, the system moved smoothly according to the preselected ROM with low rpm. As shown in Figure 77 (a), the end-user started forming the nature position (0°) then performed flexion and wrist extension gestures.

Additionally, from Figure 77 (a, b, c), we can see; (1) the desired workspace trajectories of the wrist F/E demonstrate black curve demonstrates the workspace trajectories (without the proposed system); (2) the actual motion of the wrist F/E workspace trajectories (with the proposed system) which indicated by the blue curve. In regards, the yellow highlighted value presents the current position of the wrist in the predefined coordinate frame. Besides, it can also be observed that the two trajectories are relatively identical towards

one another, and the participant has confirmed that there is no movement discomfort of the device. Eventually, the actual (with proposed system) ROMs of the wrist F/E are (0°–44°/0°–25°).

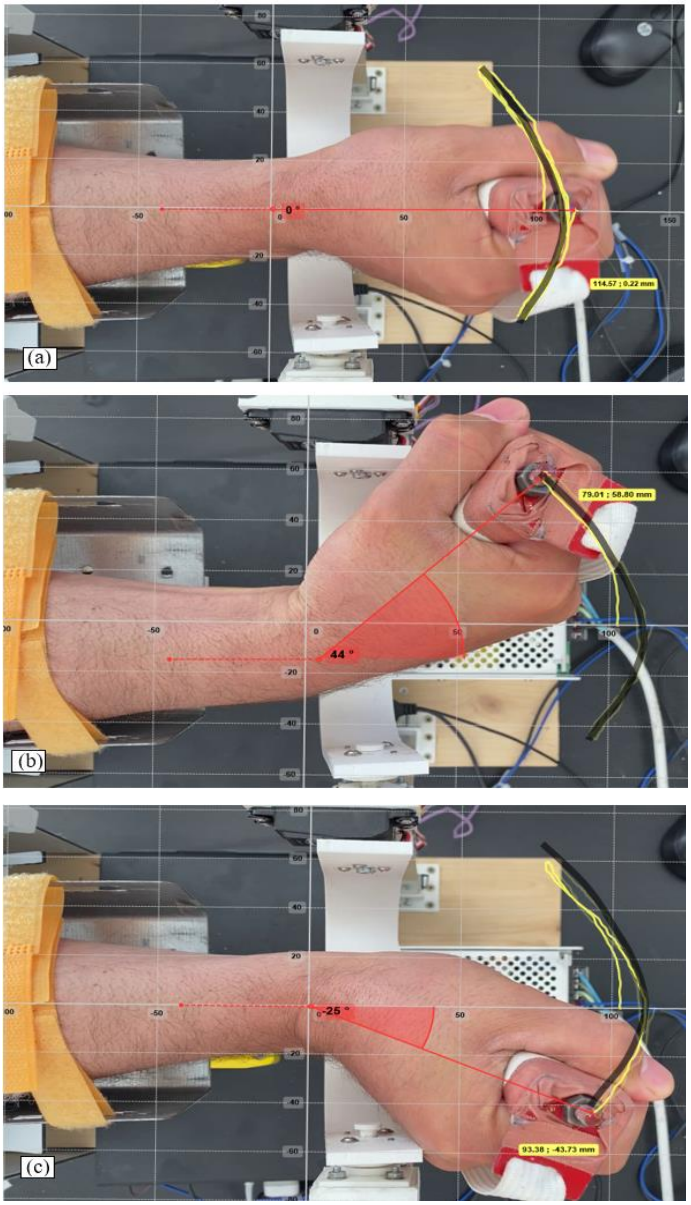

Figure 77: The real-time experiments of wrist F/E workspace trajectories and ROM.

(a), the comfortable wrist position (zero position). (b) actual wrist flexing (yellow curve) and desired (black curve) workspace trajectory, position and actual ROM angle (44°). (c), actual wrist extending (yellow curve) and desired (black curve) workspace trajectories, position and actual ROM angle (25°)

Similarly, the wrist R/U experiment was conducted to evaluate and compare the wrist R/U joint's functional region with and without the proposed machine. In this experiment, the desired R/U ROM was selected from the control dashboard to be (0°–38°/0°–49°). Once the therapy was executed, the end-user performed wrist R/U motion with slow rpm as shown in Figure 78 (a, b, c), which indicates; (1) the yellow curve, which describes the workspace trajectories without the proposed system; (2) the blue curve, which describes the real-time wrist R/U workspace trajectories induced by the proposed system.

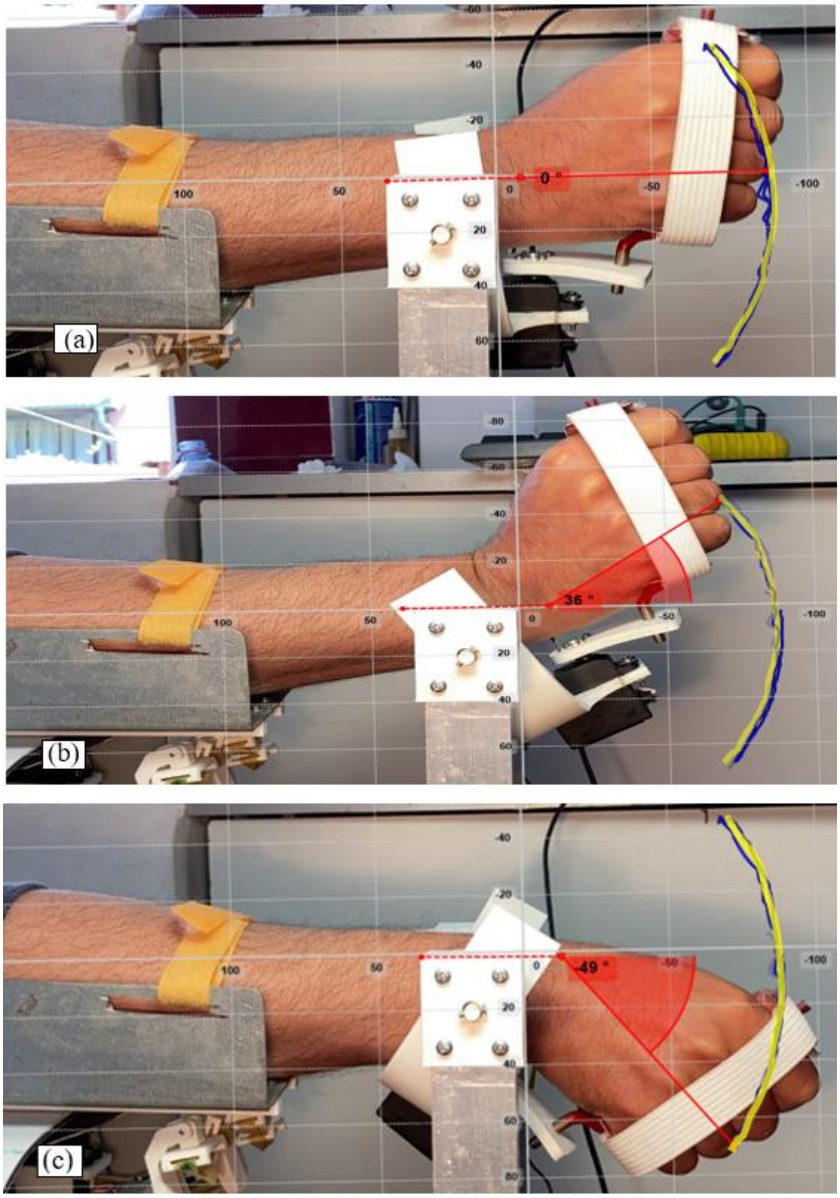

Figure 78: The real-time experiments of wrist R/U workspace trajectories and ROM.

(a), the wrist relaxing position (zero position). (b), actual wrist radial deviation (blue curve) and desired (yellow curve) workspace trajectories and actual ROM angle (36°). (c) actual wrist ulnar deviation (blue curve) and desired (yellow curve) workspace trajectory and actual ROM angle (49°).

Moreover, a graphical representation for wrist F/E and R/U ROM were created. The same applied the same previous approach in the finger F/E;. Figure 79 (a) plots a comparative analysis between the desired and actual ROMs angle of the wrist F/E during the experiment's execution. It is straightforward to observe that the end-user is performing a single F/E wrist. The vertical axis stands for the wrist's angle, while the horizontal axis stands for the execution time. The graph consists of two curves: the solid blue curve demonstrates the desired ROM angle. While the orange dash curve illustrates the actual ROM angle of the wrist F/E. It is possible to note the similarities between the two ROMs. Similarly, Figure 79 (b) plots a graphical analysis that indicates comparison graphs between the desired and actual ROM angles of the wrist R/U during the experiment's execution. The solid blue curve is plotting the desired ROM angles. In comparison, the dashed orange curve is plotting the actual ROM angles.

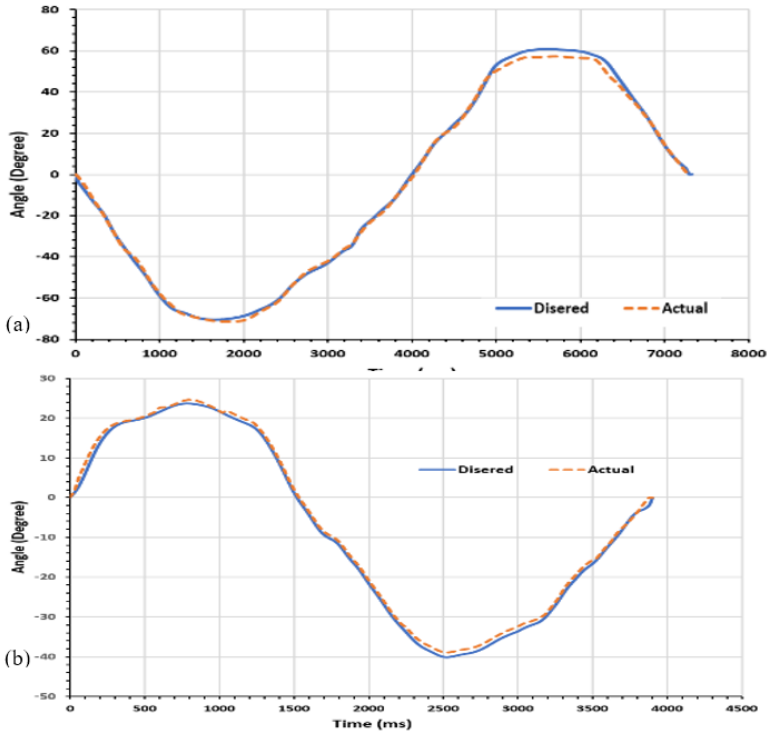

Figure 79: Continuous passive motion rehabilitation experiment of s typical.

(a) wrist flexion/ extension joint; (b) wrist radial/ulnar deviation joint.

7.4.1 Wrist F/E and U/R result's Discussion

Although comparatively both trajectories in Figure 77 and in Figure 78 and ROM angles in Figure 79 (a, and b) are functionally matching towards each other, it is slightly observable that there is a slight error between them; it is worth noting as an error; the sum calculated RMSE was 0.984 mm. However, from Figure 78 (a, b) and Figure 79 (a), we can find a negligible observable error between the two ROMs and the workspace trajectories; the sum measured by root means square error RMSE of 1.1 4mm.

Eventually, after the repeatable experimental tests, for the wrist therapies for both active and passive motions, the differences between the actual and the desired ROM were just a few millimetres for the finger's F/E and few degrees for the wrist F/E, R/U. The disparity in each measurement occurred primarily due to the mechanical frictions. However, as we have briefly explained, these differences do not affect the proposed system's training characteristics. Therefore, the results are sufficiently accurate in aspects of the stability and trajectory's alignment; the actual trajectory directly correlates to the desired trajectory, which meets the requirements of continuous passive motion training configurations.

7.4.2 Wrist uniaxial and boundary motions

The participant could actively achieve uniaxial motions with the help of the proposed system. When the patient holds the wrist handle and rotate the wrist horizontally (wrist R/U deviation) and vertically (wrist F/E deviation). From Figure 80, this result was obtained from the left hand, in which the participant performs active motion, the F/E movements within (80 to -70 degrees). And wrist R/U deviation (40 to -30 degrees).

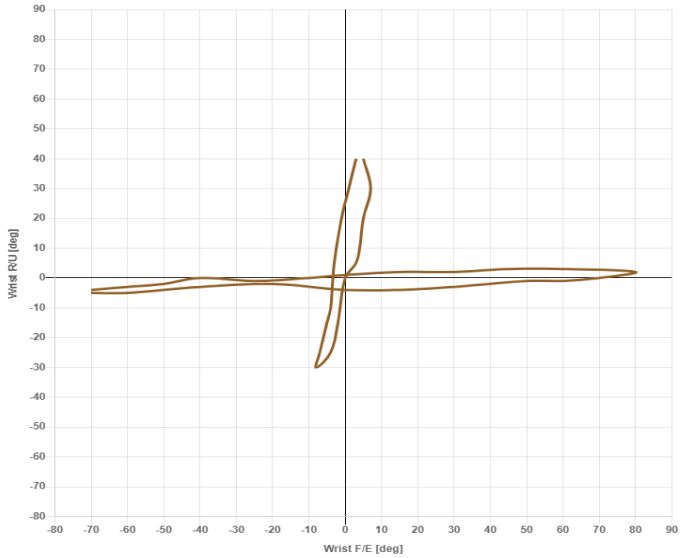

Figure 80: wrist active uniaxial motions

Additionally, the elliptical boundary motion also can be actively performed by the participant. This type of motion is vital to increase wrist therapy efficiency. Wrist ellipse motion happens when the wrist seeks to rotate along the maximal border, and the hand makes an ellipse gradually. Figure 81 depicts the trained elliptical motions for the left and right hands and the desired (blue dashed arcs) and actual values (the solid brown arcs). The proposed system needed to direct the wrist F/E and U/R deviations activated to perform the elliptical shape in the boundary motions. While Figure 81 (c) demonstrates a real-time captured active wrist elliptical training in which the participant actively holds the wrist handle and circulates it to perform a full elliptical shape.

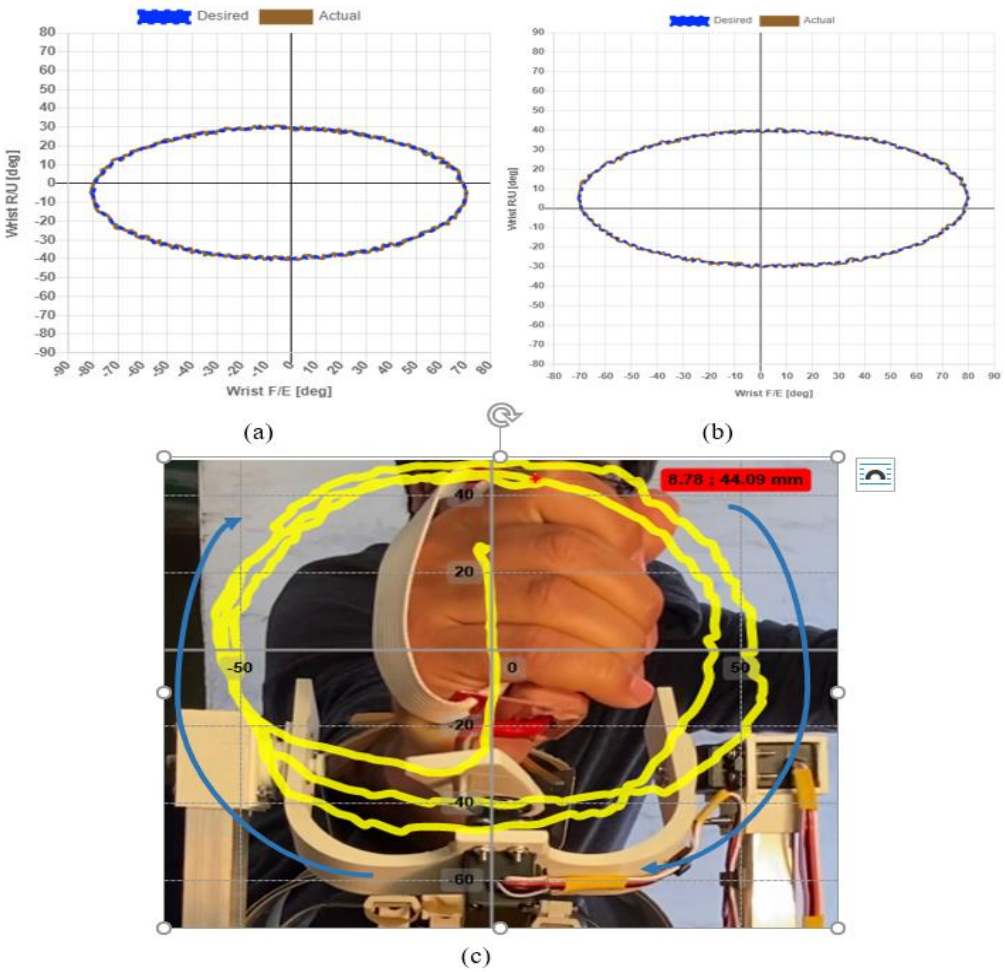

Figure 81: wrist elliptical motion:

(a), actual and desired elliptical motion of the right wrist; (b), actual and desired elliptical motion of the left wrist; (c), real-time example of captured elliptical motion

7.4.3 Interactive game-based rehabilitation experimental results

The overall purpose of the developed game is to provide an engaging and amusing experience for individuals with impaired motor capability throughout the wrist that also includes a small amount of therapeutic exercise. To test how effectively the game's interactions function with the proposed system as well

as to exhibit the proof of concept. The therapist can investigate the information and see how many times each participant has played the game. These data will be stored in the developed database, and it will list the maximum, highest game score, and date. The outcomes assessed by these test scores could be utilized to monitor and assess a patient's results throughout a period of time. Figure *82* present an example of game-based rehabilitation; while playing a game, patients interact with a virtual exporting and importing port, which receives their responses and control inputs (hand movements) by changing its status. In this particular example game, the goal was set that the patient needs to move the white container (yellow highlighted) into the white ship. The patient needs to perform one wrist flexing to achieve that goal, then wrist radial deviation flexing then one wrist extending. The exact process can be achieved to move other containers. In this way, the patient performing purely active wrist motion with different ROMs

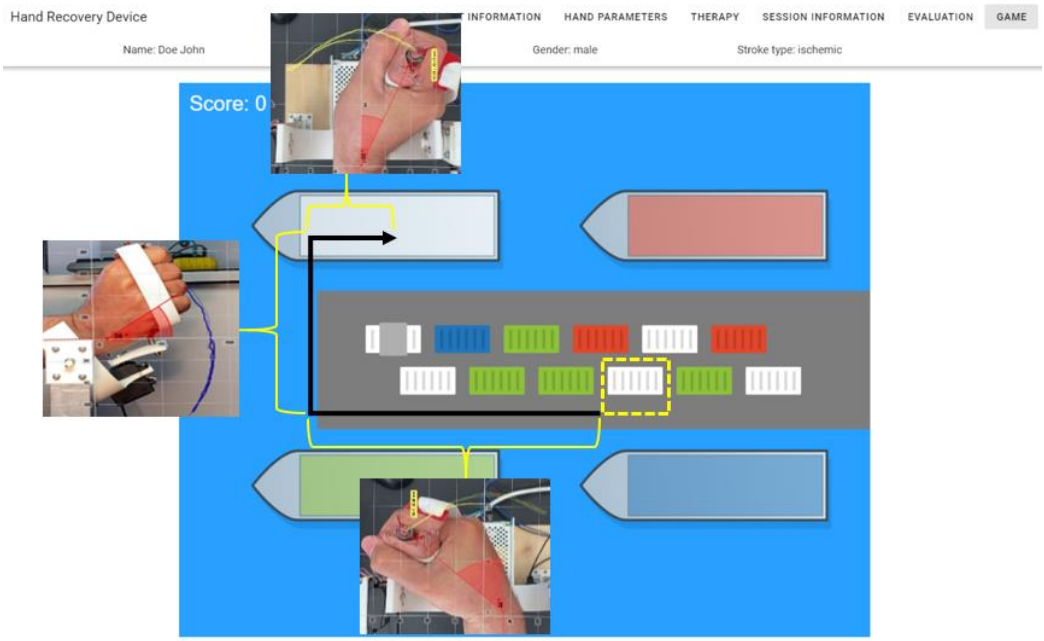

Figure 82: the developed game-based interactive rehabilitation

7.5 Time-based Performance Assessment: UI Results

At the end of each therapy session, the therapist and patient can detailly investigate and observe the recovery progress of the fingers and the wrist, based on performed maximum flexion and extension. From the developed dashboard and after hand parameters measurement and therapy, the session can be saved. It requires the date of the session, and optionally description can be added, as can be seen from Figure 83.

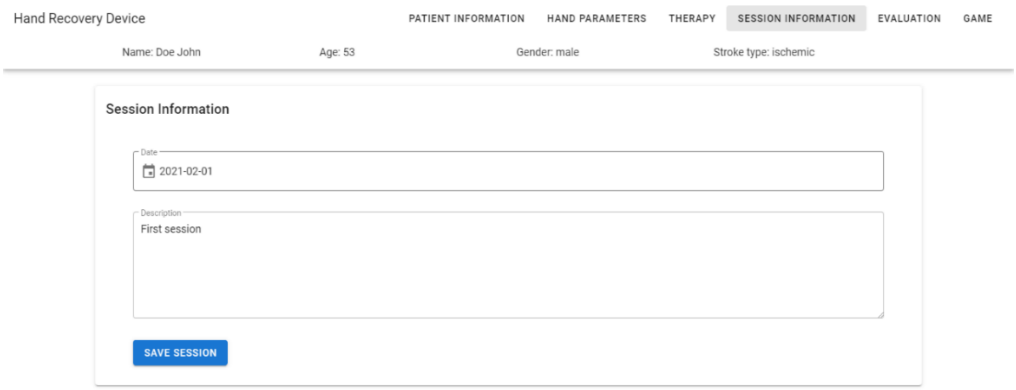

Figure 83: Session's information tab on the developed dashboard

At the end of each therapy, the therapist can store the preform sessions' parameters such as the maximum ROM, displacement, interaction force, and gaming scores. Additionally, after each session, the therapist can monitor these parameters progression that the end-user could perform throughout the session by accessing the time-based report assessment. To evaluate this feature of the proposed system. Figure 84, demonstrates the patient's time-based self-ROM assessment of various motions done over various sessions with varying dates and times. After 11 days of sessions, the progression graph Side and movement options change based on the data selected in the patient information tab. If different options are selected, the graph will be updated according to the chosen options. The graph will be saved when the save button is clicked.

The x-axis in the example graph indicates the date, while the y-axis in the case of the index, ring, middle, and pinkie shows the displacement value, and the y-axis in the case of the thumb indicates the ROM angle. Besides the data graph presentation, each therapy's comments can also be shown in the description. This gives the proposed system the feature of friendly use by saving and reminding the therapist by its comments, which can be used to describe the patient or the session status at the therapy time. It appears that assessments demonstrate considerable improvement in performance before and after training.

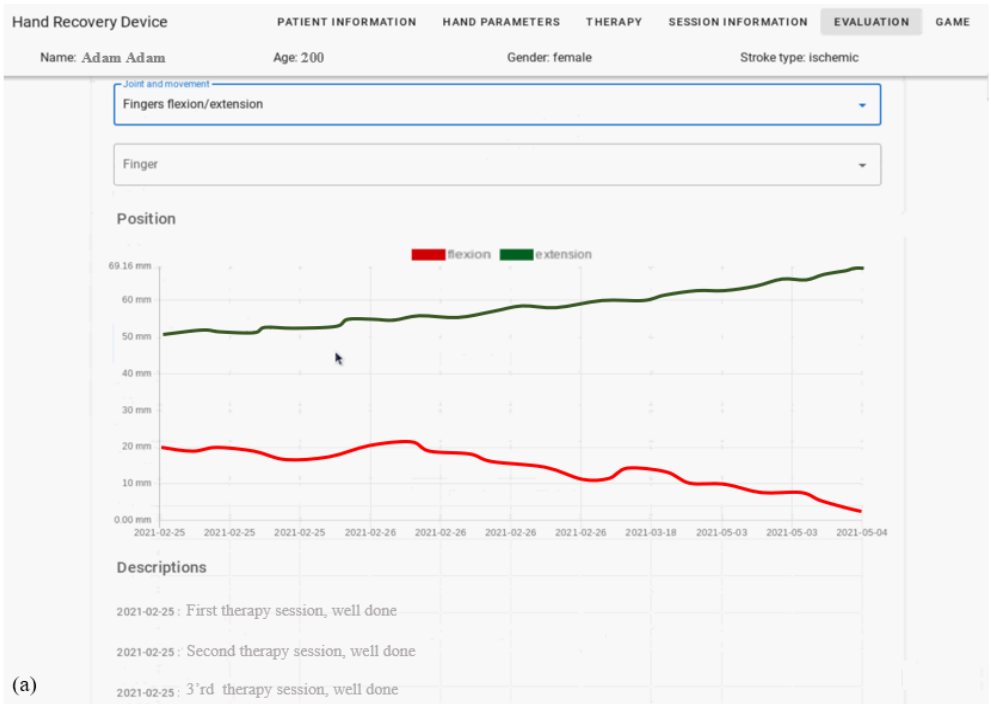

(a)

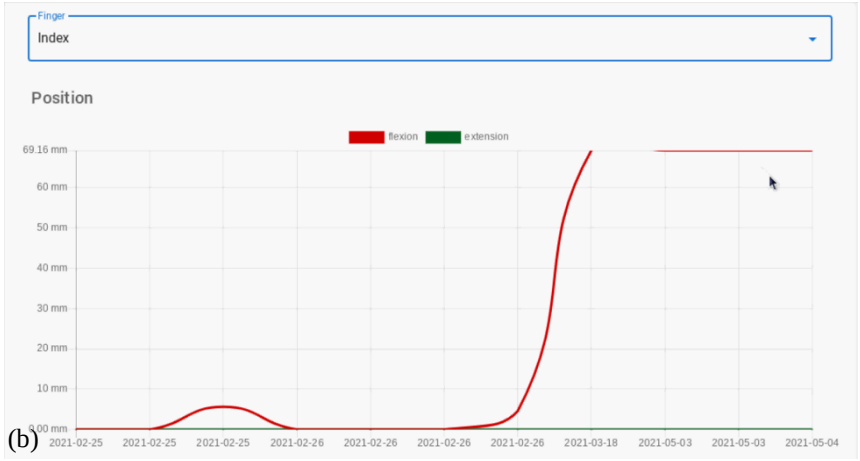

(b)

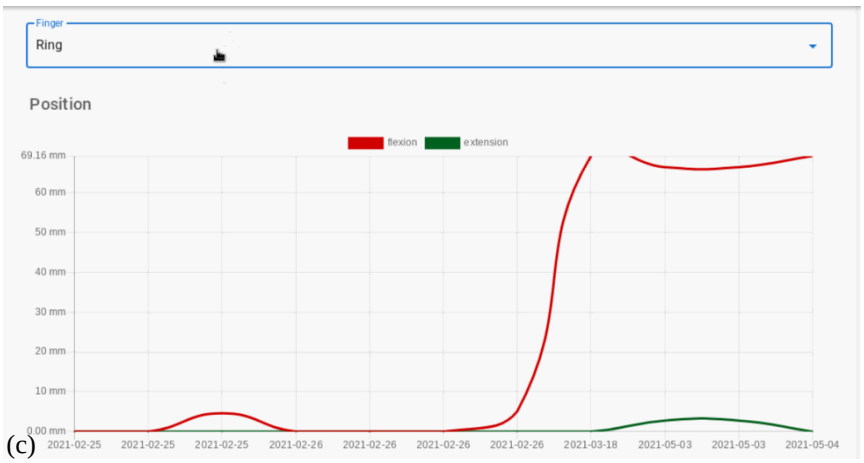

(c)

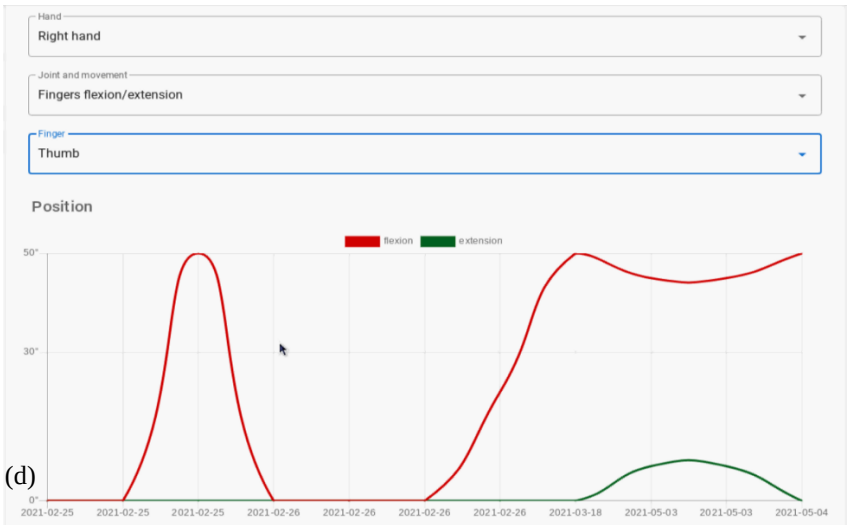

(d)

Figure 84: Time-based monitoring of the performance assessment.

(a), time-based monitoring of the performance assessment after 11 sessions. (b), time-based index finger F/E assessment. (c), time-based ring finger F/E assessment. (d), time-based thumb finger F/E assessment

7.6 Subjective Study and Results

In the experimental setup, two observations are mandatory to understand the usability and performance of this device. The first observation is based on analysing the proposed system functionality based on few parameters. Another observation is based on the device's safety and comfortability concern; it has to implement the different people before applying this on the stroke patient to understand whether this device is safest enough to be used by stroke patients. For testing this device, the six healthy participants have been asked to use this device and give their feedback on it, which is based on a carefully planned and revised questionnaire. The Participants were of different ages and different gender and from various occupational areas that perform different daily living activities.

7.6.1 Questionnaire For Cpm Device Functionality And Safety Feedback

This questionnaire consists of a variety of questions relating to the safety issues and proper functioning of the systems as given below:

Q1: How comfortable is the device in all-purpose use?

1 = Uncomfortable, 10 = Comfortable.

Q2: Was the device passive? It means that you did not need to perform active motion while the device was moving your fingers or wrist.

YES, NO

Q3: How smooth was this device during the training sessions?

1 = Very jerky, 10 = Very Smooth

Q4: How much you felt force from the CPM device on your finger while you resist?

1 = Very Strong, 10 = Not felt

Q5: Was the device's attachment on fingers was painful?

YES, NO

7.6.2 Evaluated Result With Healthy Participants

According to the feedback given by the healthy volunteers on the evaluation criteria of the proposed device based on a questionnaire proven to be safe to use and hence assuring the first observation to be fulfilled by the device which meets with the standard safety parameter. And the proposed system has achieved most of its aims and objectives. Another observation is based on the device's functionality in which users ranked it with the highest possible numbers, as shown from the bar graph illustrated in Figure 85.

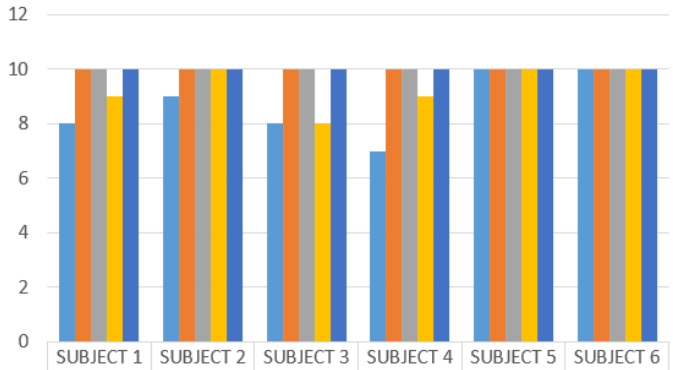

	SUBJECT 1	SUBJECT 2	SUBJECT 3	SUBJECT 4	SUBJECT 5	SUBJECT 6
(1= Uncomfortable, 10= Very Comfortable)	8	9	8	7	10	10
Device is Passive (YES, NO)	10	10	10	10	10	10
CPM motion Smoothness (1= Very Jerky, 10=Very Smooth)	10	10	10	10	10	10
Device forces the finger while applying resistance (1 = Very Strong, 10= Not felt)	9	10	8	9	10	10
Device's attachment painful (YES, NO)	10	10	10	10	10	10

Figure 86: Bar graph showing the Functionality and Safety measure of CPM device given by 06 healthy participants

Chapter 8: Conclusion and Future Work

8.1. Conclusion and Future Work

Over the years, hand rehabilitation devices have advanced drastically in terms of technological trends. However, due to the complex structure and intricateness of the human hands, it dramatically reduces efficient hand rehabilitation devices.

This dissertation addressed the concept and development of a cost-effective mechatronics rehabilitation device with a hybrid mechanism by adopting the combination of grounded-exoskeleton and end-effector mechanism. The proposed system targeted the four fingers plus the thumb and the wrist for either right or left hands. It was aimed to step forward to improve the related existing devices. The objective of the proposed system is to help the users regain both right and/or left-hand functionality and sensory-motor and reduce spasticity, muscle tone on the hand, and observe and evaluate their recovery steps. It was designed The intended system is designed to be a single device that capable of performing to aid the survivors who suffer hemiparesis of the upper arm caused by brain injury, spinal cord injury, tendon shatters, or fall-related injuries to perform four crucial movements: fingers F/E including the thumb F/E , wrist F/E, wrist E/U, and hand forearm S/P.

Unlike the related work in the literature, the proposed system's with a single design could train the mentioned joints. Additionally, the overall structure does not load the hand with a heavy and complex mechanical structure and efficiently trains the targeted joints. Additionally, owning an interactive embedded dashboard equipped with time-based self-assessment implementations enables the therapist to set then train, then evaluate the therapy control parameters conveniently. Moreover, the proposed system is equipped with specially developed game-based therapy which enabled the users to actively moves their wrist. Besides, the proposed system was

validated and tested with repeatable experimental tests to evaluate and validate the device's functionality.

The results of the tests indicate that the proposed system performed and met the requirements of an active, passive plus continuous passive motion, and interactive training modes configurations, and according to the set control parameters and the planned range of motions with minor and negligent errors. The system was designed concerning the requirements of the clinical standards at the University of Debrecen, rehabilitation department.

In future work, as this dissertation presented the prototype, some future developments. Some optimizations will be considered in the mechanical mechanism and design; besides performing clinical trials, will be considered to validate the proposed system with actual cases

8.2. Theses

This section provides the dissertation contributions related to brief analysis and publications for achieving all steps simultaneously.

Thesis I: Related publications: [P5, P8, P14]

- This thesis shaped a comprehensive guideline for building robot-based hand rehabilitation for people with brain injury, Neuroplasticity, spinal cord injury, tendon shatters, or fall-related injuries. Since there are no proper guidelines in literature could be found. Therefore, we set and defined proper guidance towards the existing state-of-the-art related technologies, and it identified the technical and clinical requirements towards design and inventing Robot-Assisted.
- This thesis identified a clinical case study that contributes to investigating and determining the level of the impact that the stroke can cause to the hand and wrist movements and force. It also helps examine the actual cases to which helped to achieve the proper design

at the Neurology and Rehabilitation department/university of Debrecen.

Thesis II: Related publications: [P2, P3, P5]

- This thesis developed a new kinematic model for single finger F/E, thumb F/E, and Ab/Ad. We have conducted several point-to-point motions for the index finger. These movements are a decent approximation of general finger F/E gestures with 3d model representation. These analyses of the hand movement configurations are needed so that a robotic system could be able to mimic its natural movement. Besides, a 2D Index finger workspace was driven to estimate the working area of the proposed system.
- This thesis introduces a new exoskeleton finger-guide design with initial fingers assist-robot system design; the initial proposed design drives the end-effector of the fingers (distal phalanx) with only one MC. This hygienic solution can guide each finger independently to the desired trajectories by integrating with the distal phalanx of the targeted finger without the need to actuate PIP and MCP joints.

Thesis III: Related publications: [P1, P2, P3]

- This thesis presented a novel solution for five-fingers robot-based rehabilitation. A forward kinematics model representation for the dynamic part of the proposed mechanism was mathematically represented to plot the predicted graphs of the robot's end-effector trajectories, positions, and velocity. A new implementation of developed control strategy of Impedance-Admittance controls, besides, an AAN controller provides active, passive and CPM therapy control modes. Eventually, quantitatively, and comparative studies

supported by biofeedback (EMG) were achieved which indicated the efficiency and usability of the proposed system.

Thesis IV Related publications: [P1]

- This dissertation presents a novel approach and implementation of five Integrative tactile sensors that were developed and validated to drive a force-feedback to the developed AAN controller designed to assist the patients with their active therapy. Additionally, it is also utilized to measure and evaluate the fingers pinch-tip strength measurement. Moreover, the developed algorithm analyses the collected forces data stored in the developed document-oriented NoSQL database (MongoDB) for progression evaluation report and presented in real-time during the therapy through the embedded developed GUI dashboard. Besides, a biofeedback sensory was implemented and detect the muscle activities through EMG signals.
- This thesis developed a time-based performance self-assessment; this feature enables the therapist and patient to detailly investigate and observe the recovery progress of the fingers in terms of grabbing force and ROM, the developed algorithm works based on performed maximum flexion and extension. This feature is taking the related technologies a step farther to make them not just robots for training but also as evaluating instruments.

Thesis V Related publications: [P1, P3]

- This thesis presents a new robot-based wrist rehabilitation system development that provided active, passive, interactive mode therapy for the wrist F/E and R/U. The proposed development was tested with a repeatable experimental test; the results are sufficiently accurate in aspects of the stability and trajectory's alignment; the actual trajectory directly correlates to the desired trajectory, which meets the requirements of continuous passive motion training configurations. In

active training mode, the proposed system could guide the participant to perform wrist F/E and R/U; additionally, uniaxial and elliptical boundary motions could be performed, which increase the participant ROM and trajectory's workspace

- This dissertation has presented the development and evaluation of new interactive game-based rehabilitation, which provided an engaging and amusing experience for individuals with wrist impaired motor capability; the game-based therapy guides the users to perform multiple wrist F/E and R/U deviation gestures with random directions. The archived scores were stored and evaluate the participant performance.

8.3. Publications

1. **Almusawi, H.**, Husi, G.: Design and Development of Continuous Passive Motion (CPM) for Fingers and Wrist Grounded-Exoskeleton Rehabilitation System. *Appl. Sci.-Basel.* 11 (2), 1-23, 2021. Folyóirat-mutatók: Q1 Engineering (miscellaneous) (2019) IF: 2.474 (2019)

2. Saadah, A., **Almusawi, H.**, Husi, G.: Computing The Kinematics Study of a 6 DOF Industrial Manipulator Prototype by Matlab. *Recent Innov. Mechatron.* 7 (1), 1-5, 2020.

3. **Almusawi, H.**, Afghan, S., Husi, G.: Designing the Mechanical Parts of a Low-Cost Hand Rehabilitation CPM Device for Stroke Patients. In: Innovation, Engineering and Entrepreneurship. Eds.: José Machado, Filomena Soares, Germano Veiga, Springer, Cham, 60-66,

2019, (Lecture Notes in Electrical Engineering, ISSN 1876-1119 ; 505) ISBN: 9783319913346

4. Afghan, S., **Almusawi, H.**, Husi, G.: Simulating the Electrical Characteristics of Solar Panels based on Practical Single-Diode Equivalent Circuit Model: Analyzing the Influence of Environmental Parameters on Output Power.
In: Innovation, Engineering and Entrepreneurship. Eds.: José Machado, Filomena Soares, Germano Veiga, Springer, Cham, 67-74, 2019, (Lecture Notes in Electrical Engineering, ISSN 1876-1119 ; 505.) ISBN: 9783319913346

5. **Almusawi, H.**, Afghan, S., Husi, G.: Recent trends in robotic systems for upper-limb stroke recovery: A low-cost hand and wrist rehabilitation device.
In: 2nd International Symposium on Small-scale Intelligent Manufacturing Systems (SIMS), 2018, IEEE, Piscataway, 1-6, 2018. ISBN: 9781538644379

   All citations+mentions: 9, External citations: 8, Self citations: 1, Unhandled citations: 0

6. Afghan, S., **Almusawi, H.**, Husi, G.: Towards the self-powered Internet of Things (IoT) by energy harvesting: Trends and technologies for green IoT.
In: 2018 2nd International Symposium on Small-scale Intelligent Manufacturing Systems (SIMS), IEEE, Piscataway, 1-5, 2018. ISBN: 9781538644379

All citations+mentions: 42, External citations: 42, Self citations: 0, Unhandled citations: 0

7. Afghan, S., **Almusawi, H.**, Husi, G.: Approximating the minimum output power for energy harvesting prototype: a case study of cell phone specifications = Minimális kimeneti teljesítmény meghatározása energy harvesting prototípushoz : egy esettanulmány mobiltelefon specifikációkra.
   In: A XXII. Fiatal Műszakiak Tudományos Ülésszak előadásai = Proceedings of the XXII-th International Scientific Conference of Young Engineers. Szerk.: Bitay Enikő, Erdélyi Múzeum Egyesület, Kolozsvár, 55-58, 2017, (Műszaki Tudományos Közlemények, ISSN 2393-1280 ; 7.) ISBN: 9789634490180

8. **Almusawi, H.**, Afghan, S., Husi, G., Molnár, Z., Erdei, T.: Reviewing the notable progress of effective techniques in the development of stroke hand rehabilitation devices = A stroke-t kapott egyének rehabilitációs eszközeiben jelentős fejlődést mutató hatékony technikák áttekintése.
   In: A XXII. Fiatal Műszakiak Tudományos Ülésszak előadásai = Proceedings of the XXII-th International Scientific Conference of Young Engineers. Szerk.: Bitay Enikő, Erdélyi Múzeum Egyesület, Kolozsvár, 63-66, 2017, (Műszaki Tudományos Közlemények, ISSN 2393-1280 ; 7.) ISBN: 9789634490180

9. Molnár, Z., Erdei, T., **Almusawi, H.**, Husi, G.: Saját CNC prototípus rendszer mint IoT eszköz = Our Own CNC Prototype System as IoT Device.
   In: A XXII. Fiatal Műszakiak Tudományos Ülésszak előadásai = Proceedings of the XXII-th International Scientific Conference of

Young Engineers. Szerk.: Bitay Enikő, Erdélyi Múzeum Egyesület (EME), Kolozsvár, 295-298, 2017. ISBN: 9789634490180

10. Afghan, S., **Almusawi, H.**, Husi, G.: Simulating the electrical characteristics of a photovoltaic cell based on a single-diode equivalent circuit model.
In: Proceedings of the Annual Session of Scientific Papers "Imt Oradea - 2017", 25th-27th May, Oradea, Romania. Eds.: Calin Baban, Florin Sandu Blaga, Gavril Grebenisan, Alexandru-Viorel Pele, Mircea Teodor Pop, Alexandru Rus, Radu Catalin Tarca, University of Oradea Publishing House, Oradea, 181-186, 2017. ISBN: 9786061015375

11. Afghan, S., **Almusawi, H.**, Husi, G.: Simulating the electrical characteristics of a photovoltaic cell based on a single-diode equivalent circuit model.
Anal. Univ. Oradea. Fasc. Ing. Manag. Technol. 26 (1), 91-96, 2017.

12. Afghan, S., **Almusawi, H.**, Husi, G.: Simulating the electrical characteristics of a photovoltaic cell based on a single-diode equivalent circuit model.
MATEC Web Conf. 126 1-6, 2017.

All citations+mentions: 4, External citations: 4, Self citations: 0, Unhandled citations: 0

13. Afghan, S., **Almusawi, H.**, Jokhio, S., Husi, G.: Estimation of minimum output power threshold for energy harvesting module: an inspection of battery and charging parameters of cell phones.
In: Proceedings of 4th International Mechatronical Student Micro-Conference. Eds.: Adrienn Dineva, István Nagy, Óbudai Egyetem, Budapest, 56-71, 2016. ISBN: 9789634490166

14. **Almusawi, H.**, Afghan, S., Husi, G.: Technological advancements in stroke hand rehabilitation devices: a review. In: Proceedings of 4th International Mechatronical Student Micro-Conference. Eds.: Adrienn Dineva, István Nagy, Óbudai Egyetem, Budapest, 80-90, 2016. ISBN: 9789634490166

References

[1] W. S. Harwin, J. L. Patton, and V. R. Edgerton, "Challenges and Opportunities for Robot-Mediated Neurorehabilitation," *Proceedings of the IEEE*, vol. 94, no. 9, 2006, doi: 10.1109/jproc.2006.880671.

[2] W. Johnson, O. Onuma, M. Owolabi, and S. Sachdev, "Stroke: a global response is needed," *Bulletin of the World Health Organization*, vol. 94, no. 9, 2016, doi: 10.2471/blt.16.181636.

[3] J. Mackay and G. A. Mensah, *The atlas of heart disease and stroke*. World Health Organization, 2004.

[4] B. H. Dobkin, "Strategies for stroke rehabilitation," *The Lancet Neurology*, vol. 3, no. 9, pp. 528–536, Sep. 2004, doi: 10.1016/S1474-4422(04)00851-8.

[5] J. S. Tutak, "Virtual reality and exercises for paretic upper limb of stroke survivors," *Tehnički vjesnik*, vol. 24, no. Supplement 2, pp. 451–458, Sep. 2017, doi: 10.17559/TV-20161011143721.

[6] R. Nudo, "Adaptive plasticity in motor cortex: Implications for rehabilitation after brain injury," *Journal of rehabilitation medicine : official journal of the UEMS European Board of Physical and Rehabilitation Medicine*, vol. 35, pp. 7–10, Jun. 2003, doi: 10.1080/16501960310010070.

[7] "Stroke - Symptoms," *nhs.uk*, Oct. 24, 2017. https://www.nhs.uk/conditions/stroke/symptoms/ (accessed Apr. 09, 2021).

[8] G. Kwakkel, B. J. Kollen, J. van der Grond, and A. J. H. Prevo, "Probability of Regaining Dexterity in the Flaccid Upper Limb," *Stroke*, vol. 34, no. 9, 2003, doi: 10.1161/01.str.0000087172.16305.cd.

[9] C.-Y. Chu and R. M. Patterson, "Soft robotic devices for hand rehabilitation and assistance: a narrative review," *J NeuroEngineering Rehabil*, vol. 15, no. 1, p. 9, Feb. 2018, doi: 10.1186/s12984-018-0350-6.

[10] B. Chen, B. Zi, Z. Wang, L. Qin, and W.-H. Liao, "Knee exoskeletons for gait rehabilitation and human performance augmentation: A state-of-the-art," *Mechanism and Machine Theory*, vol. 134, pp. 499–511, Apr. 2019, doi: 10.1016/j.mechmachtheory.2019.01.016.

[11] H. S. Lo and S. Q. Xie, "Exoskeleton robots for upper-limb rehabilitation: State of the art and future prospects," *Medical Engineering & Physics*, vol. 34, no. 3, pp. 261–268, Apr. 2012, doi: 10.1016/j.medengphy.2011.10.004.

[12] F. Ozkul and D. E. Barkana, “Upper-Extremity Rehabilitation Robot RehabRoby: Methodology, Design, Usability and Validation,” *International Journal of Advanced Robotic Systems*, vol. 10, no. 12, 2013, doi: 10.5772/57261.

[13] G. Thrane, “Arm function and constraint-induced movement in early post-stroke rehabilitation,” Sep. 2015, Accessed: Apr. 09, 2021. [Online]. Available: https://munin.uit.no/handle/10037/8208

[14] J. D. Schaechter, “Motor rehabilitation and brain plasticity after hemiparetic stroke,” *Progress in Neurobiology*, vol. 73, no. 1, pp. 61–72, May 2004, doi: 10.1016/j.pneurobio.2004.04.001.

[15] Lawrence Enas S. *et al.*, “Estimates of the Prevalence of Acute Stroke Impairments and Disability in a Multiethnic Population,” *Stroke*, vol. 32, no. 6, pp. 1279–1284, Jun. 2001, doi: 10.1161/01.STR.32.6.1279.

[16] D. Bourbonnais and S. V. Noven, “Weakness in Patients With Hemiparesis,” *Am J Occup Ther*, vol. 43, no. 5, pp. 313–319, May 1989, doi: 10.5014/ajot.43.5.313.

[17] J. Cauraugh, K. Light, S. Kim, M. Thigpen, and A. Behrman, “Chronic Motor Dysfunction After Stroke,” *Stroke*, vol. 31, no. 6, 2000, doi: 10.1161/01.str.31.6.1360.

[18] D. G. Kamper and W. Z. Rymer, “Impairment of voluntary control of finger motion following stroke: Role of inappropriate muscle coactivation,” *Muscle & Nerve*, vol. 24, no. 5, 2001, doi: 10.1002/mus.1054.

[19] S. Li, M. L. Latash, G. H. Yue, V. Siemionow, and V. Sahgal, “The effects of stroke and age on finger interaction in multi-finger force production tasks,” *Clinical Neurophysiology*, vol. 114, no. 9, 2003, doi: 10.1016/s1388-2457(03)00164-0.

[20] T. Verstynen, J. Diedrichsen, N. Albert, P. Aparicio, and R. B. Ivry, “Ipsilateral Motor Cortex Activity During Unimanual Hand Movements Relates to Task Complexity,” *Journal of Neurophysiology*, vol. 93, no. 3, 2005, doi: 10.1152/jn.00720.2004.

[21] “Hand Therapy Awareness Week 2018 | Dr Paul Jarrett, Hand, Wrist & Shoulder Surgeon.,” *Dr Paul Jarrett, Hand, Wrist & Shoulder Surgeon.*, 2018. https://pauljarrett.info/hand-therapy-awareness-week-2018/ (accessed Jan. 01, 2021).

[22] “Motor Recovery In Stroke: Recovery Considerations, Theories of Recovery, Mechanisms of Recovery,” Apr. 2021, Accessed: Apr. 09, 2021. [Online]. Available: https://emedicine.medscape.com/article/324386-overview#a1

[23] F. Coupar, A. Pollock, P. Rowe, C. Weir, and P. Langhorne, “Predictors of upper limb recovery after stroke: a systematic review and meta-analysis,” *Clinical Rehabilitation*, vol. 26, no. 4, pp. 291–313, Apr. 2012, doi: 10.1177/0269215511420305.

[24] J. BROMLEY, A. UNSWORTH, and I. HASLOCK, “CHANGES IN STIFFNESS FOLLOWING SHORT- AND LONG-TERM APPLICATION OF STANDARD

PHYSIOTHERAPEUTIC TECHNIQUES," *Rheumatology*, vol. 33, no. 6, pp. 555–561, Jun. 1994, doi: 10.1093/rheumatology/33.6.555.

[25] K. Schultz-Johnson, "Static progressive splinting," *Journal of Hand Therapy*, vol. 15, no. 2, pp. 163–178, Apr. 2002, doi: 10.1053/hanthe.2002.v15.015016.

[26] Z. Li, "Using robotic hand technology for the rehabilitation of recovering stroke patients with loss of hand power," 2003, [Online]. Available: https://repository.lib.ncsu.edu/handle/1840.16/2017

[27] J. lance, "Symposium synopsis. spasticity: Disordered motor control – ScienceOpen," Chicago 1980. https://www.scienceopen.com/document?vid=9a711532-d33b-4ecb-92ac-c11496a65f5b (accessed Apr. 09, 2021).

[28] O. Khazen, BS, "Spasticity – Causes, Symptoms and Treatments," *Spasticity*, 2021. https://www.aans.org/Patients/Neurosurgical-Conditions-and-Treatments/Spasticity (accessed Jan. 01, 2021).

[29] P. Lindberg, C. Schmitz, H. Forssberg, M. Engardt, and J. Borg, "Effects of passive-active movement training on upper limb motor function and cortical activation in chronic patients with stroke: a pilot study," *Journal of rehabilitation medicine*, vol. 36, no. 3, pp. 117–123, 2004.

[30] J. Seladi-Schulman, "Occupational Therapy vs. Physical Therapy: What to Know," *Healthline*, 2020. https://www.healthline.com/health/occupational-therapy-vs-physical-therapy (accessed Jan. 01, 2021).

[31] J. Buurke, "Walking after stroke: co-ordination patterns & functional recovery," Proefschrift Universiteit Twente, Enschede, S.l., 2005.

[32] B. Walker, "PNF Stretching Explained | Proprioceptive Neuromuscular Facilitation," Oct. 17, 2019. https://stretchcoach.com/articles/pnf-stretching/ (accessed Apr. 10, 2021).

[33] J. H. Carr and R. B. Shepherd, *A motor relearning programme for stroke*. Oxford; Rockville, Md.: Heinemann Medical Books ; Aspen Publishers, 1987. Accessed: Apr. 10, 2021. [Online]. Available: http://books.google.com/books?id=O7RrAAAAMAAJ

[34] L. C. Shaw *et al.*, "Botulinum Toxin for the Upper Limb after Stroke (BoTULS) Trial: effect on impairment, activity limitation, and pain," *Stroke*, vol. 42, no. 5, pp. 1371–1379, 2011.

[35] H. Almusawi, S. A. Afghan, and H. Geza, "Technological advancements in stroke hand rehabilitation devices: a review .," in *International Mechatronical Student Micro-Conference*, Budapest, 2016, pp. 80–90.

[36] "Functional Electrical Stimulation Enhancement of Upper Extremity Functional Recovery During Stroke Rehabilitation: A Pilot Study - Gad Alon, Alan F. Levitt, Patricia A. McCarthy, 2007." https://journals.sagepub.com/doi/abs/10.1177/1545968306297871 (accessed Apr. 10, 2021).

[37] T. Yan, C. W. Y. Hui-Chan, and L. S. W. Li, “Functional Electrical Stimulation Improves Motor Recovery of the Lower Extremity and Walking Ability of Subjects With First Acute Stroke,” *Stroke*, vol. 36, no. 1, 2005, doi: 10.1161/01.str.0000149623.24906.63.

[38] P. S. Lum, S. B. Godfrey, E. B. Brokaw, R. J. Holley, and D. Nichols, “Robotic Approaches for Rehabilitation of Hand Function After Stroke,” *American Journal of Physical Medicine & Rehabilitation*, vol. 91, no. 11, 2012, doi: 10.1097/phm.0b013e31826bcedb.

[39] E. Taub, G. Uswatte, and R. Pidikiti, “Constraint-Induced Movement Therapy: a new family of techniques with broad application to physical rehabilitation--a clinical review,” *J Rehabil Res Dev*, vol. 36, no. 3, pp. 237–251, Jul. 1999.

[40] C. Mannheimer and C.-A. Carlsson, “The analgesic effect of transcutaneous electrical nerve stimulation (TNS) in patients with rheumatoid arthritis. A comparative study of different pulse patterns,” *PAIN*, vol. 6, no. 3, pp. 329–334, Jun. 1979, doi: 10.1016/0304-3959(79)90051-4.

[41] M.-C. Smith and C. M. Stinear, “Transcranial magnetic stimulation (TMS) in stroke: Ready for clinical practice?,” *Journal of Clinical Neuroscience*, vol. 31, pp. 10–14, Sep. 2016, doi: 10.1016/j.jocn.2016.01.034.

[42] D. K. Rose and C. J. Winstein, “Bimanual Training After Stroke: Are Two Hands Better Than One?,” *Topics in Stroke Rehabilitation*, vol. 11, no. 4, pp. 20–30, Oct. 2004, doi: 10.1310/NCB1-JWAA-09QE-7TXB.

[43] D. B. Gandhi, A. Sterba, H. Khatter, and J. D. Pandian, “Mirror Therapy in Stroke Rehabilitation: Current Perspectives,” *Ther Clin Risk Manag*, vol. 16, pp. 75–85, Feb. 2020, doi: 10.2147/TCRM.S206883.

[44] T. Cowles, A. Clark, K. Mares, G. Peryer, R. Stuck, and V. Pomeroy, “Observation-to-Imitate Plus Practice Could Add Little to Physical Therapy Benefits Within 31 Days of Stroke: Translational Randomized Controlled Trial,” *Neurorehabil Neural Repair*, vol. 27, no. 2, pp. 173–182, Feb. 2013, doi: 10.1177/1545968312452470.

[45] M. Ietswaart *et al.*, “Mental practice with motor imagery in stroke recovery: randomized controlled trial of efficacy,” *Brain*, vol. 134, no. 5, pp. 1373–1386, May 2011, doi: 10.1093/brain/awr077.

[46] R. Bertani, C. Melegari, M. C. De Cola, A. Bramanti, P. Bramanti, and R. S. Calabrò, “Effects of robot-assisted upper limb rehabilitation in stroke patients: a systematic review with meta-analysis,” *Neurol Sci*, vol. 38, no. 9, pp. 1561–1569, Sep. 2017, doi: 10.1007/s10072-017-2995-5.

[47] N. Norouzi-Gheidari, P. S. Archambault, and J. Fung, “Effects of robot-assisted therapy on stroke rehabilitation in upper limbs: systematic review and meta-analysis of the literature,” *J Rehabil Res Dev*, vol. 49, no. 4, pp. 479–496, 2012, doi: 10.1682/jrrd.2010.10.0210.

[48] L. E. Kahn, P. S. Lum, W. Z. Rymer, and D. J. Reinkensmeyer, “Robot-assisted movement training for the stroke-impaired arm: Does it matter what the

robot does?," *Bulletin of prosthetics research*, vol. 43, no. 5, pp. 619–629, Sep. 2006, doi: 10.1682/JRRD.2005.03.0056.

[49] L. D. L. da Silva, T. F. Pereira, V. R. Q. Leithardt, L. O. Seman, and C. A. Zeferino, "Hybrid Impedance-Admittance Control for Upper Limb Exoskeleton Using Electromyography," *Applied Sciences*, vol. 10, no. 20, Art. no. 20, Jan. 2020, doi: 10.3390/app10207146.

[50] F. Zhang, L. Lin, L. Yang, and Y. Fu, "Design of an Active and Passive Control System of Hand Exoskeleton for Rehabilitation," *Applied Sciences*, vol. 9, no. 11, Art. no. 11, Jan. 2019, doi: 10.3390/app9112291.

[51] L. Zhang, J. Li, Y. Cui, M. Dong, B. Fang, and P. Zhang, "Design and performance analysis of a parallel wrist rehabilitation robot (PWRR)," *Robotics and Autonomous Systems*, vol. 125, p. 103390, Mar. 2020, doi: 10.1016/j.robot.2019.103390.

[52] Z. Pang, T. Wang, Z. Wang, J. Yu, Z. Sun, and S. Liu, "Design and Analysis of a Wearable Upper Limb Rehabilitation Robot with Characteristics of Tension Mechanism," *Applied Sciences*, vol. 10, no. 6, Art. no. 6, Jan. 2020, doi: 10.3390/app10062101.

[53] D. Wang, Y. Wang, B. Zi, Z. Cao, and H. Ding, "Development of an active and passive finger rehabilitation robot using pneumatic muscle and magnetorheological damper," *Mechanism and Machine Theory*, vol. 147, p. 103762, May 2020, doi: 10.1016/j.mechmachtheory.2019.103762.

[54] A. Tyromotion, "AMADEO," *Tyromotion*. https://tyromotion.com/en/products/amadeo/ (accessed Apr. 11, 2021).

[55] S. E. Palsbo and P. Hood-Szivek, "Effect of Robotic-Assisted Three-Dimensional Repetitive Motion to Improve Hand Motor Function and Control in Children With Handwriting Deficits: A Nonrandomized Phase 2 Device Trial," *Am J Occup Ther*, vol. 66, no. 6, pp. 682–690, Nov. 2012, doi: 10.5014/ajot.2012.004556.

[56] H. I. Krebs, N. Hogan, M. L. Aisen, and B. T. Volpe, "Robot-aided neurorehabilitation," *IEEE Transactions on Rehabilitation Engineering*, vol. 6, no. 1, pp. 75–87, Mar. 1998, doi: 10.1109/86.662623.

[57] B. T. Volpe, H. I. Krebs, N. Hogan, L. Edelsteinn, C. M. Diels, and M. L. Aisen, "Robot training enhanced motor outcome in patients with stroke maintained over 3 years," *Neurology*, vol. 53, no. 8, pp. 1874–1874, Nov. 1999, doi: 10.1212/WNL.53.8.1874.

[58] B. Inc, "BIONIK | Rehabilitation Robotics Manufacturer." https://www.bioniklabs.com (accessed Apr. 11, 2021).

[59] H. I. Krebs *et al.*, "Rehabilitation robotics: pilot trial of a spatial extension for MIT-Manus," *J NeuroEngineering Rehabil*, vol. 1, no. 1, p. 5, Oct. 2004, doi: 10.1186/1743-0003-1-5.

[60] B. Inc, "Solutions - InMotion® Robotic Therapy for Stroke Treatment." https://www.bioniklabs.com/products/overview (accessed Apr. 11, 2021).

[61] B. Inc, “InMotion ARM/HAND® | Robotic Assisted Therapy for Treating Stroke.” https://www.bioniklabs.com/products/inmotion-arm-hand (accessed Apr. 11, 2021).
[62] P. S. Lum, C. G. Burgar, P. C. Shor, M. Majmundar, and M. Van der Loos, “Robot-assisted movement training compared with conventional therapy techniques for the rehabilitation of upper-limb motor function after stroke,” *Archives of Physical Medicine and Rehabilitation*, vol. 83, no. 7, pp. 952–959, Jul. 2002, doi: 10.1053/apmr.2001.33101.
[63] S. Hesse, H. Schmidt, C. Werner, and A. Bardeleben, “Upper and lower extremity robotic devices for rehabilitation and for studying motor control,” *Current Opinion in Neurology*, vol. 16, no. 6, pp. 705–710, Dec. 2003.
[64] B.-M. Trainer, “Bi-Manu-Trainer - Reha-Stim Medtec AG,” *Reha-Stim*. https://reha-stim.com/bi-manu-trainer/ (accessed Apr. 11, 2021).
[65] S. Hesse, G. Schulte-Tigges, M. Konrad, A. Bardeleben, and C. Werner, “Robot-assisted arm trainer for the passive and active practice of bilateral forearm and wrist movements in hemiparetic subjects11An organization with which 1 or more of the authors is associated has received or will receive financial benefits from a commercial party having a direct financial interest in the results of the research supporting this article.,” *Archives of Physical Medicine and Rehabilitation*, vol. 84, no. 6, pp. 915–920, Jun. 2003, doi: 10.1016/S0003-9993(02)04954-7.
[66] A. (Lex) E. Q. van Delden, C. (Lieke) E. Peper, G. Kwakkel, and P. J. Beek, “A Systematic Review of Bilateral Upper Limb Training Devices for Poststroke Rehabilitation,” *Stroke Research and Treatment*, vol. 2012, p. e972069, Nov. 2012, doi: 10.1155/2012/972069.
[67] G. Rosati, P. Gallina, and S. Masiero, “Design, implementation and clinical tests of a wire-based robot for neurorehabilitation,” *IEEE Trans Neural Syst Rehabil Eng*, vol. 15, no. 4, pp. 560–569, Dec. 2007, doi: 10.1109/TNSRE.2007.908560.
[68] A. A. Timmermans, H. A. Seelen, R. D. Willmann, and H. Kingma, “Technology-assisted training of arm-hand skills in stroke: concepts on reacquisition of motor control and therapist guidelines for rehabilitation technology design,” *Journal of NeuroEngineering and Rehabilitation*, vol. 6, no. 1, p. 1, Jan. 2009, doi: 10.1186/1743-0003-6-1.
[69] D. J. Reinkensmeyer, B. D. Schmit, and W. Z. Rymer, *Can Robots Improve Arm Movement Recovery After Chronic Brain Injury? A Rationale for Their Use Based on Experimentally Identified Motor Impairments*.
[70] D. J. Reinkensmeyer, B. D. Schmit, and W. Z. Rymer, “Assessment of Active and Passive Restraint During Guided Reaching After Chronic Brain Injury,” *Annals of Biomedical Engineering*, vol. 27, no. 6, pp. 805–814, Nov. 1999, doi: 10.1114/1.233.
[71] L. E. Kahn, M. L. Zygman, W. Z. Rymer, and D. J. Reinkensmeyer, “Robot-assisted reaching exercise promotes arm movement recovery in chronic

hemiparetic stroke: a randomized controlled pilot study," *Journal of NeuroEngineering and Rehabilitation*, vol. 3, no. 1, p. 12, Jun. 2006, doi: 10.1186/1743-0003-3-12.

[72] T. Nef, M. Guidali, V. Klamroth-Marganska, and R. Riener, "ARMin - Exoskeleton Robot for Stroke Rehabilitation," in *World Congress on Medical Physics and Biomedical Engineering, September 7 - 12, 2009, Munich, Germany*, Berlin, Heidelberg, 2009, pp. 127–130. doi: 10.1007/978-3-642-03889-1_35.

[73] T. Nef, M. Mihelj, and R. Riener, "ARMin: a robot for patient-cooperative arm therapy," *Med Bio Eng Comput*, vol. 45, no. 9, pp. 887–900, Sep. 2007, doi: 10.1007/s11517-007-0226-6.

[74] R. C. V. Loureiro, B. Lamperd, C. Collin, and W. S. Harwin, "Reach grasp therapy: Effects of the Gentle/G System assessing sub-acute stroke whole-arm rehabilitation," in *2009 IEEE International Conference on Rehabilitation Robotics*, Jun. 2009, pp. 755–760. doi: 10.1109/ICORR.2009.5209509.

[75] H. Kawasaki *et al.*, "Development of a Hand Motion Assist Robot for Rehabilitation Therapy by Patient Self-Motion Control," in *2007 IEEE 10th International Conference on Rehabilitation Robotics*, Jun. 2007, pp. 234–240. doi: 10.1109/ICORR.2007.4428432.

[76] S. Balasubramanian *et al.*, "RUPERT: An exoskeleton robot for assisting rehabilitation of arm functions," in *2008 Virtual Rehabilitation*, Aug. 2008, pp. 163–167. doi: 10.1109/ICVR.2008.4625154.

[77] O. Lambercy, L. Dovat, R. Gassert, E. Burdet, C. L. Teo, and T. Milner, "A Haptic Knob for Rehabilitation of Hand Function," *IEEE Transactions on Neural Systems and Rehabilitation Engineering*, vol. 15, no. 3, pp. 356–366, Sep. 2007, doi: 10.1109/TNSRE.2007.903913.

[78] Rehab Robotics Cmp Ltd, "Innovative way of stroke rehabilitation|Rehab-Robotics." http://www.rehab-robotics.com.hk/ (accessed Apr. 11, 2021).

[79] C. D. Takahashi, L. Der-Yeghiaian, V. Le, R. R. Motiwala, and S. C. Cramer, "Robot-based hand motor therapy after stroke," *Brain*, vol. 131, no. Pt 2, pp. 425–437, Feb. 2008, doi: 10.1093/brain/awm311.

[80] C. D. Takahashi, L. Der-Yeghiaian, V. H. Le, and S. C. Cramer, "A robotic device for hand motor therapy after stroke," in *9th International Conference on Rehabilitation Robotics, 2005. ICORR 2005.*, Jun. 2005, pp. 17–20. doi: 10.1109/ICORR.2005.1501041.

[81] A. Frisoli, M. Bergamasco, S. L. Wu, and E. Ruffaldi, "11 Evaluation of Multipoint Contact Interfaces in Haptic Perception of Shapes," in *Multi-point Interaction with Real and Virtual Objects*, F. Barbagli, D. Prattichizzo, and K. Salisbury, Eds. Berlin, Heidelberg: Springer, 2005, pp. 177–188. doi: 10.1007/11429555_11.

[82] T. Yoshikawa, T. Endo, T. Maeno, and H. Kawasaki, "Multi-Fingered Bimanual Haptic Interface with Three-Dimensional Force Presentation,"

IFAC Proceedings Volumes, vol. 42, no. 16, pp. 651–656, Jan. 2009, doi: 10.3182/20090909-4-JP-2010.00110.

[83] K. D. Fitle, A. U. Pehlivan, and M. K. O'Malley, "A robotic exoskeleton for rehabilitation and assessment of the upper limb following incomplete spinal cord injury," in *2015 IEEE International Conference on Robotics and Automation (ICRA)*, May 2015, pp. 4960–4966. doi: 10.1109/ICRA.2015.7139888.

[84] A. U. Pehlivan, O. Celik, and M. K. O'Malley, "Mechanical design of a distal arm exoskeleton for stroke and spinal cord injury rehabilitation," in *2011 IEEE International Conference on Rehabilitation Robotics*, Jun. 2011, pp. 1–5. doi: 10.1109/ICORR.2011.5975428.

[85] A. U. Pehlivan, D. P. Losey, and M. K. O'Malley, "Minimal Assist-as-Needed Controller for Upper Limb Robotic Rehabilitation," *IEEE Transactions on Robotics*, vol. 32, no. 1, pp. 113–124, Feb. 2016, doi: 10.1109/TRO.2015.2503726.

[86] Kinetec Maestra™, "Kinetec Maestra - Kinetec Maestra - Hand & Wrist - Continuous Passive Motion (CPM) - Kinetec - Brands." https://www.kinetecusa.com/brands/kinetec/cpm/continuous-passive-motion-hand-and-wrist/kinetec-maestra/kinetec-maestra (accessed Apr. 11, 2021).

[87] R. Riener, T. Nef, and G. Colombo, "Robot-aided neurorehabilitation of the upper extremities," *Med. Biol. Eng. Comput.*, vol. 43, no. 1, pp. 2–10, Feb. 2005, doi: 10.1007/BF02345116.

[88] A. H. AbdulKareem, A. S. Adila, and G. Husi, "Recent trends in robotic systems for upper-limb stroke recovery: A low-cost hand and wrist rehabilitation device," in *2018 2nd International Symposium on Small-scale Intelligent Manufacturing Systems (SIMS)*, Apr. 2018, pp. 1–6. doi: 10.1109/SIMS.2018.8355302.

[89] P. Maciejasz, J. Eschweiler, K. Gerlach-Hahn, A. Jansen-Troy, and S. Leonhardt, "A survey on robotic devices for upper limb rehabilitation," *Journal of NeuroEngineering and Rehabilitation*, vol. 11, no. 1, p. 3, Jan. 2014, doi: 10.1186/1743-0003-11-3.

[90] T.-Y. Ho, Y.-J. Chen, and P.-H. Chen, "The design and implementation of a motor drive for foot rehabilitation," *Computers & Electrical Engineering*, vol. 56, pp. 795–806, Nov. 2016, doi: 10.1016/j.compeleceng.2016.07.017.

[91] R. Sanchez *et al.*, "Monitoring functional arm movement for home-based therapy after stroke," in *The 26th Annual International Conference of the IEEE Engineering in Medicine and Biology Society*, Sep. 2004, vol. 2, pp. 4787–4790. doi: 10.1109/IEMBS.2004.1404325.

[92] E. J. Koeneman, R. S. Schultz, S. L. Wolf, D. E. Herring, and J. B. Koeneman, "A pneumatic muscle hand therapy device," in *The 26th Annual International Conference of the IEEE Engineering in Medicine and Biology*

Society, Sep. 2004, vol. 1, pp. 2711–2713. doi: 10.1109/IEMBS.2004.1403777.

[93] P. Cordo, H. Lutsep, L. Cordo, W. G. Wright, T. Cacciatore, and R. Skoss, "Assisted Movement With Enhanced Sensation (AMES): Coupling Motor and Sensory to Remediate Motor Deficits in Chronic Stroke Patients," *Neurorehabil Neural Repair*, vol. 23, no. 1, pp. 67–77, Jan. 2009, doi: 10.1177/1545968308317437.

[94] Yasuhisa Hasegawa, Yasuyuki Mikami, Kosuke Watanabe, and Yoshiyuki Sankai, "Five-fingered assistive hand with mechanical compliance of human finger," in *2008 IEEE International Conference on Robotics and Automation*, May 2008, pp. 718–724. doi: 10.1109/ROBOT.2008.4543290.

[95] L. Zhang, S. Guo, and Q. Sun, "Development and Assist-As-Needed Control of an End-Effector Upper Limb Rehabilitation Robot," *Applied Sciences*, vol. 10, no. 19, Art. no. 19, Jan. 2020, doi: 10.3390/app10196684.

[96] I. H. Ertas, E. Hocaoglu, D. E. Barkana, and V. Patoglu, "Finger exoskeleton for treatment of tendon injuries," in *2009 IEEE International Conference on Rehabilitation Robotics*, Jun. 2009, pp. 194–201. doi: 10.1109/ICORR.2009.5209487.

[97] J. Lee and J. Bae, "Design of a hand exoskeleton for biomechanical analysis of the stroke hand," in *2015 IEEE International Conference on Rehabilitation Robotics (ICORR)*, Aug. 2015, pp. 484–489. doi: 10.1109/ICORR.2015.7281246.

[98] A. Polotto, F. Modulo, F. Flumian, Z. G. Xiao, P. Boscariol, and C. Menon, "Index finger rehabilitation/assistive device," in *2012 4th IEEE RAS EMBS International Conference on Biomedical Robotics and Biomechatronics (BioRob)*, Jun. 2012, pp. 1518–1523. doi: 10.1109/BioRob.2012.6290676.

[99] J. Wang, J. Li, Y. Zhang, and S. Wang, "Design of an exoskeleton for index finger rehabilitation," in *2009 Annual International Conference of the IEEE Engineering in Medicine and Biology Society*, Sep. 2009, pp. 5957–5960. doi: 10.1109/IEMBS.2009.5334779.

[100] D. Popov, I. Gaponov, and J. Ryu, "Portable Exoskeleton Glove With Soft Structure for Hand Assistance in Activities of Daily Living," *IEEE/ASME Transactions on Mechatronics*, vol. 22, no. 2, pp. 865–875, Apr. 2017, doi: 10.1109/TMECH.2016.2641932.

[101] P. W. Ferguson, B. Dimapasoc, Y. Shen, and J. Rosen, "Design of a Hand Exoskeleton for Use with Upper Limb Exoskeletons," in *Wearable Robotics: Challenges and Trends*, Cham, 2019, pp. 276–280. doi: 10.1007/978-3-030-01887-0_53.

[102] M. A. Rahman and A. Al-Jumaily, "Design and Development of a Hand Exoskeleton for Rehabilitation Following Stroke," *Procedia Engineering*, vol. 41, pp. 1028–1034, Jan. 2012, doi: 10.1016/j.proeng.2012.07.279.

[103] L. Cui, A. Phan, and G. Allison, "Design and fabrication of a three dimensional printable non-assembly articulated hand exoskeleton for

rehabilitation," in *2015 37th Annual International Conference of the IEEE Engineering in Medicine and Biology Society (EMBC)*, Aug. 2015, pp. 4627–4630. doi: 10.1109/EMBC.2015.7319425.

[104] I. Jo and J. Bae, "A Force-Controllable Compact Actuator Module for a Wearable Hand Exoskeleton," *IFAC Proceedings Volumes*, vol. 47, no. 3, pp. 4453–4458, Jan. 2014, doi: 10.3182/20140824-6-ZA-1003.01863.

[105] M. Sarac, M. Solazzi, E. Sotgiu, M. Bergamasco, and A. Frisoli, "Design and kinematic optimization of a novel underactuated robotic hand exoskeleton," *Meccanica*, vol. 52, no. 3, pp. 749–761, Feb. 2017, doi: 10.1007/s11012-016-0530-z.

[106] J. Arata, K. Ohmoto, R. Gassert, O. Lambercy, H. Fujimoto, and I. Wada, "A new hand exoskeleton device for rehabilitation using a three-layered sliding spring mechanism," in *2013 IEEE International Conference on Robotics and Automation*, May 2013, pp. 3902–3907. doi: 10.1109/ICRA.2013.6631126.

[107] H. Almusawi and G. Husi, "Design and Development of Continuous Passive Motion (CPM) for Fingers and Wrist Grounded-Exoskeleton Rehabilitation System," *Applied Sciences*, vol. 11, no. 2, Art. no. 2, Jan. 2021, doi: 10.3390/app11020815.

[108] A. Chiri *et al.*, "HANDEXOS: Towards an exoskeleton device for the rehabilitation of the hand," in *2009 IEEE/RSJ International Conference on Intelligent Robots and Systems*, Oct. 2009, pp. 1106–1111. doi: 10.1109/IROS.2009.5354376.

[109] M. Cortese, M. Cempini, P. R. D. A. Ribeiro, S. R. Soekadar, M. C. Carrozza, and N. Vitiello, "A Mechatronic System for Robot-Mediated Hand Telerehabilitation," *IEEE/ASME Transactions on Mechatronics*, vol. 20, no. 4, pp. 1753–1764, Aug. 2015, doi: 10.1109/TMECH.2014.2353298.

[110] P. M. Aubin, H. Sallum, C. Walsh, L. Stirling, and A. Correia, "A pediatric robotic thumb exoskeleton for at-home rehabilitation: the Isolated Orthosis for Thumb Actuation (IOTA)," *IEEE Int Conf Rehabil Robot*, vol. 2013, p. 6650500, Jun. 2013, doi: 10.1109/ICORR.2013.6650500.

[111] H. Yamaura, K. Matsushita, R. Kato, and H. Yokoi, "Development of hand rehabilitation system for paralysis patient – universal design using wire-driven mechanism –," in *2009 Annual International Conference of the IEEE Engineering in Medicine and Biology Society*, Sep. 2009, pp. 7122–7125. doi: 10.1109/IEMBS.2009.5332885.

[112] B. Allotta, R. Conti, L. Governi, E. Meli, A. Ridolfi, and Y. Volpe, "Development and experimental testing of a portable hand exoskeleton," in *2015 IEEE/RSJ International Conference on Intelligent Robots and Systems (IROS)*, Sep. 2015, pp. 5339–5344. doi: 10.1109/IROS.2015.7354131.

[113] M. Mulas, M. Folgheraiter, and G. Gini, "An EMG-controlled exoskeleton for hand rehabilitation," in *9th International Conference on Rehabilitation Robotics, 2005. ICORR 2005.*, Jun. 2005, pp. 371–374. doi: 10.1109/ICORR.2005.1501122.

[114] T. M. W. Burton, R. Vaidyanathan, S. C. Burgess, A. J. Turton, and C. Melhuish, “Development of a parametric kinematic model of the human hand and a novel robotic exoskeleton,” in *2011 IEEE International Conference on Rehabilitation Robotics*, Jun. 2011, pp. 1–7. doi: 10.1109/ICORR.2011.5975344.

[115] M. Bouzit, G. Burdea, G. Popescu, and R. Boian, “The Rutgers Master II-new design force-feedback glove,” *IEEE/ASME Transactions on Mechatronics*, vol. 7, no. 2, pp. 256–263, Jun. 2002, doi: 10.1109/TMECH.2002.1011262.

[116] H. Li and L. Cheng, “Preliminary study on the design and control of a pneumatically-actuated hand rehabilitation device,” in *2017 32nd Youth Academic Annual Conference of Chinese Association of Automation (YAC)*, May 2017, pp. 860–865. doi: 10.1109/YAC.2017.7967530.

[117] L. Connelly, Y. Jia, M. L. Toro, M. E. Stoykov, R. V. Kenyon, and D. G. Kamper, “A Pneumatic Glove and Immersive Virtual Reality Environment for Hand Rehabilitative Training After Stroke,” *IEEE Transactions on Neural Systems and Rehabilitation Engineering*, vol. 18, no. 5, pp. 551–559, Oct. 2010, doi: 10.1109/TNSRE.2010.2047588.

[118] P. Polygerinos, Z. Wang, K. C. Galloway, R. J. Wood, and C. J. Walsh, “Soft robotic glove for combined assistance and at-home rehabilitation,” *Robotics and Autonomous Systems*, vol. 73, pp. 135–143, Nov. 2015, doi: 10.1016/j.robot.2014.08.014.

[119] P. Maeder-York *et al.*, “Biologically Inspired Soft Robot for Thumb Rehabilitation1,” *Journal of Medical Devices*, vol. 8, no. 020933, Apr. 2014, doi: 10.1115/1.4027031.

[120] Zhongsheng Sun, Xiaodong Miao, and Xiaoning Li, “Design of a bidirectional force feedback dataglove based on pneumatic artificial muscles,” in *2009 International Conference on Mechatronics and Automation*, Aug. 2009, pp. 1767–1771. doi: 10.1109/ICMA.2009.5246223.

[121] P. Agarwal, P. Kuo, R. R. Neptune, and A. D. Deshpande, “A novel framework for virtual prototyping of rehabilitation exoskeletons,” in *2013 IEEE 13th International Conference on Rehabilitation Robotics (ICORR)*, Jun. 2013, pp. 1–6. doi: 10.1109/ICORR.2013.6650382.

[122] J. Wu, J. Huang, Y. Wang, and K. Xing, “A Wearable Rehabilitation Robotic Hand Driven by PM-TS Actuators,” in *Intelligent Robotics and Applications*, Berlin, Heidelberg, 2010, pp. 440–450. doi: 10.1007/978-3-642-16587-0_41.

[123] V. D. Lee and J. H, “Constraint-induced therapy for stroke: more of the same or something completely different?,” *Current Opinion in Neurology*, vol. 14, no. 6, pp. 741–744, Dec. 2001.

[124] H. C. Fischer, K. Stubblefield, T. Kline, X. Luo, R. V. Kenyon, and D. G. Kamper, “Hand Rehabilitation Following Stroke: A Pilot Study of Assisted Finger Extension Training in a Virtual Environment,” *Topics in Stroke Rehabilitation*, vol. 14, no. 1, pp. 1–12, Jan. 2007, doi: 10.1310/tsr1401-1.

[125] “Bohannon RW, Smith MB. (1987) Interrater reliability of a modified Ashworth scale of muscle spasticity. Phys Ther 67:206-7.”.
[126] F. J. Valero-Cuevas, M. E. Johanson, and J. D. Towles, “Towards a realistic biomechanical model of the thumb: the choice of kinematic description may be more critical than the solution method or the variability/uncertainty of musculoskeletal parameters,” *Journal of Biomechanics*, vol. 36, no. 7, pp. 1019–1030, Jul. 2003, doi: 10.1016/S0021-9290(03)00061-7.
[127] F. C. Chen *et al.*, “Human Hand: Kinematics, Statics, and Dynamics,” in *41st International Conference on Environmental Systems*, American Institute of Aeronautics and Astronautics. doi: 10.2514/6.2011-5249.
[128] J. Lenarčič, T. Bajd, and M. M. Stanišić, “Kinematic Model of the Human Hand,” in *Robot Mechanisms*, J. Lenarcic, T. Bajd, and M. M. Stanišić, Eds. Dordrecht: Springer Netherlands, 2013, pp. 313–326. doi: 10.1007/978-94-007-4522-3_10.
[129] A. Soska, “Surface electrode array-based electrical stimulation and iterative learning control for hand rehabilitation,” Ph.D., University of Southampton, 2015. Accessed: Jun. 07, 2021. [Online]. Available: https://eprints.soton.ac.uk/388627/
[130] J. Angeles and J. Angeles, *Fundamentals of robotic mechanical systems*, vol. 2. Springer, 2002.
[131] P. N. SOUCACOS, “Indications and Selection for Digital Amputation and Replantation,” *Journal of Hand Surgery*, vol. 26, no. 6, pp. 572–581, Dec. 2001, doi: 10.1054/jhsb.2001.0595.
[132] J. G. Andrews and Y. Youm, “A biomechanical investigation of wrist kinematics,” *Journal of Biomechanics*, vol. 12, no. 1, pp. 83–93, Jan. 1979, doi: 10.1016/0021-9290(79)90012-5.
[133] M. A. Gull, S. Bai, and T. Bak, “A Review on Design of Upper Limb Exoskeletons,” *Robotics*, vol. 9, no. 1, Art. no. 1, Mar. 2020, doi: 10.3390/robotics9010016.
[134] F. Ragazzo, “Review on Upper Limb Continuous Passive Motion Devices,” *MATEC Web of Conferences*, vol. 53, p. 01062, 2016, doi: 10.1051/matecconf/20165301062.
[135] T. R. P. Foundation, “Buy a Raspberry Pi 3 Model B+,” *Raspberry Pi*. https://www.raspberrypi.org/products/raspberry-pi-3-model-b-plus/ (accessed Jun. 09, 2021).
[136] U. Eben, “Raspberry Pi 3 Model B+ on sale now at $35 - Raspberry Pi,” Mar. 14, 2018. https://www.raspberrypi.org/blog/raspberry-pi-3-model-bplus-sale-now-35/ (accessed Jun. 09, 2021).
[137] M. Richardson and S. Wallace, *Getting Started with Raspberry Pi*. O’Reilly Media, Inc., 2012.
[138] S. Monk, *Raspberry Pi Cookbook: Software and Hardware Problems and Solutions*. O’Reilly Media, Inc., 2016.

[139] B. Earl, “Adafruit PCA9685 16-Channel Servo Driver,” *Adafruit Learning System*, 2012. https://learn.adafruit.com/16-channel-pwm-servo-driver (accessed Jan. 01, 2021).
[140] “MCP3424 - Analog to Digital Converters,” *Microchip.com*, 2018. https://www.microchip.com/wwwproducts/en/mcp3424 (accessed Jan. 01, 2021).
[141] I. Texas, “LM324/324A, Quadruple Operational Amplifiers - TI | DigiKey.” https://www.digikey.com/en/product-highlight/t/texas-instruments/lm324-324a-quadruple-operational-amplifiers (accessed Jun. 12, 2021).
[142] Olimex, “SHIELD-EKG-EMG - Open Source Hardware Board,” *Olimex*, 2021. https://www.olimex.com/Products/Duino/Shields/SHIELD-EKG-EMG/open-source-hardware (accessed Jan. 01, 2021).
[143] N. Pinckney, “Pulse-width modulation for microcontroller servo control,” *IEEE Potentials*, vol. 25, no. 1, pp. 27–29, Jan. 2006, doi: 10.1109/MP.2006.1635026.
[144] O. Sudjana and M. Hutagalung, “Trajectory control of analog servo motor with limited state information using estimated discrete time model,” in *2013 International Conference on Robotics, Biomimetics, Intelligent Computational Systems*, Nov. 2013, pp. 73–76. doi: 10.1109/ROBIONETICS.2013.6743581.
[145] D. M. Ştefănescu and M. A. Anghel, “Electrical methods for force measurement – A brief survey,” *Measurement*, vol. 46, no. 2, pp. 949–959, Feb. 2013, doi: 10.1016/j.measurement.2012.10.020.
[146] A. S. Sadun, J. Jalani, and J. A. Sukor, “Force Sensing Resistor (FSR): a brief overview and the low-cost sensor for active compliance control,” in *First International Workshop on Pattern Recognition*, Jul. 2016, vol. 10011, p. 1001112. doi: 10.1117/12.2242950.
[147] H. E. Nabilah *et al.*, “Analysis of touching sensation based on weights of rectangular object,” in *2015 2nd International Conference on Biomedical Engineering (ICoBE)*, Mar. 2015, pp. 1–6. doi: 10.1109/ICoBE.2015.7235883.
[148] R. Pallás-Areny and J. G. Webster, *Sensors and Signal Conditioning*. John Wiley & Sons, 2012.
[149] K. Flores De Jesus, M. H. Cheng, L. Jiang, and E. G. Bakhoum, “Resolution Enhancement Method Used for Force Sensing Resistor Array,” *Journal of Sensors*, vol. 2015, p. e647427, Jan. 2015, doi: 10.1155/2015/647427.
[150] A. G. U. Bakshi, *Basics Of Electrical And Electronics Engineering.* 2007.
[151] M. Mrinal, J. Jaijee, P. Bhulania, A. Mehra, H. Rana, and S. Khanna, “Study and Designing of Fourth Order BEC Circuit for Flash Analog to Digital Converter using MUX based Encoder,” *Indian Journal of Science and Technology*, vol. 10, pp. 1–7, May 2017, doi: 10.17485/ijst/2017/v10i18/106370.
[152] S. Jakhar, V. S. Mandloi, R. Goswami, and K. Kandpal, “A Low Power, High Speed 1.2 V Dynamic Comparator for Analog-to-Digital Converters,”

Procedia Computer Science, vol. 171, pp. 1018–1026, Jan. 2020, doi: 10.1016/j.procs.2020.04.109.
[153] A. Sahu, R. S. Mishra, and P. Gour, “Design and Interfacing of High speed model of FPGA using I2C protocol,” *International Journal of Computer Technology and Applications*, vol. 3, 2011.
[154] J. Mankar, C. Darode, K. Trivedi, M. Kanoje, and P. Shahare, “Review of I2C protocol,” *International Journal of Research in Advent Technology*, vol. 2, no. 1, 2014.
[155] V. Pandey, S. Kumar, V. Kumar, and P. Goel, “A Review Paper on I2C Communication Protocol,” *undefined*, 2018, Accessed: Jun. 12, 2021. [Online]. Available: /paper/A-Review-Paper-on-I2C-Communication-Protocol-Pandey-Kumar/66617d4cc786491b4dbb0d072c45f718617f9f2c
[156] T. instruments, “LM2596,” *Ti.com*, 2021. https://www.ti.com/product/LM2596 (accessed Jan. 01, 2021).
[157] M. Lutz, *Programming Python*. O’Reilly Media, Inc., 2001.
[158] A. Kazarian, V. Teslyuk, I. Tsmots, and J. Greguš, “Development of a «smart» home system based on the modular structure and architectural data flow pattern Redux,” *Procedia Computer Science*, vol. 155, pp. 35–42, Jan. 2019, doi: 10.1016/j.procs.2019.08.009.
[159] A. B. M. Moniruzzaman and S. A. Hossain, “NoSQL Database: New Era of Databases for Big data Analytics - Classification, Characteristics and Comparison,” *arXiv:1307.0191 [cs]*, Jun. 2013, Accessed: Jun. 12, 2021. [Online]. Available: http://arxiv.org/abs/1307.0191
[160] A. Castelltort and A. Laurent, “Rogue behavior detection in NoSQL graph databases,” *Journal of Innovation in Digital Ecosystems*, vol. 3, no. 2, pp. 70–82, Dec. 2016, doi: 10.1016/j.jides.2016.10.004.
[161] Z. Bicevska and I. Oditis, “Towards NoSQL-based Data Warehouse Solutions,” *Procedia Computer Science*, vol. 104, pp. 104–111, Jan. 2017, doi: 10.1016/j.procs.2017.01.080.
[162] V. Abramova, J. Bernardino, and P. Furtado, “Which NoSQL Database? A Performance Overview,” *Open Journal of Databases (OJDB)*, vol. 1, no. 2, pp. 17–24, 2014.
[163] N. K. Gundla and Z. Chen, “Creating NoSQL Biological Databases with Ontologies for Query Relaxation,” *Procedia Computer Science*, vol. 91, pp. 460–469, Jan. 2016, doi: 10.1016/j.procs.2016.07.120.
[164] K. Chodorow, *MongoDB: The Definitive Guide: Powerful and Scalable Data Storage*. O’Reilly Media, Inc., 2013.
[165] O. Lehrmann, B. Moller-Pedersen, and K. Nygaard, *Object-oriented programming in the BETA programming language*. ACM Press, 1993.
[166] I. Afyouni *et al.*, “A therapy-driven gamification framework for hand rehabilitation,” *User Model User-Adap Inter*, vol. 27, no. 2, pp. 215–265, Jun. 2017, doi: 10.1007/s11257-017-9191-4.

[167] admin, “Responsive HTML5 and CSS3 Tutorial,” *Tutorial And Example*, May 10, 2019. https://www.tutorialandexample.com/responsive-html5-and-css3-tutorial/ (accessed Jun. 12, 2021).
[168] joan charmant, *Kinovea*. 2021. Accessed: Jan. 01, 2021. [Online]. Available: https://www.kinovea.org/
[169] A. Puig-Diví, C. Escalona-Marfil, J. M. Padullés-Riu, A. Busquets, X. Padullés-Chando, and D. Marcos-Ruiz, “Validity and reliability of the Kinovea program in obtaining angles and distances using coordinates in 4 perspectives,” *PLOS ONE*, vol. 14, no. 6, p. e0216448, Jun. 2019, doi: 10.1371/journal.pone.0216448.
[170] J. A. Moral-Muñoz, B. Esteban-Moreno, M. Arroyo-Morales, M. J. Cobo, and E. Herrera-Viedma, “Agreement Between Face-to-Face and Free Software Video Analysis for Assessing Hamstring Flexibility in Adolescents,” *The Journal of Strength & Conditioning Research*, vol. 29, no. 9, pp. 2661–2665, Sep. 2015, doi: 10.1519/JSC.0000000000000896.
[171] C. H. Guzmán-Valdivia, A. Blanco-Ortega, M. A. Oliver-Salazar, and J. L. Carrera-Escobedo, “Therapeutic motion analysis of lower limbs using Kinovea,” *Int J Soft Comput Eng*, vol. 3, no. 2, pp. 2231–307, 2013.
[172] A. R. Youssef, “PHOTOGRAMMETRIC QUANTIFICATION OF FORWARD HEAD POSTURE IS SIDE DEPENDENT IN HEALTHY PARTICIPANTS AND PATIENTS WITH MECHANICAL NECK PAIN,” *International Journal of Physiotherapy*, pp. 326–331, Jun. 2016, doi: 10.15621/ijphy/2016/v3i3/100838.
[173] P. Fernández-González, A. Koutsou, A. Cuesta-Gómez, M. Carratalá-Tejada, J. C. Miangolarra-Page, and F. Molina-Rueda, “Reliability of Kinovea® Software and Agreement with a Three-Dimensional Motion System for Gait Analysis in Healthy Subjects,” *Sensors*, vol. 20, no. 11, Art. no. 11, Jan. 2020, doi: 10.3390/s20113154.
[174] J. A. Balogun, C. T. Akomolafe, and L. O. Amusa, “Grip strength: Effects of testing posture and elbow position,” *Archives of Physical Medicine and Rehabilitation*, vol. 72, no. 5, pp. 280–283, Apr. 1991, doi: 10.5555/uri:pii:000399939190241A.